

# Collective defenses of garden ants against a fungal pathogen

by

**Barbara Elisa Casillas Pérez**

7th May 2019

*A thesis presented to the  
Graduate School of the  
Institute of Science and Technology Austria,  
Klosterneuburg, Austria  
in partial fulfillment of the requirements  
for the degree of  
Doctor of Philosophy*



*Institute of Science and Technology*



The thesis of Barbara Elisa Casillas Pérez, titled *Collective defenses of garden ants against a fungal pathogen*, is approved by:

**Supervisor:** Sylvia Cremer, IST Austria, Klosterneuburg, Austria

Signature: \_\_\_\_\_

**Committee Member:** Gašper Tkačik, IST Austria, Klosterneuburg, Austria

Signature: \_\_\_\_\_

**Committee Member:** Iain D. Couzin, Max Planck Institute of Ornithology and  
University of Konstanz, Germany

Signature: \_\_\_\_\_

**Defense Chair:** Beatriz Vicoso, IST Austria, Klosterneuburg, Austria

Signature: \_\_\_\_\_

signed page is on file



© by Barbara Elisa Casillas Pérez, 7th May 2019

All Rights Reserved

IST Austria Thesis, ISSN: 2663-337X

I hereby declare that this thesis is my own work and that it does not contain other people's work without this being so stated; this thesis does not contain my previous work without this being stated, and the bibliography contains all the literature that I used in writing the dissertation.

I declare that this is a true copy of my thesis, including any final revisions, as approved by my thesis committee, and that this thesis has not been submitted for a higher degree to any other university or institution.

I certify that any republication of materials presented in this thesis has been approved by the relevant publishers and co-authors.

Signature: \_\_\_\_\_

Barbara Elisa Casillas Pérez

7th May 2019

signed page is on file



## Abstract

Social insect colonies tend to have numerous members which function together like a single organism in such harmony that the term “super-organism” is often used. In this analogy the reproductive caste is analogous to the primordial germ cells of a metazoan, while the sterile worker caste corresponds to somatic cells. The worker castes, like tissues, are in charge of all functions of a living being, besides reproduction. The establishment of new super-organismal units (i.e. new colonies) is accomplished by the co-dependent castes. The term oftentimes goes beyond a metaphor. We invoke it when we speak about the metabolic rate, thermoregulation, nutrient regulation and gas exchange of a social insect colony. Furthermore, we assert that the super-organism has an immune system, and benefits from “social immunity”.

Social immunity was first summoned by evolutionary biologists to resolve the apparent discrepancy between the expected high frequency of disease outbreak amongst numerous, closely related tightly-interacting hosts, living in stable and microbially-rich environments, against the exceptionally scarce epidemic accounts in natural populations. Social immunity comprises a multi-layer assembly of behaviours which have evolved to effectively keep the pathogenic enemies of a colony at bay. The field of social immunity has drawn interest, as it becomes increasingly urgent to stop the collapse of pollinator species and curb the growth of invasive pests. In the past decade, several mechanisms of social immune responses have been dissected, but many more questions remain open.

I present my work in two experimental chapters. In the first, I use invasive garden ants (*Lasius neglectus*) to study how pathogen load and its distribution among nest-mates affect the grooming response of the group. Any given group of ants will carry out the same total grooming work, but will direct their grooming effort towards individuals carrying a relatively higher spore load. Contrary to expectation, the highest risk of

transmission does not stem from grooming highly contaminated ants, but instead, we suggest that the grooming response likely minimizes spore loss to the environment, reducing contamination from inadvertent pickup from the substrate.

The second is a comparative developmental approach. I follow black garden ant queens (*Lasius niger*) and their colonies from mating flight, through hibernation for a year. Colonies which grow fast from the start, have a lower chance of survival through hibernation, and those which survive grow at a lower pace later. This is true for colonies of naïve and challenged queens. Early pathogen exposure of the queens changes colony dynamics in an unexpected way: colonies from exposed queens are more likely to grow slowly and recover in numbers only after they survive hibernation.

In addition to the two experimental chapters, this thesis includes a co-authored published review on organisational immunity, where we enlist the experimental evidence and theoretical framework on which this hypothesis is built, identify the caveats and underline how the field is ripe to overcome them. In a final chapter, I describe my part in two collaborative efforts, one to develop an image-based tracker, and the second to develop a classifier for ant behaviour.



## Acknowledgments

During my PhD, I have welcomed plenty of opportunities to learn, to develop ideas and I have enjoyed immense practical and philosophical support from numerous people.

First, I would like to thank my supervisor, Sylvia Cremer, whose scientific openness and enthusiasm encouraged me to explore many of my interests and whose patience and direction allowed me to focus and follow some of them to an end. It was a privilege to be her PhD student.

During my first year, Christoph Lampert, Gašper Tkačik and Fabian Theis, agreed to supervise my first attempts to obtain motion trajectories from ants to analyze their behaviour. My lab rotations in their groups were key to start shaping this dissertation and they were a point of no return in my development as a scientist as I tapped into their fields of expertise and into their ways of approaching science. I am grateful for their continued support, encouragement and also for introducing me to my amazing collaborators.

Fabian Theis introduced me to his PhD student, Michael Schwarzfischer, who kindly took me under his wing during my first steps into image analysis and data analysis. Thanks to Christoph Lampert I met Jiri Matas and his student Filip Naiser who took on the giant challenge of developing a better multi-target motion tracker. Filip additionally took the challenge of bringing me up to speed with version control software, virtual environments, cloud-based collaboration, python libraries and machine learning algorithms, while making it fun. Through Gašper Tkačik I met Katka Bod'ová and with both I still enjoy trying to work out what type of information ants might use to direct their grooming response. I was also unbelievably lucky to have worked close together with Anna V. Grasse, Christopher D. Pull, Elisabeth Naderlinger, Nathalie Stroeymeyt and Christoph Sommer, who besides their impeccable work, they were truly a joy to work with.

I have a big appreciation for the scientific support units at IST. In particular, thanks to Robert Hauschild (Imaging Facility), who shared his expertise to buy our imaging equipment and Thomas Adletzberger (Electronic Workshop), who built our light system, to Mond, Jean St-Laurent and Janos Kiss (IT Support team) helped me troubleshoot the multiple camera acquisition system on different occasions and they also succeeded in dissipating the accompanying frustration with humour, to Wanda Gorecka (Life Science Facility) for her help rearing my *Lasius neglectus*, and to Alois Schlögl who introduced me to parallel computing and provided unparalleled support (Scientific-Computing and HP-Cluster).

I would like to thank Iain Couzin for his spot on feedback and advice and for setting the bar high in Behavioural Biology.

I collectively acknowledge all the members of the Social Immunity Lab (past and current), for expanding my scientific horizons while filling my time at IST with happy memories. *Danke vielmals* to the people that happily crossed my path during these years at IST.

*Tantísimas gracias* also to those, back home, who often crossed my mind. My warmest gratitude goes to my family, who encouraged me to take on every challenge that came my way and immensely supported me when these challenges felt larger than I could handle.

My endless gratitude to my partner, Victor Mireles. Choosing a finite set of reasons from an infinite set, seems pointless here. Thank you !

## About the Author

Barbara Casillas Pérez completed her BSc in Biology at Facultad de Ciencias, Universidad Nacional Autónoma de México (UNAM), before joining IST Austria in September 2011. Her main research interest is animal behavioural ecology and evolution, in particular, decision making processes. She also has a predilection for method development. During her PhD, she has focused on the individual, group and colony level decisions of ants facing a fungal pathogen.

## List of Publications

1. Stroeymeyt N, **Casillas-Pérez B**, Cremer S. 2014.  
Organisational Immunity in Social Insects.  
**Current Opinions in Insect Science**  
(doi:10.1016/j.cois.2014.09.001)

## Table of Contents

<b>Abstract</b>	<b>v</b>
<b>Acknowledgments</b>	<b>vii</b>
<b>About the Author</b>	<b>ix</b>
<b>List of Publications</b>	<b>x</b>
<b>List of Figures</b>	<b>xiii</b>
<b>List of Abbreviations</b>	<b>xv</b>
<b>1 Background</b>	<b>xvi</b>
1.1 Collective disease defenses and social immunity . . . . .	1
1.2 Study system . . . . .	5
1.3 Thesis aims and outline . . . . .	8
<b>2 Organisational Immunity in Social Insects</b>	<b>10</b>
2.1 Abstract . . . . .	11
2.2 Introduction . . . . .	12
2.3 Evidence for organisational immunity in social insects . . . . .	14
2.4 From individual behaviour to interaction patterns . . . . .	21
2.5 Conclusions . . . . .	26
2.6 Acknowledgements . . . . .	28

<b>3</b>	<b>Sanitary care dynamics and pathogen transmission</b>	<b>35</b>
3.1	Abstract . . . . .	35
3.2	Introduction . . . . .	36
3.3	Results . . . . .	41
3.4	Discussion and Conclusion . . . . .	77
3.5	Method . . . . .	83
3.6	Supplement . . . . .	93
<b>4</b>	<b>Effect of queen pathogen-contamination on colony development</b>	<b>96</b>
4.1	Abstract . . . . .	97
4.2	Introduction . . . . .	98
4.3	Results and Discussion . . . . .	102
4.4	Conclusion . . . . .	121
4.5	Method . . . . .	124
4.6	Supplement . . . . .	133
<b>5</b>	<b>Computational analysis of behavior</b>	<b>137</b>
5.1	Abstract . . . . .	137
5.2	Introduction and approach . . . . .	139
5.3	Method . . . . .	145
5.4	Results . . . . .	151
5.5	Conclusions . . . . .	152
5.6	Contribution . . . . .	153
5.7	Introduction . . . . .	154
5.8	Approach . . . . .	155
5.9	Method . . . . .	158
5.10	Results . . . . .	160
5.11	Conclusions . . . . .	161
5.12	Contribution . . . . .	162
	<b>Bibliography</b>	<b>163</b>

## List of Figures

2.1	Mechanisms of organisational immunity in insect societies . . . . .	29
3.1	Experimental plan . . . . .	40
3.2	Changes in time allocated to grooming . . . . .	42
3.3	Expulsion of pellets . . . . .	46
3.4	Time-resolved behavior . . . . .	51
3.4	Time-resolved behaviour (Continued) . . . . .	52
3.5	Timing of pellet expulsion by nestmates . . . . .	54
3.6	First allogrooming interaction . . . . .	56
3.7	Effect of dose given and dose of partner on allogrooming received during peak allogrooming response . . . . .	57
3.8	Example of grooming choice per window and estimated spore load dif- ference . . . . .	61
3.9	Nestmate preference . . . . .	62
3.10	Possible routes in which spores move within the system . . . . .	65
3.11	Body to head spore load ratio . . . . .	68
3.12	Spores in pellets . . . . .	71
3.13	Spore reduction and acquisition . . . . .	74
3.14	Proportional loss estimated with exposure-controls . . . . .	75
3.15	Proportion of nestmates contaminated . . . . .	76
4.1	Experimental design . . . . .	101

4.2	Individual colony growth trajectories . . . . .	104
4.3	Colony growth . . . . .	107
4.4	Colony size split by growth mode . . . . .	108
4.5	Brood production before hibernation . . . . .	111
4.6	Brood production and overwintering outcome . . . . .	112
4.7	Colony behaviour . . . . .	116
4.8	Worker size change in time . . . . .	121
5.1	Examples of dataset and behavioral categories . . . . .	159
5.2	Partial occlusion visualization in Picasso visualizer . . . . .	161



## List of Abbreviations

**GLM** General(ised) linear model

**LMER** Linear mixed effects regression

**LR** Likelihood ration test

**ddPCR** Droplet digital PCR

**MWW** Mann-Whitney-U test or Mann-Whitney-Wilcoxon test



# 1 Background

## 1.1 Collective disease defenses and social immunity

Group living is a strategy with many benefits, and some costs [Krause and Ruxton, 2002]. One of the costs associated to group living is an increased susceptibility to disease. This is because the transmission opportunities of a pathogen grow with the number of potentially infectious interactions among the members of the group. Also, a large density of susceptible individuals would ensure that the pathogen finds an opportunity for infection. Moreover, a population of group-living individuals, often family groups with a shared genetic background, can have a relatively uniform susceptibility, further increasing the chance that a pathogen prevails. Indeed, group size and genetic homogeneity correlate with pathogen prevalence and intensity in a number of study organisms [Schmid-Hempel, 2017]. However, there can be considerable deviation from the expectation, for instance, when there is structure in the social interactions (e.g. resulting from dominance hierarchies in mammals or division of labour in social insects) which can impede pathogens from reaching all parts of the population [Schmid-Hempel, 2017; Nunn *et al.*, 2015]. Group-living animals have evolved a variety of adaptations that offset the costs of pathogens [Schmid-Hempel, 2017].

Social insects represent a peculiar case, as they live in particularly dense populations with high genetic relatedness, maintaining a stable homeostatic environment which should favour microbial invasion [Schmid-Hempel, 1998], but instead exhibit a barrage of individual and collective anti-pathogenic defenses [Cremer *et al.*, 2007].

These defenses have evolved to limit the uptake of pathogens from the environment and into the nest, to avoid the contamination of colony members or the replication of the

pathogens inside them [Cremer *et al.*, 2007]. The strategies have also been broadly categorized into avoidance, resistance and tolerance strategies based on their effect. Avoidance strategies prevent the acquisition of a parasite altogether. Resistance refers to strategies that limit pathogen replication, whereas tolerance strategies do not affect the pathogen but merely compensate for its effects [Cremer *et al.*, 2018]. Finally, they can be classified according to when they happen, as prophylactic (happening inherently, constantly), as pathogen-induced (happening only upon pathogen exposure) or both (present always, but intensified with a pathogen trigger). For examples of collective strategies against disease see Table 1.1.

Avoidance of possibly contaminated areas, food or individuals reduces overall exposure to pathogens (e.g. territoriality, aversion, nest guards) [Cremer *et al.*, 2007]. Given the ubiquity of pathogens, complete avoidance seems unachievable, and this possibly explains the scarcity of avoidance examples in social insects [Cremer *et al.*, 2018]. The actions of colony members tend to be located in space and restricted to certain tasks (e.g. spatial fidelity [Mersch *et al.*, 2013], task-allocation [Hart and Ratnieks, 2001; Schmid-Hempel and Schmid-Hempel, 1993b]) and this substructuring of the interaction network can protect the queen and vulnerable brood from pathogens carried inside the nest by foragers (e.g. organisational immunity, see Chapter 2). The isolation of sick individuals (self-actuated [Bos *et al.*, 2012] or socially enforced [Baracchi *et al.*, 2012; Leclerc and Detrain, 2016]) has also been observed.

Resistance strategies can remove pathogens from the nest or from individuals and/or neutralize them. Preventively, the nest can be kept clear by removing sources of contamination (e.g. removing corpses and placing them down-stream so they are not washed in with the next rain [Howard and Tschinkel, 1975]) and applying disinfectants to the nest walls (e.g. resin collection, fecal pellets) [Cremer *et al.*, 2007]. Triggered by the presence of a heat-sensitive pathogen, honeybees are known to increase the comb temperature, a feat known as collective fever [Starks *et al.*, 2000].

Tolerance is the capacity of a colony to cope with the damage directly caused by the pathogen or caused by the measures taken against the pathogen. A colony can increase worker production to replace losses after an infection, and it is also hypothesized that it produces a buffer worker force before it incurs a major loss (e.g. inactive “lazy” workers) [Cremer *et al.*, 2018]. Colony-level tolerance is starting to gain atten-

COLLECTIVE STRATEGIES			
STAGE	AVOIDANCE	RESISTANCE	TOLERANCE
UPTAKE	territoriality aversion		
NEST CONTAMINATION	nest guards nest architecture	resin collection fecal pellets nechrophoresis	
TRANSMISSION AND INFECTION	spatial-fidelity task allocation	mechanical removal (allogrooming)	
	self-removal or isolation	chemical disinfection (antimicrobial glandular compounds)	
REPLICATION		collective fever destructive disinfection	changes in colony pace or composition

Table 1.1: **Examples of collective disease defenses.** The strategies can be broadly categorized based on the stage of the pathogen which they prevent or on the effect they have over the pathogen. They can also be presented prophylactically (blue), be pathogen-induced defenses (pink), or both (purple). This is by no means an exhaustive list.

tion in the field, and it should gain momentum as it becomes easier to experimentally monitor colonies long-term (see Chapter 4).

Collective defenses, can be complex and dynamic. To illustrate these properties, take destructive disinfection [Pull *et al.*, 2018], which targets the replication of a fungal pathogen once it has successfully invaded an individual in the ant colony (an immobile and vulnerable pupae) . The individual can no longer be helped by the colony and it relies only on its immune system to fight the pathogen. If it were to fail, it poses an imminent threat to the colony, as the pathogen will complete its cycle and produce an overwhelming amount of new infectious propagules to release into the colony. The brood tending ants sense a chemical cue emitted by the infected pupae, which triggers unpacking, biting and spraying, killing both the pupae and the fungus inside. The group moves from prophylactic brood-care to pathogen-triggered intensified grooming, to destructive disinfection, in a thrilling race against the pathogen.

Because of their reliance on interactions among individuals, collective strategies can have, both, a beneficial and a detrimental outcome. For example, the effects of allogrooming on fungal spore transmission depend on at least two parameters: (i) the ability of spores to transmit and (ii) the ability of ants to remove the spores. Depending on these parameters, allogrooming can have opposing effects, that is, allogrooming can lead both to the propagation or containment of the pathogen. When the spores are highly transmissible (infectious) or the ants are inefficient at removing them, the best strategy to contain the pathogen is to avoid allogrooming and rely on self-grooming. When the spores are not so transmissible (infectious), or the ants are very efficient at removing them, allogrooming becomes advantageous [Theis *et al.*, 2015].

Epidemic parameters are not necessarily fixed in time. For example, in the ant-fungus host-pathogen system, transmissibility decreases as the spores attach and penetrate the cuticle of the contaminated ant. For the same reason, grooming efficiency is also expected to decrease. Given a certain pathogen-host system, we may start at a fixed point in the parameter space and move away from it, as time goes by. Correspondingly, the host response should be adjusted dynamically.

This dependency on time does not end when one pathogen invasion is eliminated. Rather, the outcome of a given strategy can influence the response to subsequent challenges. For example, while a low-level infection can lower susceptibility to the

same pathogen in a second challenge [Ugelvig and Cremer, 2007; Konrad *et al.*, 2012], it can increase susceptibility to a different pathogen [Konrad *et al.*, 2018]. Interestingly, ants adjust their sanitary care to their infection history and the presented challenge. Specifically, ants allogroom when presented to a homologous threat and use poison spraying when presented to a heterologous threat, to which they are more susceptible [Konrad *et al.*, 2018].

Despite the wealth of studies on mechanical removal and chemical disinfection, the behavior dynamics of sanitary care are not entirely understood. Points above illustrate the complexity of the phenomenon and from these examples stem new questions. To name a few, how are contaminated individuals detected? Is the information of contaminated-status broadcast to the group? How do contaminated individuals take part? Ants constantly encounter soil-borne fungal pathogens and at any point in time it is likely that more than a single ant is contaminated. Given that infection risk is dose-dependent, can ants (individually or collectively) assess the risk to the colony (overall spore load) based on the number of individuals contaminated or their loads? And do they adjust sanitary care according to this risk? It is thus worth revisiting the most popular strategy against pathogen transmission and infection, sanitary care. We do this in Chapter 3.

## 1.2 Study system

In this work, two different host-pathogen systems were used for study of fungal infections in ants. The first consists of the ant *Lasius neglectus* as host, and *Metarhizium robertsii* as a fungal pathogen; the second, of the ant *Lasius niger* and the fungus *Metarhizium brunneum*. In general terms, both fungi are prevalent in plants and soil, and their spores are known to attach to the foraging ants, whereby they penetrate their cuticle, eventually sporulating from the dead body. Each of these organisms is described in more detail below.

### 1.2.1 Ant hosts

*Lasius neglectus* is an invasive garden ant which is found in most continental Europe [Seifert, 2000; Chultz and Eifert, 2005] after being, most likely, accidentally introduced from Asia Minor [Chultz and Eifert, 2005; Ugelvig *et al.*, 2008]. Its wide distribution is due in part to its ability to survive extended periods of frost [Seifert, 2000]. Populations dwell in networks of several cooperating nests, each containing several queens that mate within the nests, and can thus be considered super-colonies [Helanterä *et al.*, 2009]. The workers of *L. neglectus* are specially proficient at collecting honeydew from aphids, which allows them to out-compete other local species, but causing a damage to vegetation [Cremer *et al.*, 2006]. The species has become a very common model organism for the study of social immunity [Cremer *et al.*, 2018; Ugelvig and Cremer, 2007; Konrad *et al.*, 2012], for four main reasons: their role as an urban pest [Konrad *et al.*, 2012], its interaction with fungal pathogens, the ease with which they are collected and the ease of maintenance in laboratory environments over several years.

*Lasius niger*, also known as the black garden ant, is a species distributed throughout the Holarctic region. They live in colonies with a single queen (*i.e.* monogynic) and several thousand workers, which are aggressive to other colonies [Sommer *et al.*, 1995]. Colonies are founded after a nuptial flight in which queens and males from several colonies in the same region, emerge simultaneously to the surface [Aron *et al.*, 2009], after sensing environmental cues [Bourke *et al.*, 1995]. After mid-air mating, the queen lands, sheds its wings, finds a suitable place to dig and buries itself never to emerge again. Inside its chamber, the *L. niger* queen must survive without foraging, metabolizing parts of its own body and fat reserves [Janet, 1907], as well as raising the first batch of workers. During this period, the incipient colonies are especially vulnerable to predators and pathogens and in the case where queens share a nest a fight to death imminently takes place [Bourke *et al.*, 1995]. In the surviving colonies, workers take over brood care and start to forage, allowing the colony to survive for years or decades [Kramer *et al.*, 2016; Fowler *et al.*, 1986]. Fertilized *L. niger* queens can be captured during nuptial flight in large numbers and let to initiate colonies in laboratory conditions, which makes them a good model organism for the study of colony development.



## 1.2.2 Fungal pathogens

***Metarhizium*** is a genus of Ascomycete which is present in all continents except Antarctica [Roberts and St. Leger, 2004], dwelling in the roots of plants and surrounding soil, with a very high prevalence [Keller *et al.*, 2003]. Most of the species are generalist pathogens of insects, with some species being able to infect hosts of seven different orders, which has led to its use as a biological insecticide [Deacon, 2013]. In this work, we use two different species of the genus: *M. robertsii* and *M. brunneum*, which were until recently considered a single species *M. anisopliae* [Bischoff *et al.*, 2009]. Apart from their genetically-derived phylogeny, their differences are most evident in habitat, with *M. brunneum* found in forested habitats and *M. robertsii* more in open or agricultural fields [Wyrebek *et al.*, 2011].

Both species have a similar interaction cycle with their insect host. The sexual spores of the fungus (*i.e.* conidiospores) are acquired from the environment, attaching loosely to the insect cuticle. Under the right humidity conditions, these germinate and attach firmly, producing a specialized infection structure called an “appressorium”, which penetrates into the body by enzymatically breaking down the insect’s cuticle [Deacon, 2013]. Inside the host, the conidiospores produce sexual spores (*i.e.* blastospores) which spread through the insect’s hemolymph, consuming sugars and producing toxins, which kill cells and suppress the immune system of insect [Pedras *et al.*, 2002]. The host dies because its organs are colonized. The fungus produces filaments (*i.e.* mycelia) that grow out of the corpse and in their tips produce new conidiospores [Deacon, 2013].

In this work we had access to a strain of *M. robertsii* which had been genetically modified to include one of two molecular labels, either an eGFP or an mRFP1 gene. These were used in the experiments described in Chapter 3, to distinguish their transit through a group of ants. For the experiment described in Chapter 4, *M. brunneum* was used.

## 1.3 Thesis aims and outline

This thesis has the aim of advancing our understanding of two processes. First, the changes in the behaviour of ants upon contact with individuals that have been exposed to pathogens, and how these changes mediate the transmission of the pathogen. Second, the development of colonies when the queen has been exposed after mating, in particular, the effect on overwintering survival. These two processes have repercussions on the survival of the colony, and so the studies lead to a better understanding of the mechanisms that insects have evolved to cope with disease. Furthermore, the refinement of the techniques, both theoretical and experimental, necessary for these studies, firmly establish them in a field that has seen much technical transformation.

The second chapter presents the basis of the organizational immunity hypothesis. The hypothesis refers to properties of interaction networks of insect societies which inhibit disease transmission. The hypothesis is presented and supported with theoretical and empirical evidence. The chapter was published as a review in 2014 in the Journal *Current Opinions in Insect Science*, and written with N. Stroeymeyt and S. Cremer. This chapter also puts the study of disease defenses in insect societies into context, mentioning the important findings and major challenges of this field.

In the third chapter, an experiment in which the behaviour of small groups of ants upon contact with a pathogen-exposed individual, is described. The experiment, combining molecular techniques for spore quantification, behavioural observations and mathematical models, sheds light on the effect that pathogen doses and infestation level have on the behaviour of both exposed and unexposed individuals, and on how this behaviour affects the transmission of pathogens. The study presents several novelties: the sheer amount of data which was manually generated gives unprecedented statistical power to make inferences, behaviours which had not been studied in detail are observed, and molecular quantification on two labelled spores simultaneously add significant resolution to the tracing of infection pathways. This work was done in collaboration with A. V. Grasse, G. Tkačik and S. Cremer. Furthermore, it serves as the basis for a theoretical exploration of individual ant behaviour being undertaken in collaboration with G. Tkačik and K. Boďová.

The fourth chapter reports an experiment in which the effect of pathogens on the development of newly founded colonies is studied, with particular attention to its overwintering survival. The experiment monitored queens exposed to a pathogenic fungus immediately after mating, and followed them throughout a year, observing periodically both their demographics and their behaviour. Of special interest is the description of different strategies that colonies follow to optimize their resources and allow them to survive the winter, independently of their exposure to pathogens. Importantly, this experiment introduced the use of an image-based tracking software (developed in a collaboration described in the next chapter), which allows for quantitative assessment of behaviour in unprecedented scales, both in terms of number of colonies, and of total observation time. The experimental work described in this chapter was carried out with C. Pull. Additional experimental measurements are carried out with help from Elisabeth Näderlinger.

In the fifth and final chapter, the previously mentioned image-based tracking software is described in detail. After a review of the state of the art in automated behavioural observation, its successes and potentialities, as well as detailed analysis of one of the most prominent solutions, the need for the development of new software, called Ferda, is motivated. Ferda is capable of following individuals of different sizes, recorded in videos of diverse quality and of very large sizes. This last property is essential for the experiment described in the previous chapter, and required the use of parallel algorithms and a high performance computing environment. The development of Ferda was done in close collaboration with F. Naiser and J. Matas, is still in progress and expected to lead to a publication (F. Naiser, B. Casillas-Pérez, S. Cremer, J. Matas). Finally, the chapter ends with a report on preliminary results of automated behaviour classification, which consist of machine learning algorithms being trained to recognize different behaviours. Essential to this project was the data produced by Ferda, as well as human annotation of data. These final experiments were performed in collaboration with C. Sommer and expected to be included in future experiments by the Cremer Lab.



## 2 Organisational Immunity in Social Insects

The work presented in this chapter was published as a review article, with the same title, in *Current Opinions in Insect Science* [Stroeymeyt *et al.*, 2014], and reproduced here with minimal changes. The manuscript was written together with the principal author, Nathalie Stroeymeyt and corresponding author, Sylvia Cremer. All authors contributed to the literature search, concept development, discussions and manuscript drafting. The review collects the work which has been relevant to formulate the “organisational immunity” hypothesis. In brief, the hypothesis states that eusocial insect networks should possess properties which hinder disease spread. The literature was roughly split into theoretical work and the empirical evidence which support the hypothesis. I was mainly responsible for compiling, selecting and condensing the theoretical studies on the propagation-inhibiting properties of networks, as well as, the modeling approaches which predict the emergence of such properties and which are used in combination with empirical studies. My work is best illustrated in items Box1 and Figure B1. A recent study [Stroeymeyt *et al.*, 2018] demonstrated the existence of both constitutive and induced transmission-inhibiting properties in the interaction networks of ant colonies, providing the hypothesis with strong empirical support.

### 2.1 Abstract

Selection for disease control is believed to have contributed to shape the organisation of insect societies – leading to interaction patterns that mitigate disease transmission risk within colonies, conferring them “organisational immunity”. Recent studies combining epidemiological models with social network analysis have identified general prop-

erties of interaction networks that may hinder propagation of infection within groups. These can be prophylactic and/or induced upon pathogen exposure. Here we review empirical evidence for these two types of organisational immunity in social insects and describe the individual-level behaviours that underlie it. We highlight areas requiring further investigation, and emphasise the need for tighter links between theory and empirical research and between individual- and collective-level analyses.

## 2.2 Introduction

Disease transmission in animal societies is believed to depend greatly on the structure and dynamics of their social interaction networks, which represent pathways over which infectious propagules can be transmitted [Newman, 2010; Mersch *et al.*, 2013; Charbonneau *et al.*, 2013; Keeling, 2005; Barthelemy *et al.*, 2005; Pei and Makse, 2013; House and Keeling, 2011; Miller, 2009; Newman and Girvan, 2004; Salathe and Jones, 2010; Shao and Jiang, 2012; Bisset and Marathe, 2009; Bansal *et al.*, 2010; Cremer *et al.*, 2007; Naug and Camazine, 2002; Naug and Smith, 2007; Schmid-Hempel, 1998; Schmid-Hempel and Schmid-Hempel, 1993a]. The effects of interaction patterns on epidemic dynamics have been thoroughly investigated in theoretical studies (Fig. B1). However, empirical validation of their predictions has been scarce due to the difficulty of obtaining comprehensive datasets on interactions and disease transmission in large animal groups. Studying experimentally amenable model systems such as colonies of social insects (social bees and wasps, all ants and termites) may help overcome this constraint and gain new insights on how social organisation influences disease dynamics and epidemic outcomes in social groups (Fig. B1).

Social insects are particularly vulnerable to disease because the frequent and close interactions among genetically related colony members favour pathogen transmission. In addition to their individual immune system, they have evolved collective disease defences known as “social immunity” [Cremer *et al.*, 2007]. Social immunity is expressed through a variety of sanitary behaviours and the use of antimicrobials, which reduce the infection risk and pathogen load of exposed individuals [Cremer *et al.*, 2007; de Roode and Lefèvre, 2012; Evans and Spivak, 2010; Wilson-Rich *et al.*, 2009]. Moreover, the organisation of insect societies may also contribute to social immunity [Cremer *et al.*,

2007; Naug and Camazine, 2002; Naug and Smith, 2007; Schmid-Hempel, 1998; Schmid-Hempel and Schmid-Hempel, 1993a]. In particular, certain patterns of interactions among group members have been claimed to limit pathogen spread at the colony-level and decrease the infection risk of valuable individuals, such as the queen, brood or young workers, providing a form of “organisational immunity” [Naug and Smith, 2007]. Interaction patterns that reduce disease risk may be constitutively expressed in healthy colonies and play a preventative or prophylactic role, or be induced upon contact with pathogens, through behavioural changes that further reduce transmission risk from infectious to healthy individuals [Cremer *et al.*, 2007].

Testing the organisational immunity hypothesis in social insects has been facilitated by the recent development of data collection techniques and analytical approaches, such as high-throughput automated tracking of individuals within colonies (reviewed in [Charbonneau *et al.*, 2013; Pinter-Wollman *et al.*, 2014]) and the application of social network theory to epidemiology and behavioural ecology [Keeling, 2005; Krause *et al.*, 2009]. However, unequivocal testing remains challenging because it is experimentally difficult to: (i) manipulate colony-level interaction patterns without modifying other potentially epidemic-relevant parameters such as colony size, hunger levels or health status; (ii) track the propagation of pathogens and/or non-pathogenic proxies in real time and thus (iii) establish a clear causal relationship between the structure of interaction networks and transmission dynamics; and (iv) understand how individual behaviour influences collective dynamics. Empirical work has therefore often been limited to partially addressing different aspects of organisational immunity (Table 1). Here we present an overview of the existing empirical support for organisational immunity in social insects and the individual behavioural rules that are believed to underlie it. We attempt to elucidate general concepts of organisational immunity and highlight areas deserving further investigation.

## 2.3 Evidence for organisational immunity in social insects

### 2.3.1 Interaction patterns and colony-level disease spread

Explicit simulations of disease spread over simulated interaction networks have proven a powerful approach to formally investigate the role of social organisation in disease dynamics. These analyses revealed that the structural properties of interaction networks (*e.g.*, degree distribution, clustering coefficient, and community structure) have a crucial influence on transmission dynamics and final epidemic size ([Keeling, 2005; House and Keeling, 2011; Salathe and Jones, 2010; Hock and Fefferman, 2012]; detailed in Box 1). Similarly, the extent to which disease spreads within groups depends on the temporal dynamics of interactions among individuals, such as the time ordering and temporal overlap of interactions, or the existence of repeated contacts [Bansal *et al.*, 2010; Read *et al.*, 2008]. Empirical studies that combined social network analysis with the physical tracking of non-pathogenic proxies spreading through colonies (*e.g.*, microbeads [Naug and Smith, 2007; Naug, 2008] or food [Feigenbaum and Naug, 2010; Sendova-Franks *et al.*, 2010]; Table 1) confirmed that social network properties influence transmission in social insects. Indeed, changes in network structure induced by experimentally manipulating food quality or foraging motivation led to predicted changes in transmission patterns in the honeybee *Apis mellifera* [Naug and Smith, 2007; Naug, 2008; Feigenbaum and Naug, 2010] and the ant *Temnothorax al-bipennis* [Sendova-Franks *et al.*, 2010]. In particular, non-pathogenic proxies spread less broadly and less evenly over networks of lower density [Naug and Smith, 2007; Naug, 2008; Feigenbaum and Naug, 2010; Sendova-Franks *et al.*, 2010] and/or increased clustering [Naug and Smith, 2007; Naug, 2008], and spread faster and more uniformly in groups with higher spatial mixing among individuals and higher temporal overlap of interactions [Sendova-Franks *et al.*, 2010].

It remains unproven, however, whether the structure of interaction networks naturally observed in social insects really contributes to limit disease spread through the colony (*i.e.* whether it provides prophylactic organisational immunity). Most support for this hypothesis comes from agent-based models showing that social heterogeneities,



arising for example from division of labour or differences in life history and disease susceptibility among different types individuals, help contain disease in social insect colonies [Naug and Camazine, 2002; Schmid-Hempel, 1998; Fefferman *et al.*, 2007]. Social heterogeneities result in interaction heterogeneities, *i.e.* interactions are not distributed uniformly within the colony, but some pairs of workers interact more frequently than others. This leads to the formation of partially isolated groups of individuals, or communities, with reduced transmission rates across groups [Cremer *et al.*, 2007; Naug and Camazine, 2002; Fefferman *et al.*, 2007]. Empirical evidence that social networks do contribute to mitigate disease risk is however still scarce. Testing the effect of interaction heterogeneities on disease spread can be achieved by comparing the transmission properties of real social insect networks with appropriate null models (Table 1). So far, most such studies have focused on information flow over networks [Mersch *et al.*, 2013; Blonder and Dornhaus, 2011; Pinter-Wollman *et al.*, 2011]; however, their outcome can be reinterpreted in terms of disease transmission because they use similar modelling approaches to those investigating pathogen spread [Quevillon *et al.*, 2015]. Analysis of time-ordered contact networks in the ant *Temnothorax rugatulus* revealed slower colony-level propagation compared to a diffusion null model [Blonder and Dornhaus, 2011], which could lend support to the organisational immunity hypothesis. By contrast, the interaction skew observed among *Pogonomyrmex barbatus* ant workers near the nest entrance was shown to enhance information flow compared to uniform interaction null models [Pinter-Wollman *et al.*, 2011]. These examples illustrate the difficulty of determining the adaptive value of interaction patterns observed in social insect colonies. These have indeed evolved under conflicting selection pressures and likely represent a compromise between the need to reduce disease spread on one hand, and to ensure high work output, fast information flow, and colony resilience on the other hand [Charbonneau *et al.*, 2013; Naug and Camazine, 2002; Pinter-Wollman *et al.*, 2011]. Studies that explicitly address the differences in transmission properties between information and pathogens will be crucial to better understand the significance of interaction networks in terms of disease control and colony efficiency.

It also remains unproven whether social insects can alter their interaction patterns upon encountering pathogens to further reduce disease propagation (*i.e.* whether they

show induced organisational immunity). So far there has been only one investigation of group-level transmission dynamics in pathogen-exposed colonies [Otterstatter and Thomson, 2007], and this study lacked comparison with non-exposed control colonies (Table 1). Theory may help generate testable predictions for future empirical studies of induced organisational immunity (Box 1).

### **2.3.2 Interaction patterns and individual probability of infection**

The fitness consequences of infection in social insects depend not only on overall disease incidence, but also on the identity of individuals contracting the disease. For example, losing a queen is more costly to the colony than losing workers. Similarly, losing young workers is more costly than losing older workers, which have shorter expected life expectancy [Woyciechowski and Moron, 2009]. Highly valuable individuals appear to be protected against disease via interaction heterogeneities, which result in their social isolation from 'high-risk' individuals (*i.e.* old workers that have a high chance of having encountered pathogens and perform high disease-risk tasks such as foraging [Mersch *et al.*, 2013], waste management [Hart and Ratnieks, 2001; Hart and Ratnieks, 2002], undertaking [Sun and Zhou, 2013] and hygienic behaviour [Wilson-Rich *et al.*, 2009]). There is good evidence that the queen and young workers are protected from potentially harmful external agents. Studies tracking the propagation of non-pathogenic proxies through honeybee colonies indeed revealed lower prevalence and intensity in young workers [Naug and Camazine, 2002; Feigenbaum and Naug, 2010] and the queen [Feigenbaum and Naug, 2010] than in older workers. Moreover, time-ordered analysis of trophallaxis (*i.e.* social food sharing) networks in the ant *Camponotus pennsylvanicus* showed that there is a long delay between foragers introducing new food into the colony and the queen receiving it, which was suggested to decrease the risk of transmission of external pathogens to the queen [Quevillon *et al.*, 2015]. In honeybees, the protection of the queen and young workers was assumed to derive from the consistently observed biases towards within-age-group interactions [Naug and Smith, 2007; Naug, 2008; Scholl and Naug, 2011; Baracchi and Cini, 2014], which lead to between-age-group compartmentalisation [Baracchi and Cini, 2014]. This hypothesis is supported by a study of the social interaction net-

works in the ant *Camponotus fellah*. Colonies of this species appear to be loosely organised into three groups, or communities, showing more frequent within-group than between-group interactions: the queen and young nurses, middle-aged workers performing nest maintenance and cleaning, and old foragers [Mersch *et al.*, 2013]. Simulation of propagation over these empirical networks revealed faster information spread within than between communities when the source originated from the foragers [Mersch *et al.*, 2013]. These results indicate that age-and-task interaction biases play a crucial role in isolating the queen and young workers from the outside environment. Interaction heterogeneities leading to colony compartmentalisation into groups that differ in their value for the colony and/or in their disease exposure risk are likely to be widespread in the organisation of insect societies. For example, workers performing high disease-risk tasks are usually highly specialised and have few interactions with other workers [Hart and Ratnieks, 2002; Hart and Ratnieks, 2001; Sun and Zhou, 2013; Arathi *et al.*, 2000], which leads to their social isolation.

Regardless of the identity of their interaction partners, individuals could also be at higher or lower risk of infection depending on their position within the interaction network. For example, individuals with a high number of interaction partners, or individuals that occupy an intermediary 'bridge' position between communities, may be more vulnerable than isolated individuals. In network analysis, this can be formally quantified via measures of node centrality (*e.g.*, degree or betweenness; Box 1). The only empirical study that specifically tested for a correlation between the degree centrality of individuals and their infection rate did not find evidence for this hypothesis [Otterstatter and Thomson, 2007], but that study involved very small, incipient colonies. Because colony size limits the complexity of colony organisation [Anderson and McShea, 2001], these may have been too small for organisational immunity to develop.

### Box 1. Modelling social interactions and disease transmission

Most epidemic models classify individuals in a group according to their disease state (*e.g.* susceptible-infectious in the simplest SI model). This type of models traditionally assume random mixing of individuals, *i.e.* every individual interacts with any other with the same probability [Newman, 2010]. Yet, the contact patterns observed in social groups, in particular social insect societies [Salathe and Jones, 2010], deviate widely from the assumption of random mixing. Recent studies have therefore focused on simulating epidemic spread over networks, which explicitly describe all interactions. In such an approach, an edge between two nodes represents an interaction between two individuals (*e.g.* grooming, trophallaxis), potentially leading to disease transmission. At every time-step, disease may 'travel' – with a given probability – from an infectious node to a neighbouring susceptible node, making it infectious. Other studies have defined networks in different ways (*e.g.* nodes as areas and weighted edges as the number of individuals moving across them [Charbonneau *et al.*, 2013]).

Compared to a 'random mixing' model, an individual in a network has a relatively small number of susceptible contacts, which quickly become infected. This local depletion of susceptible contacts is present in all networks and, to different extents, leads to reduced early growth rate and smaller final epidemic sizes [Keeling, 2005]. The following network features further influence epidemic outcome.

**Density.** *Proportion of all possible edges that are actually present* (Fig. B1a). In the simplest scenario, a random network where all nodes have the same number of edges (*i.e.* they have the same degree), an increased density will ensure faster spread [Barthelemy *et al.*, 2005]. This trend can be countered by other structural features of a network.

**Degree heterogeneity (D).** *Variance in degree of nodes* (Fig. B1a,b). In a random network where nodes have different numbers of edges, diffusion (*e.g.* of a pathogen) accelerates with increasing heterogeneity. In these networks, disease cascades from high-degree nodes ("hubs") to low-degree nodes, which is why hubs have been a target for vaccination efforts [Mersch *et al.*, 2013], although, influential nodes or "super-spreaders" (*i.e.* individuals that have a disproportionately high likelihood of spreading the disease to others) are not necessarily high-degree nodes [Pei and Makse, 2013].

**Clustering.** *Propensity of two neighbours of a given node to also be directly linked to each other* (Fig. B1a,b). Clustering coefficient (**C**) is a common measure to describe clustering. Epidemic simulations over networks with a large C show reduced initial growth rate and smaller epidemic sizes, given a fixed global transmission rate [House and Keeling, 2011; Miller, 2009]. Nevertheless, the hampering effect of clustering on initial growth rate can be counterbalanced by increasing the transmission rate parameter, in which case, larger C results in larger final epidemic sizes [Lentz *et al.*, 2012].

**Community structure.** *A network is said to show community structure if it is a loosely connected set of tightly connected nodes* (Fig. B1a,b). Modularity (**Q**) is a commonly used measure of community structure. Greater Q can lead to a smaller final epidemic size and peak prevalence [Newman and Girvan, 2004]. Interestingly, it can also increase the total duration of the epidemic [Barthelemy *et al.*, 2005]. In contrast, in traffic-driven epidemic models, community structure accelerates the speed of epidemic propagation [Shao and Jiang, 2012].

Characterising social insect interaction networks for the above-mentioned structural features, and measuring their effect on disease spread over networks will lay a strong basis for the organisational immunity hypothesis (Fig. B1c,d). It will be particularly interesting to determine the effect of the network structure on the “vulnerability” (*i.e.* the probability that a node is reached by a pathogen, if the outbreak starts from a random node) and “criticality” (*i.e.* the reduction in epidemic size if a given node is removed from the network by vaccination or isolation) of particular individuals in the network [Bisset and Marathe, 2009] (Fig. B1c,d).

Static networks with undirected links have provided useful and fruitful models to understand epidemics. However, the relaxation of both conditions has also been explored. Directed links can be important in cases where pathogen transmission is linked to inherently non-symmetric processes, such as food sharing. Furthermore, the field of temporal (or dynamic) networks has emerged to include more realistic time-ordered interactions where the sequence of interactions dictates the paths of disease. Lastly, networks that change in time can change adaptively. The latest studies of epidemiology examine social networks in which nodes can disconnect links as soon as they detect the infection [Bansal *et al.*, 2010].

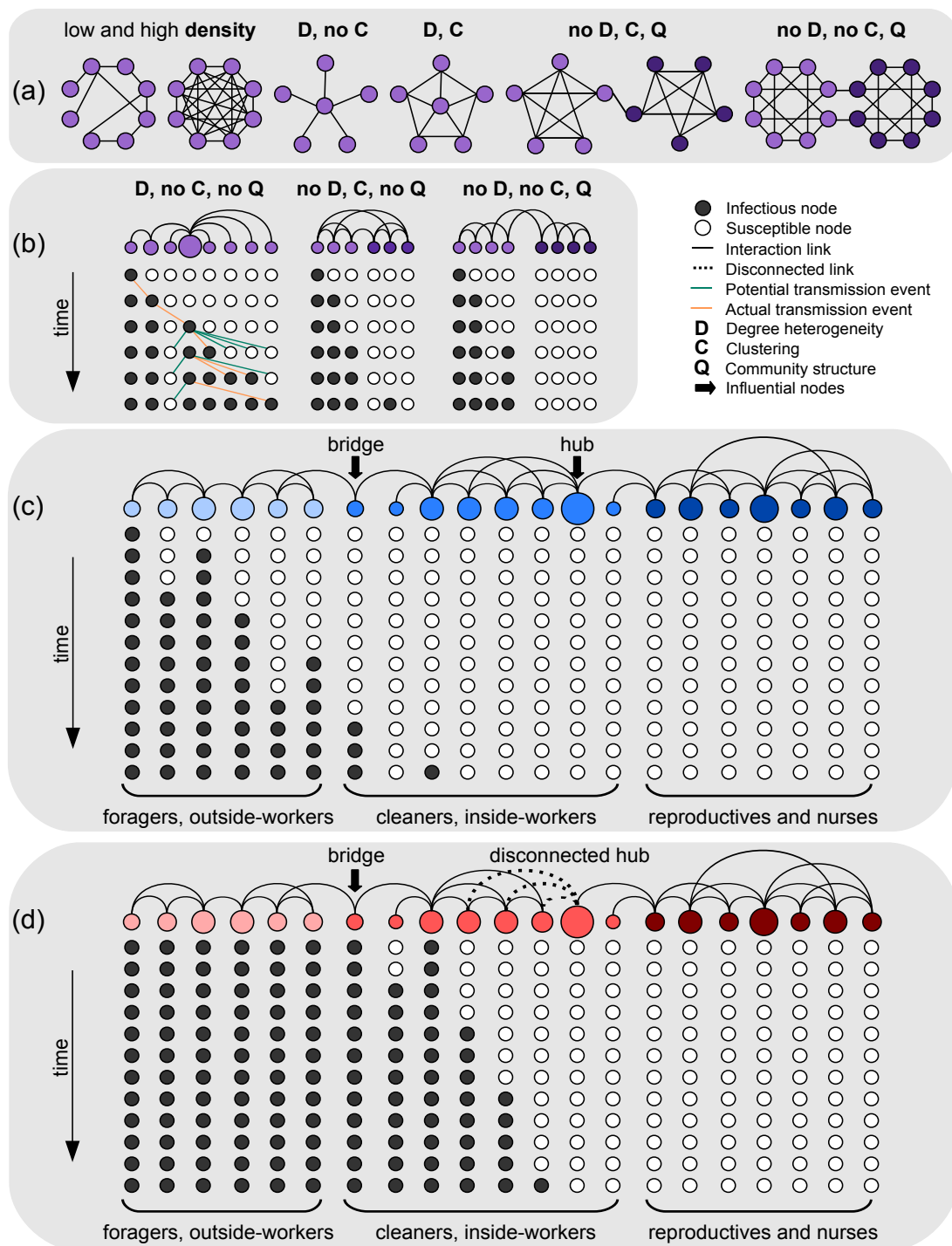


**Figure B1. Network properties and disease spread.** a) Structural features relevant in epidemic spread. (b-d) Epidemic propagation in networks showing different structural features. Nodes coloured according to their disease state: a pathogen may travel, stochastically, from infectious nodes (black circles) to neighbouring susceptible nodes (white circles)(continued...).

**Figure B1. Network properties and disease spread (continued...).** The network is a time-aggregate of all interactions which could lead to transmission (interaction link), yet at each time point, transmission events are possible only from currently infectious to currently susceptible nodes. An explicit epidemic sequence is exemplified (orange lines for actual, turquoise lines for potential transmission events, respectively); notice the fluctuation in the number of possible transmission events (orange + turquoise lines). (b) Degree heterogeneity can lead to the existence of “super-spreaders” which, once infectious, quickly spread the pathogen to a large portion of the group. Clustering leads to susceptible depletion, which slows down spreading. Community structure can confine epidemics inside a single community. (c) Example propagation over a network with three distinct communities and containing high-degree nodes, illustrating a possible configuration of an insect colony; the epidemic is constrained to the outer-most community of foragers for a long time, making it unlikely that the high-valued individuals of the inner-most community become infectious. (d) Example propagation over the same network later in time, illustrating adaptive edge modification, where inside-nest workers cut their links to the community hub (dotted line), when one of their neighbours becomes infectious. Notice that it would also make sense to target a community bridge. In all networks, colour is according to relevance in prophylactic (blue), induced (red), or both types of organisational immunity (purple). Shading marks different communities, and node size signifies degree.

## 2.4 From individual behaviour to interaction patterns

Interaction heterogeneities mediating prophylactic organisational immunity arise from three main factors (Figure 1): spatial organisation of the colony, temporal activity patterns and behavioural modulation of interactions among workers. The effects of spatial segregation on colony compartmentalisation are particularly well established, whereas temporal and interaction modulation effects have been less well studied. Pathogen-induced changes in space use and pairwise interactions have usually been interpreted as adaptive host responses that help contain disease. However, one should note that they could also correspond to side effects of disease and/or immune responses, or even to pathogen manipulation. Whereas studies using non-pathogenic

proxies partially bypass these difficulties [Alaux *et al.*, 2012; Aubert and Richard, 2008; de Souza *et al.*, 2008; Hamilton *et al.*, 2011; Richard *et al.*, 2008; Richard *et al.*, 2012], more investigations of real pathogens attempting to discriminate between these three potential underlying causes [Ugelvig and Cremer, 2007] are required to properly test the induced organisational immunity hypothesis.

### **Spatial segregation**

Spatial heterogeneities arising from division of labour in social insect colonies are a crucial underlying factor of prophylactic organisational immunity. Space-embedded epidemiological models involving explicit spatial constraints indeed showed that spatial structuring *per se* can limit disease spread [Buscarino *et al.*, 2010; Pie *et al.*, 2004; Hagerstrand *et al.*, 2004; Lindholm and Britton, 2007]. In addition, empirical studies of *Temnothorax* ant networks suggested that spatial fidelity of individuals hinders the propagation of spreading agents through the colony, such as food or pathogens, because it results in spatial segregation [Sendova-Franks *et al.*, 2010; Blonder and Dornhaus, 2011]. The effect of spatial segregation on disease spread can be explained because space use strongly influences interaction patterns at both individual and collective levels. For example, ants moving over small areas interact infrequently and form long-lasting associations with a small number of social partners only, whereas mobile individuals have a denser, broader and more homogeneous interaction spectrum [Pinter-Wollman *et al.*, 2011; Jeanson, 2012]. Although the implication of these findings for disease risk was not considered formally, this suggests that the movement characteristics of individuals might affect their likelihood of being exposed to disease. Moreover, in the ant *C. fellah* and in the honeybee, within-colony interaction heterogeneities were shown to emerge solely as the consequence of spatial segregation between groups of individuals [Mersch *et al.*, 2013; Baracchi and Cini, 2014]. Spatial segregation thus appears to be a crucial underlying cause of the social compartmentalisation of the colony into communities, which is believed to greatly contribute to prophylactic organisational immunity.

Spatial segregation is common within social insect colonies, as individuals do not occupy space uniformly, but spend most of their time in small, distinct spatial fidelity zones [Mersch *et al.*, 2013; Naug, 2008; Sendova-Franks and Franks, 1995; See-



ley, 1982; Jandt and Dornhaus, 2009; Baracchi *et al.*, 2010]. Spatial segregation is mainly explained by the strong division of labour characterising most insect societies combined with the existence of spatially distinct nest areas where different tasks are performed [Mersch *et al.*, 2013; Baracchi and Cini, 2014; Seeley, 1982; Jandt and Dornhaus, 2009], and it can be reinforced by specific nest geometries [Pie *et al.*, 2004]. Division of labour and nest spatial structuring contribute to prophylactic organisational immunity in two main aspects. First, they decrease the spatial overlap between age groups, differing both in their value for the colony and in their potential for infection. This occurs as a direct consequence of age polyethism: as they age, workers in many social insect species shift from inside tasks distant from the nest entrance, such as brood and queen care, to peripheral tasks like food processing and nest maintenance, eventually performing outside-nest tasks at the end of their lives [Mersch *et al.*, 2013; Scholl and Naug, 2011; Seeley, 1982]. Second, they ensure the spatial isolation of workers performing high disease risk tasks. For example, in the leaf-cutter ant *Atta colombica*, waste is kept in separate nest chambers in which waste heap workers are confined, decreasing their rate of contacts with fungus garden workers [Hart and Ratnieks, 2001].

Since spatial heterogeneities can lead to prophylactic organisational immunity, induced organisational immunity could be mediated by an increase in spatial segregation between potentially infectious and healthy individuals. Such spatial changes have been repeatedly shown to occur upon pathogen exposure, although their effect on colony-level disease spread has not been studied formally. In many cases, pathogen exposure leads to the complete exclusion of exposed individuals. For example, ants exposed to an entomopathogenic fungus voluntarily leave the nest, a behaviour known as 'self-removal' [Ugelvig and Cremer, 2007; Heinze and Walter, 2010; Bos *et al.*, 2012] (see [Heinze and Walter, 2010; Rueppell *et al.*, 2010] for a general effect of health condition on self-removal). Moreover, diseased individuals are sometimes actively excluded by their nestmates: in termites, nematode-infected individuals are walled in [Cremer *et al.*, 2007], whereas in the honeybee, infected workers are declined entrance [Cremer *et al.*, 2007] or dragged out of the hive [Baracchi *et al.*, 2012]. Certain species have evolved devoted communication channels to respond to pathogen threat: upon contact with contaminated substrates, workers of the termite *Zootermopsis angusticollis* pro-

duce vibrational alarm signals triggering escape behaviour in unexposed nestmates [Rosengaus *et al.*, 1999]. In other cases, spatial segregation is increased indirectly, via a decrease in mobility [Aubert and Richard, 2008] or changes in the task repertoire of exposed workers. For example, *Pogonomyrmex barbatus* ants are more likely to perform waste work if they interact more frequently with waste workers [Gordon and Mehdiabadi, 1999]. In ants and honeybees, workers subjected to pathogen exposure or immune stimulation stop tending the queen and brood [Alaux *et al.*, 2012; Ugelvig and Cremer, 2007; Bos *et al.*, 2012; Wang and Moeller, 1970] and switch to outdoors tasks like foraging or defence against intruders [Woyciechowski and Moron, 2009; Alaux *et al.*, 2012; Bos *et al.*, 2012; Wang and Moeller, 1970; Dussaubat *et al.*, 2013; Goblirsch *et al.*, 2013], thereby increasing their distance to valuable individuals. In honeybees infected by microsporidians of the genus *Nosema*, these behavioural changes are concomitant with physiological changes, including an above normal increase in production of Ethyl Oleate (EO) by infected workers [Dussaubat *et al.*, 2010; Dussaubat *et al.*, 2013]. EO is a pheromone that inhibits the behavioural maturation of in-hive workers [Leoncini *et al.*, 2004]. This leads to the testable hypothesis that in addition to becoming early foragers [Woyciechowski and Moron, 2009; Wang and Moeller, 1970; Dussaubat *et al.*, 2013; Goblirsch *et al.*, 2013], *Nosema*-infected workers may also delay the onset of foraging in their healthy nestmates. Such social readjustment could be beneficial for infected colonies, because it would both decrease the spatial overlap of healthy with infected workers and delay the draining of the nursing force induced by *Nosema* infection [Khoury *et al.*, 2013].

### 2.4.1 Temporal Heterogeneities

Theory shows that the temporal dynamics of interactions influence disease spread (Section 'Interaction patterns and colony-level disease spread'). Because they contribute to shape the dynamics of interactions within social insect colonies, worker activity rhythms might be an important factor affecting pathogen transmission and might even underlie certain aspects of organisational immunity. Although this hypothesis has received little attention so far, it is supported by one recent empirical study on social networks in the ant *Temnothorax albipennis* (T Richardson and T Gorochofski, un-

published). This study investigated the spread of agents with indirect transmission mode, such as pheromones or pathogens transferred via contaminated substrates, and showed that activity bursts at the colony level hinder agent propagation, because they introduce heterogeneities in the temporal sequence of interactions.

## 2.4.2 Modulation of social contacts

Spatial and temporal aspects of worker activity determine the likelihood of individuals meeting. Upon meeting, individuals can however decide whether or not to prolong their interaction and to initiate closer contact, such as grooming or trophallaxis. Because the duration and closeness of an interaction directly influence pathogen transmission risk, these decisions are expected to have a strong impact on disease spread, although the link between individual behaviour and colony-level disease dynamics remains to be investigated in more detail.

It has been suggested that honeybee workers might modulate social contacts depending on the age of interacting partners, thus reinforcing social segregation between age groups and providing prophylactic organisational immunity [Scholl and Naug, 2011]. Electro-physiological recordings indeed showed that the antennae of old and middle-aged honeybee workers are more sensitive to stimulations with the odour of workers from their own age groups than with the odour of young bees, which could constitute the basis for age-dependent modulation of social contacts. Disentangling the respective roles of spatial segregation and individual decisions in generating age-based interaction biases will be crucial in determining the importance of behavioural modulation in mediating organisational immunity.

In ants and in the honeybee, pathogen exposure is known to trigger changes in interaction frequencies among workers, although it is still unclear whether these changes constitute the basis for induced organisational immunity. There have been multiple reports of either increases [de Souza *et al.*, 2008; Hamilton *et al.*, 2011] or decreases [Aubert and Richard, 2008; Bos *et al.*, 2012; Naug and Gibbs, 2009] in the frequency of trophallaxis involving pathogen-exposed or immune-stimulated workers (but see [Konrad *et al.*, 2012]). In honeybees, *Nosema*-infected workers both increase their food intake and decrease their willingness to share food with nestmates [Naug and Gibbs,

2009]. They may therefore turn into 'sinks' in the trophallaxis network of the colony, because they have higher incoming than outgoing food flow. It was hypothesised that this may help contain disease by decreasing pathogen transmission risk from infected to healthy workers. Moreover, grooming of treated workers has been consistently reported to increase following pathogen exposure or immune stimulation in ants, termites and honeybees [Aubert and Richard, 2008; Richard *et al.*, 2008; Richard *et al.*, 2012; Bos *et al.*, 2012; Konrad *et al.*, 2012; Hughes *et al.*, 2002; Walker and Hughes, 2009; Reber *et al.*, 2011; Rosengaus *et al.*, 1998a] (but see [de Souza *et al.*, 2008]). While grooming reduces the infection risk of pathogen-exposed individuals via mechanical removal of infectious particles from their body surface [Hughes *et al.*, 2002; Rosengaus *et al.*, 1998a], sometimes combined with chemical disinfection [Tragust *et al.*, 2013], it also increases the risk of pathogen transmission to the grooming individuals [Konrad *et al.*, 2012; Hughes *et al.*, 2002]. The effects of increased grooming of infectious workers on colony-level epidemic size are still unknown, either because pathogen transmission was not monitored or because the groups studied involved too few individuals (Table 1). Colony-level pathogen spread could be either enhanced or hindered depending, for example, on the number, identity and degree of specialisation of the grooming workers, and these parameters should be considered in future studies. It should be noted that grooming workers usually show no or little increase in mortality [Konrad *et al.*, 2012; Hughes *et al.*, 2002; Rosengaus *et al.*, 1998a], and that social contact with infectious workers can instead confer protection against later exposure to the same pathogen via social immunisation [Hamilton *et al.*, 2011; Ugelvig and Cremer, 2007; Konrad *et al.*, 2012; Traniello *et al.*, 2002]. Transmission of low numbers of pathogenic propagules may therefore not be harmful to the host in certain host-pathogen systems [Konrad *et al.*, 2012]. It would be interesting to test whether colonies show more drastic changes in individual behaviour and collective organisation when exposed to more virulent pathogens.

## 2.5 Conclusions

Despite its recent formulation, the organisational immunity hypothesis has already stimulated many studies (Table 1). However, study effort has been taxonomically uneven,

with disproportionately more work on bees and ants than on wasps and termites. In addition, group-level and individual-level approaches have not been equally applied in studies of prophylactic versus induced organisational immunity. On one hand, many studies investigated interaction networks in healthy colonies, revealing potential baseline pathways for transmission, although these have rarely been confirmed by the tracking of real, non-pathogenic proxies. On the other hand, behavioural changes induced by pathogen exposure have been mostly studied in small groups, and their effects on overall network structure and colony-level transmission dynamics are yet unclear. Studies investigating further the interplay between individual and collective processes, and confirming group-level dynamics by physically tracking real pathogens or non-pathogenic proxies, are therefore called for. A particularly interesting avenue for research would be to investigate how colony size might influence the manifestation and effectiveness of organisational immunity.

We believe that empirical studies of organisational immunity would also benefit from a tighter connection with theory. Epidemiology has generated many useful analytical tools and testable predictions that are usually not exploited to their full potential in empirical work. In addition, theory may help understand the idiosyncrasies of specific host-pathogen systems: different interaction networks underlie the spread of pathogens with different transmission modes, and this should influence both disease spread dynamics and the potential for the host to express organisational immunity. Combining empirical work with models fitted to specific host-pathogen systems is thus likely to be informative.

Understanding the effect of organisational immunity on epidemiology of insect societies poses both technical and theoretical challenges. First, studies on whole colonies have been rare, due to the technical difficulties of tracking a large number of individuals. However, automated approaches overcoming this constraint are becoming increasingly available (reviewed in [Charbonneau *et al.*, 2013]). Second, choosing appropriate null models in theoretical studies can be challenging. Third, the empirical establishment of constitutive transmission pathways in healthy colonies requires the use of non-pathogenic proxies. Choosing an appropriate proxy, having similar transmission properties as real pathogens but inducing no behavioural changes in the host, is not trivial. Fourth, caution is required when interpreting pathogen-induced behavi-

oural changes, since they can reflect pathogen manipulation or disease side-effects rather than host adaptation. Finally, it should be noted that pathogen transmission *per se* does not necessarily reflect disease spread, since transmission of low pathogen levels across the network can sometimes confer reduced susceptibility to disease by social immunisation [Konrad *et al.*, 2012]. This highlights the necessity to study the effects of pathogen transmission on the host in detail and to incorporate immunisation effects into epidemiological models.

## 2.6 Acknowledgements

We thank Tom Richardson and Line V. Ugelvig for discussion and the Social Immunity Team at IST Austria for comments on the manuscript. S.C. and N.S. acknowledge funding by the European Research Council by an ERC Starting Grant (Social Vaccines, no. 243071, to S.C.) and an ERC Advanced Grant (Social Life, no. 249375, to Laurent Keller), respectively.

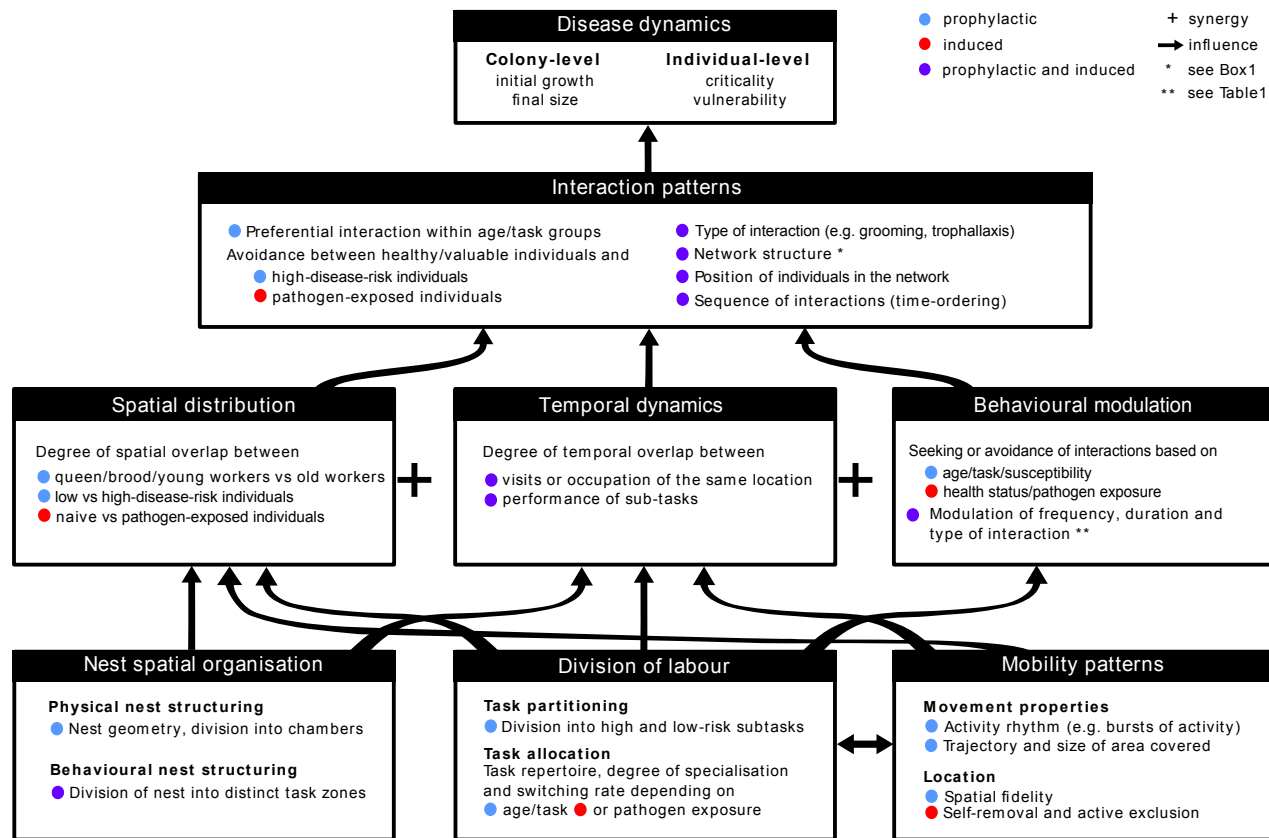


Figure 2.1: **Mechanisms of organisational immunity in insect societies.** The diagram identifies collective and individual properties influencing group-level disease spread and their mutual interdependence. Properties known to play a role in prophylactic, induced, or both prophylactic and induced organisational immunity are shown in blue, red, and purple, respectively.

Table 2.1: **Agent-based models and empirical studies of organisational immunity in social insects.** For each study, the host species and (if relevant) the pathogen or non-pathogenic proxy considered are given, as well as the individual behaviour(s) studied, the size of experimental groups, and a mention of whether the authors formally investigated interaction patterns, whether they monitored the propagation of pathogens, non-pathogenic proxies, or information through the group, and whether experimental controls and/or theoretical null models were used. For studies involving pathogen-exposure or immune-stimulation of individuals, we provide the number of treated individuals first, followed by the number of non-treated individuals in each experimental group (e.g. '1 + 5 workers' means 1 treated worker put in contact with 5 untreated nestmates). In these studies pairs workers were inferred to be interacting if they were close to one another (spatial proximity); if they were close to one another and facing one another (spatial configuration); or if they were observed at the same location at the same or different times (spatial coincidence).

Prophylactic organisational immunity in insect societies								
Interaction patterns and group-level transmission: cellular automata models								
Naug & Smith 2002	model social insect	∅	contact	<300 workers	interaction bias btw. 2 worker classes	group-level spread modelled	homogeneous null model	
Pie et al 2004	model social insect	∅	contact	<1000 workers	spatial heterogeneities	group-level spread modelled	null model	
Fefferman et al 2007	model social insect	∅	contact ; allogrooming	<1200 workers	spatial heterogeneities	group-level spread modelled	null model	
Interaction patterns and group-level transmission: empirical studies								
Naug & Smith 2007	honeybee <i>Apis mellifera</i>	microbeads	trophallaxis	observation hive (c. 4000 individuals)	frequency & duration of trophallaxis	group-level spread physically tracked	no	
Naug 2008	honeybee <i>Apis mellifera</i>	∅	trophallaxis	observation hive (c. 1000 individuals)	static network analysis	no	no	
Feigenbaum & Naug 2010	honeybee <i>Apis mellifera</i>	radioactive food	food transfer	observation hive (c. 5000 individuals)	no	group-level spread physically tracked	no	
Scholl & Naug 2011	honeybee <i>Apis mellifera</i>	∅	trophallaxis ; antennal contacts	observation hive (c.1500 individuals)	contact frequencies	no	no	



Study	Host	Pathogen	Behaviour studied	Group size	Interaction patterns investigated	Transmission monitored	Null model / control
Baracchi & Cini 2014	honeybee <i>Apis mellifera</i>	∅	spatial proximity <sup>a</sup>	worker subset (n = 300) from observation hive (c. 4000 workers)	static network analysis	no	no
Sendova-Franks et al 2010	ant <i>Temnothorax albipennis</i>	food	trophallaxis	whole colony (lab)(42-95 individuals)	static network analysis	group-level spread inferred from trophallaxis duration	no
Blonder & Dornhaus 2011	ant <i>Temnothorax rugatulus</i>	∅	antennal contacts	whole colony (lab)(6-90 individuals)	static & dynamical network analysis	group-level spread modelled	null model for spread
Pinter-Wollman 2011	ant <i>Pogonomyrmex barbatus</i>	∅	spatial proximity <sup>a</sup>	entrance chamber of whole colony (lab) (<131 workers)	static network analysis	group-level spread modelled	null models for spread
Jeanson 2012	ant <i>Odontomachus hastatus</i>	∅	spatial proximity <sup>a</sup>	worker subsets (n= 55-58) from field colony (c. 300 individuals)	static network analysis	no	no
Mersch et al 2013	ant <i>Camponotus fellah</i>	∅	spatial configuration <sup>a</sup>	whole colony (lab) (122-192 individuals)	static network analysis	group-level spread modelled	no null model for spread, but see below
Quevillon et al 2014	ant <i>Camponotus pennsylvanicus</i>	∅	trophallaxis	standardised colony (1 queen+75 workers)	static & dynamical network analysis	group-level spread modelled	no
Richardson & Gorochoowski (unpublished)	ant <i>Temnothorax albipennis</i>	∅	spatial coincidence <sup>a</sup>	subset (queen + 14 workers)from lab colonies (47-134 workers)	dynamical network analysis	group-level spread modelled	null models for spread
<b>Heterogeneities in space use leading to spatial segregation</b>							
Seeley 1982	honeybee <i>Apis mellifera</i>	∅	spatial segregation	worker subset (n = 100) from observation hive (c. 21000 workers)	no	no	no
Naug 2008	honeybee <i>Apis mellifera</i>	∅	spatial segregation	observation hive (c. 1000 workers)	static network analysis	no	no
Baracchi & Cini 2014	honeybee <i>Apis mellifera</i>	∅	spatial fidelity	worker subset (n = 300) from observation hive (c. 4000 workers)	static network analysis	no	no
Jandt & Dornhaus 2009	bumblebee <i>Bombus impatiens</i>	∅	spatial fidelity	whole colony (lab) (90-154 individuals)	no	no	no
Sendova-Franks & Franks 1995	ant <i>Temnothorax unifasciatus</i>	∅	spatial fidelity	whole colony (lab) (28-165 individuals)	no	no	no
Sendova-Franks et al 2010	ant <i>Temnothorax albipennis</i>	food	spatial segregation	whole colony (lab)(42-95 individuals)	static network analysis	group-level spread inferred	no

Study	Host	Pathogen	Behaviour studied	Group size	Interaction patterns investigated	Transmission monitored	Null model / control
Jeanson 2012	ant <i>Odotonmachus hastatus</i>	∅	mobility	worker subsets (n= 55-58) from field colony (c. 300 individuals)	static network analysis	no	no
Mersch et al 2013	ant <i>Camponotus fellah</i>	∅	spatial fidelity	whole colony (lab) (122-192 individuals)	static network analysis	group-level spread modelled	null model for spatial fidelity
Quevillon et al 2014	ant <i>Camponotus pennsylvanicus</i>	∅	mobility	standardised colony (1 queen+75 workers)	static & dynamical network analysis	group-level spread modelled	no
Baracchi et al 2010	wasp <i>Polistes dominulus</i>	∅	spatial fidelity	lab and field colonies (9-20 individuals)	no	no	no
<b>High-pathogen risk tasks: specialisation &amp;/or spatial isolation</b>							
Arathi et al 2000	honeybee <i>Apis mellifera</i>	freeze-killed brood	hygienic behaviour	observation hive (c. 3500 individuals)	no	no	no
Gordon & Mehdiabadi 1999	ant <i>Pogonomyrmex barbatus</i>	∅	waste management	whole colony (lab)(500-1500 individuals)	yes	no	no
Hart & Ratnieks 2001	ant <i>Atta cephalotes</i>	∅	waste management	whole colony (lab)(1-3.104 individuals)	no	no	no
Hart & Ratnieks 2002	ant <i>Atta colombica</i>	∅	waste management	whole colony (field)(103-106 individuals)	no	no	no
<b>Recognition mechanisms and interaction heterogeneities</b>							
Scholl & Naug 2011	honeybee <i>Apis mellifera</i>	∅	responsiveness to age-specific CHC	observation hive (c.1500 workers)	contact frequencies	no	no
Hart & Ratnieks 2001	ant <i>Atta cephalotes</i>	∅	aggression towards waste workers	whole colony (lab)(1-3.104 individuals)	no	no	no
<b>Induced organisational immunity in insect societies</b>							
<b>Interaction patterns and group-level transmission: empirical studies</b>							
Otterstatter & Thomson 2007	bumblebee <i>Bombus impatiens</i>	protozoan <i>Crithidia bombi</i>	all contacts	incipient colonies (1 queen + 4-6 workers)	static network analysis	group-level spread physically tracked	no
<b>Modulation of interactions with pathogen-exposed individuals</b>							
Richard et al 2008	honeybee <i>Apis mellifera</i>	immune stimulation (LPS injection)	locomotion ; all contacts	1 + 10 workers	no	no	sham handling ; saline injection
Naug & Gibbs 2009	honeybee <i>Apis mellifera</i>	microsporidian <i>Nosema ceranae</i>	trophallaxis	2 workers	no	no	sucrose control

Study	Host	Pathogen	Behaviour studied	Group size	Interaction patterns investigated	Transmission monitored	Null model / control
Richard et al 2012	honeybee <i>Apis mellifera</i>	immune stimulation (injection of freeze-killed bacteria <i>Escherichia coli</i> ; bead injection)	locomotion ; all contacts	1 + 10 workers	no	no	sham handling ; saline injection
Hughes et al 2002	ant <i>Acromyrmex echinator</i>	fungus <i>Metarhizium anisopliae</i>	transmission ; survival	1 worker ; 1 + 2-5 workers	no	transmission to nestmates	Triton X application
Aubert & Richard 2008	ant <i>Formica polyctena</i>	immune stimulation (LPS injection)	locomotion ; all contacts	1 + 10 workers	no	no	sham handling ; saline injection
de Souza et al 2008	ant <i>Camponotus fellah</i>	immune stimulation (PGN injection)	allogrooming ; trophallaxis	2 workers ; 1 + 1 workers	no	no	Ringer injection
Walker & Hughes 2009	ant <i>Acromyrmex echinator</i>	fungus <i>Metarhizium anisopliae</i>	allogrooming	4-6 + 21 workers	no	transmission to nestmates	Triton X application
Bos et al 2011	ant <i>Camponotus aethiops</i>	fungus <i>Metarhizium brunneum</i>	allogrooming ; trophallaxis	5 + 42-45 workers	no	no	Triton X application
Hamilton et al 2011	ant <i>Camponotus pennsylvanicus</i>	bacteria <i>Serratia marcescens</i> ; immune stimulation (LPS injection)	trophallaxis	2 workers ; 1 + 1 workers	no	no	Ringer injection
Reber et al 2011	ant <i>Formica selysi</i>	fungus <i>Metarhizium anisopliae</i>	allogrooming	11 workers ; 1-2 + 3-28 workers	no	transmission to nestmates	Tween-20 application
Konrad et al 2012	ant <i>Lasius neglectus</i>	fungus <i>Metarhizium anisopliae</i>	allogrooming	1 + 5 workers	no	transmission to nestmates	Triton X application
Rosengaus et al 1998	termite <i>Zootermopsis angusticollis</i>	fungus <i>Metarhizium anisopliae</i>	allogrooming	1-25 workers; 5 + 10 workers	no	transmission to nestmates	Tween-80 application
<b>Spatial exclusion of pathogen-exposed or moribund individuals</b>							
Rueppell et al. 2010	honeybee <i>Apis mellifera</i>	CO2 exposure ; hydroxyurea injection	self-removal	observation hive (c.1500 individuals)	no	group-level spread modelled	null model
Baracchi et al 2012	honeybee <i>Apis mellifera</i>	deformed wing virus	enforced exclusion	observation hive (c. 3000 individuals)	no	no	healthy control
Ugelvig et al 2007	ant <i>Lasius neglectus</i>	fungus <i>Metarhizium anisopliae</i>	self-removal	1 + 5 workers	no	no	Triton X application ; UV-killed conidia
Heinze & Walter 2010	ant <i>Temnothorax unifasciatus</i>	fungus <i>Metarhizium anisopliae</i> ;CO2 exposure	self-removal	20 workers; 10 + 10 workers	no	no	natural death
Bos et al 2011	ant <i>Camponotus aethiops</i>	fungus <i>Metarhizium brunneum</i>	self-removal	5 + 42-45 workers	no	no	Triton X application

Study	Host	Pathogen	Behaviour studied	Group size	Interaction patterns investigated	Transmission monitored	Null model / control
Rosengaus et al 1999	termite <i>Zootermopsis angusticollis</i>	fungus <i>Metarhizium anisopliae</i>	alarm behaviour ; escape behaviour	10 + 10 nymphs	no	no	no
<b>Changes in tasks performed by pathogen-exposed individuals</b>							
Wang & Moeller 1970	honeybee <i>Apis mellifera</i>	microsporidian <i>Nosema apis</i>	foraging ; guarding ; queen care	observation hive (c. 2500 individuals)	no	no	healthy control
Woyciechowski & Moron 2009	honeybee <i>Apis mellifera</i>	microsporidian <i>Nosema apis</i> ;CO2 exposure	foraging	observation hive (size unknown)	no	no	sham handling
Alaux et al 2012	honeybee <i>Apis mellifera</i>	immune stimulation (LPS injection)	queen care ; foraging	observation hive (size unknown)	no	no	sham handling ; Ringer injection
Dussaubat et al 2013	honeybee <i>Apis mellifera</i>	microsporidian <i>Nosema ceranae</i>	foraging ; flight activity	observation hive (c. 4500 individuals)	no	no	healthy control
Goblirsch et al 2013	honeybee <i>Apis mellifera</i>	microsporidian <i>Nosema ceranae</i>	foraging	whole colony (field)(size unknown)	no	no	sucrose control
Ugelvig et al 2007	ant <i>Lasius neglectus</i>	fungus <i>Metarhizium anisopliae</i>	brood care	1 + 5 workers	no	no	Triton X application ; UV-killed conidia
Bos et al 2011	ant <i>Camponotus aethiops</i>	fungus <i>Metarhizium brunneum</i>	brood care ; nest defence	5 + 42-45 workers	no	no	Triton X application

## 3 Sanitary care dynamics and pathogen transmission

The work described in this chapter was done in collaboration with Anna V. Grasse, Gašper Tkačik and Sylvia Cremer. The study was designed jointly with SC, data interpretation was performed with GT and SC. I performed the experiment and analyzed the videos together with AVG (50% BCP, 50% AVG). AVG performed the final ddPCR run. I performed preliminary experiments to calibrate the method and design of this experiment (*e.g.* selection of exposure dose, observation period, spore quantification method, etc), and I analyzed the data. Further analysis by Katarína Bod'ová (assistant professor at Comenius University, Department of Mathematical Analysis and Numerical Mathematics) is to be combined with these results for final submission.

### 3.1 Abstract

Eusocial insects show an impressive set of collective solutions to numerous problems, such as sorting and tending brood, gathering and storing food or building and defending a nest. These complex behaviors emerge from social interactions, which often also represent pathways for disease spread. While close and frequent associations can promote epidemics, they can also be the key to their efficient control. Insect societies have accrued a varied repertoire of collective defenses against disease. The mechanical removal of infectious particles via grooming, sometimes complemented by chemical inactivation, is commonplace among eusocials. Here we look at the complete sequence of sanitary behaviors of a small group of ants and the immediate changes triggered by exposure of a couple of individuals with a fungal pathogen. In particular, we investigate how the distribution of pathogen load between the pair of treated indi-

viduals affects the dynamics of sanitary care behavior and pathogen spread among the group. As expected, the allogrooming response is directed towards treated individuals. Moreover, the group preferentially allocates their effort towards an individual with a higher spore load. To estimate the disease consequences of this preference, we separately measured (i) spores acquired on body, (ii) collected in the head and (iii) discarded as pellets, since only the first largely retain their ability to infect. At an individual level, while the time an ant spends grooming an exposed individual and its exposure level predict the number of spores collected in the groomers head, they do not explain the spores acquired on its body. At the group level, while the number of pellets produced depends on the global spore dose, it does not predict nestmate contamination. However, groups with two spore-exposed individuals have a higher rate of contamination than groups with a single exposed, independently of the global spore dose. Concurrently, in groups with two spore-exposed individuals we estimate a higher spore loss (*i.e.* difference between number applied to controls and number recovered from experimental samples). We contend that preferential grooming of individuals with a higher spore load may reduce the loss of spores to the environment, thus limiting the contamination of nestmates by inadvertent pickup. Directed grooming of spore exposed individuals implies a lower-than-expected risk for an individual, and besides reducing the load and infection probability of exposed ants, it protects the colony by minimizing indirect transmission.

## 3.2 Introduction

Across biological systems, one can identify complex collective behaviors which stem from local interactions among the elements that constitute them [Sumpter, 2006]. Eusocial insects provide numerous examples of collective animal behavior [Schmid-Hempel, 2017] which emerge from repeated interactions among members of a colony. Collective behavior is often described as a function of group size [Sumpter, 2006] when the switch towards an output "larger than the sum of its parts" happens above a certain critical size. The size of a colony can reach massive proportions [Burchill and Moreau, 2016] and with a growing number of individuals comes a growing number of interactions between them. Beside the benefits (*e.g.* division of labour [Ferguson-Gow *et al.*,

2014]), numerous interactions predict increased disease transmission [Anderson and May, 1979]. To counter this, social insects have evolved numerous collective strategies against disease, which, on top of their individual defences confer them an added level of protection, termed 'social immunity' [Cremer *et al.*, 2007].

Grooming is commonplace inside the social insect colony. This conspicuous behavior – performed by individuals to themselves (selfgrooming) or to others (allogrooming) – has been extensively studied as a response to pathogens, since it can mechanically remove [Mersch *et al.*, 2013] infectious particles from the surface of an insect, reducing their risk of infection and mortality [Walker and Hughes, 2009]. Individuals resort to selfgrooming in isolation [Okuno *et al.*, 2012; Graystock and Hughes, 2011] but also in a social context [Bos *et al.*, 2012; Theis *et al.*, 2015; Yek *et al.*, 2013] upon direct exposure to pathogenic fungi or when it is present in the environment [Yek *et al.*, 2013].

Allogrooming is common, as well, in the presence of a pathogen, and while it could benefit the exposed individual, it is also assumed to come at a risk of contagion for the groomer. This risk can never be completely avoided, as allogrooming is primary for insect communication and for colony functioning (*e.g.* CHCs exchange and colony odour establishment [van Zweden and D'Ettorre, 2010]). This conflict has drawn much attention, leading to many interesting studies on the effects of grooming and, more generally, of sanitary behavior in colony fitness [Theis *et al.*, 2015; Konrad *et al.*, 2018].

Grooming behaviors can be followed by chemical disinfection [Tragust *et al.*, 2013; Fernández-Marín *et al.*, 2015] through the use of glandular compounds with antimicrobial properties. These can be directly applied (to the nest or to a colony member, sometimes leading to its death [Pull *et al.*, 2018]). Alternatively, they can be collected in the mouth parts and applied via grooming in a controlled manner [Tragust *et al.*, 2013]. The transient deposit of these substances in the mouth parts also disinfects the material collected in them (*e.g.* spores accumulate in the infrabuccal pocket, a sieve tissue, to be discarded in compact neutralized pellets [Tragust *et al.*, 2013]).

When the pathogen is not completely neutralized, its effects depends on many factors. For instance, a small sub-lethal infection can activate the immune system of an individual and provide protection in a second challenge to the same pathogen [Konrad *et al.*, 2012], or it can render an individual more susceptible to a different pathogen [Konrad *et al.*, 2018]. Eusocial insects are known to adjust their sanitary

care according to risk, that is, according to their history of previous exposure [Konrad *et al.*, 2018]. More over, the effects are dose dependent [Graystock and Hughes, 2011; Hughes *et al.*, 2002], and insects are known to respond in a dose-dependent manner (*i.e.* ants [Konrad *et al.*, 2018; Okuno *et al.*, 2012; Currie and Stuart, 2001; Jaccoud *et al.*, 1999] and termites [Reber *et al.*, 2011; Yanagawa *et al.*, 2009]).

Sanitary care can be present in a colony continuously (*i.e.* prophylactically) and modulated upon pathogen presence (*i.e.* to dead [Ugelvig and Cremer, 2007] and live fungal spores [Howard and Tschinkel, 1975; Chultz and Eifert, 2005; Ugelvig *et al.*, 2008]). The exact mechanism that triggers the allogrooming of contaminated individuals is still subject of investigation. One possibility is an active signaling by the compromised individuals (*e.g.* vibratory display [Rosengaus *et al.*, 1998b], chemical changes in the cuticle [Pull *et al.*, 2018]). Another is the detection of chemical cues of pathogen origin (*e.g.* octenol (Ugelvig, L.V., unpublished data).

Social insects seem to sense and respond to pathogens or cues related to their presence, rapidly [Ugelvig *et al.*, 2010]. We do not know whether they gather cues locally (*e.g.* requiring contact) or globally (*e.g.* volatile). Similarly, we do not know if and how they can integrate this pathogen-related information. Insects have astounding sensing and cognitive capabilities, at the individual and colony level underlying all sorts of feats. It is worth examining these capabilities in the context of disease defence.

In this work, we studied the immediate sanitary response of a group of ants upon contamination with a fungal pathogen, as well as the consequences of their behaviors, in terms of pathogen transmission. In particular, we aimed to find out whether ants make use of local cues (*i.e.* sensing their own pathogen load or that of their interacting partner) or rather, use global information (*i.e.* sensing the overall pathogen load) to mount a group response. Moreover, we wanted to explain the emerging collective dynamics from the elementary behaviors of individual ants.

To this end we use the invasive garden ant, *Lasius neglectus* and the generalist insect pathogen *Metarhizium robertsii*, a well-studied host-pathogen system. We obtain the complete sequence of sanitary behaviors of groups of six ants, before (*i.e.* baseline behavior, during thirty minutes) and after treatment (*i.e.* pathogen induced behavior, during ninety minutes). The treatment consisted of taking two ants from the group and applying a high dose (H), a low dose (L), or a pathogen-free solution (T) (*i.e.*



sham control), to yield six combinations (*i.e.* HH, HL, HT, LL,LT and TT) or treatment groups. The high dose contained twice the number of fungal conidiospores than the low dose (*i.e.* H = 2L). In this way, we could compare two groups with the same global dose, but evenly or unevenly distributed among the treated pair (*i.e.* HT vs LL).

We used conidiospores (hereafter, simply referred to as spores) of a strain of *M. robertsii*, containing a plasmid with one of two genes (mRFP or eGFP), targeted for quantification with a high resolution method, ddPCR (See Methods section). Importantly, in treatments with two exposed ants (HH,LL,HL), one ant carried mRFP-labelled spores and the other eGFP-labelled spores. For each ant, we separately estimated the number of spores in their head and on their body, to discriminate between spores collected in their infrabuccal pocket – destined to be chemically inactivated and discarded as pellets – and disease relevant spores – remaining on exposed ants or transmitted to others. The labeled spores allowed us to keep track of the origin of the spores measured on the ants. In addition, we collected and measured spores on the discarded pellets (See Figure 3.1 for a summary of the experimental plan). We lay out the results in four parts. The first three parts present the behavioral response, each in increasing detail. The fourth presents the outcome of the response in terms of spores.

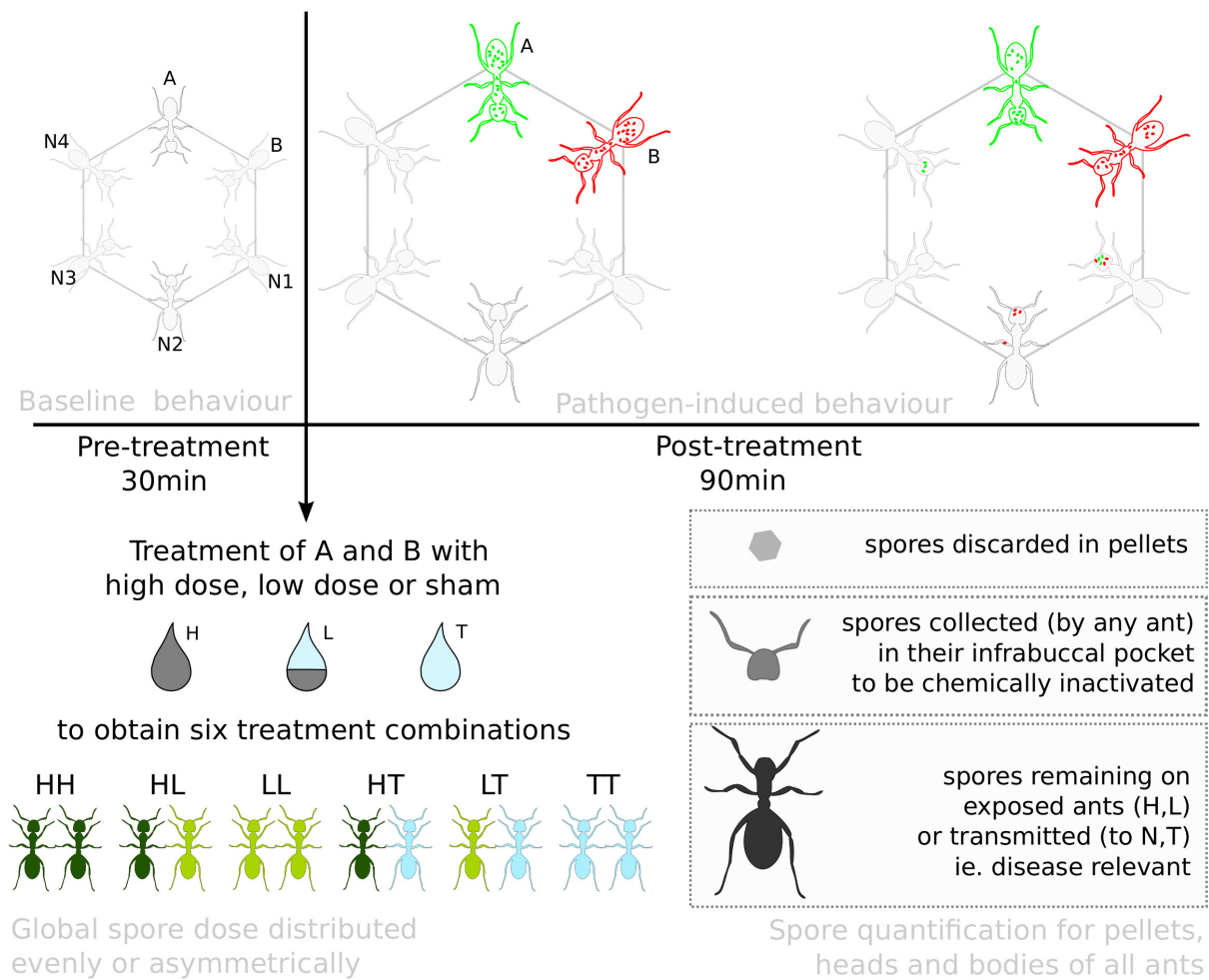


Figure 3.1: Experimental plan. The sanitary behaviors of a group of ants were scored during a 30 minute pre-treatment period to obtain a baseline. Two ants were randomly selected for treatment (A and B) and reintroduced for a second, 90 minute, period of observation. Treatment consisted of applying, to each of A and B, one of two pathogen loads (high and low) or a control (sham), to yield six groups. We used eGFP-labeled spores and mRFP-labeled spores (depicted in bright green and red) of the same fungus (*M. robertsii*). By using two labels, we know from which spore-treated ant the spores came from. We quantified spores from all ants (head and body separately), and from a pool of pellets collected. Spores in ant head samples represent spores collected in the infrabuccal pocket by selfgrooming – in the case of spore-treated ants (H,L) – and allogrooming – in the case of nestmates (N) or sham treated (T), and spore-treated ants when they collect spores from one another (H,L). These would eventually be neutralized and discarded as pellets. On the other hand, spores on the body of ant hold the highest potential to infect.

## 3.3 Results

### 3.3.1 Time-aggregated response

First, we looked at the relative change in the time allocated to a given behavior during the post-treatment period with respect to the time allocated during the pre-treatment period. The unit employed was “effective time” which is the proportion of time spent selfgrooming and performing grooming towards other, but for grooming received, it is the sum allocated by different ants to the receiver (See Method for further detail). We compared spore-contaminated (S) – at this point, disregarding individual dose and treatment group – to sham-treated (T) and untreated nestmates (N).

#### (i) Allogrooming is directed and is modulated by pathogen presence

Both spore-contaminated and sham-treated ants, received more allogrooming (Figure 3.2 A; [paired-Wilcoxon Test] spore-contaminated  $V = 117$ ,  $p < 0.001$ ; sham-treated  $V = 122$ ,  $p < 0.001$ ), while they allocated less time to grooming others (Figure 3.2 B; [paired-Wilcoxon Test] spore-contaminated  $V = 7340$ ,  $p < 0.001$ ; sham-treated  $V = 1854$ ,  $p < 0.001$ ). Conversely, nestmates allocated more time to allogrooming others (Figure 3.2 B; [paired-Wilcoxon Test]  $V = 13179$ ,  $p < 0.001$ ) while they received less (Figure 3.2 A; [paired-Wilcoxon Test]  $V = 62923$ ,  $p < 0.001$ ). Moreover, spore-contaminated ants received more grooming than sham-treated ants. (Figure 3.2 A; [LMER]: LR  $\chi^2 = 16.57$ ,  $df = 1$ ,  $p < 0.001$ ). However, spore-contaminated and sham-treated equally reduced the allogrooming performed (Figure 3.2 B; [LMER]: LR  $\chi^2 = 0.06$ ,  $df = 1$ ,  $p = 0.799$ ).

The allogrooming response of untreated nestmates was elicited by the treatment of their group members and elevated by the presence of the pathogenic spores. This was not necessarily expected, as allogrooming can reduce the load of an individual but lead to transmission of spores to others, and this is likely system dependent (*e.g.* contingent on pathogen infectiousness and the efficiency of host defences [Theis *et al.*, 2015]). Termites seem to consistently groom fungus infected individuals [Rosengaus *et al.*, 1998a; Yanagawa *et al.*, 2011], yet the prediction has not been reported so concurrently for ants. Many studies observed that ants increased their allogrooming

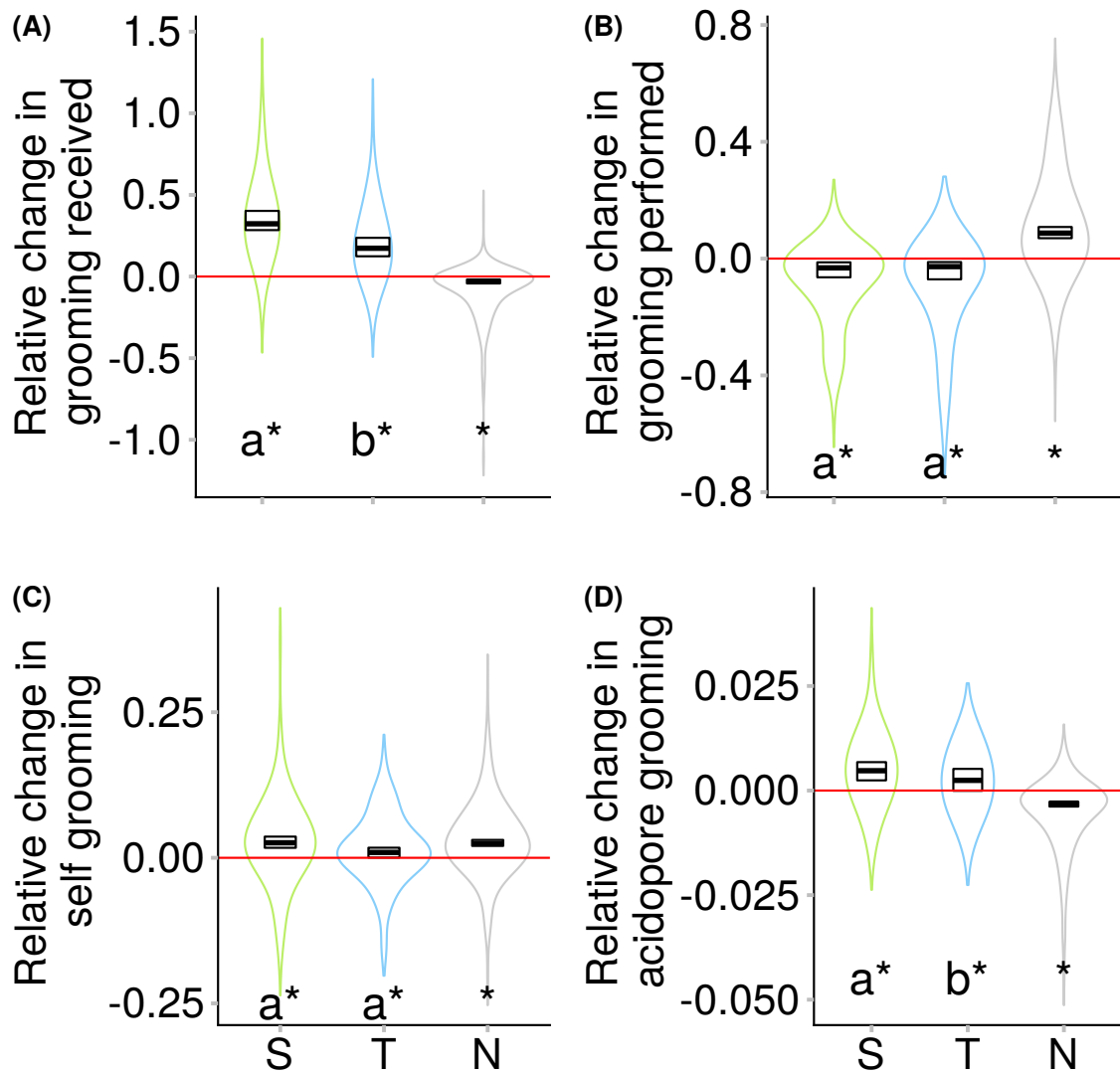


Figure 3.2: Changes in time allocated to grooming, between pre- and post-treatment observation periods. For every ant, we look at the difference in the proportion of time allocated, before and after treatment, to (A) grooming received, (B) grooming performed, (C) selfgrooming and (D) selfgrooming of acidopore. Ants are grouped into spore-contaminated (S; green), sham-treated (T; blue) and untreated nestmates (N; grey) across experimental groups. Spore-contaminated ants are pooled together regardless of individual dose and treatment group (global dose). Shown in boxes are the median and 95% CI, and in outlines are violin plots. The red line denotes no change between pre- and post-treatment periods, and stars denote a significant change in time allocated (paired-Wilcoxon Test, statistics in text). Letters denote the differences between spore and sham-treatment (LMER, statistics in text).

towards infectious individuals [Bos *et al.*, 2012; Walker and Hughes, 2009; Okuno *et al.*, 2012; Yek *et al.*, 2013; Hughes *et al.*, 2002], but some found it unchanged compared to sham-treated ([Theis *et al.*, 2015; Reber *et al.*, 2011; Graystock and Hughes, 2011]).

Most studies have concentrated on the positive effect that allogrooming can have on survival, and tend to report only on the allogrooming received by the exposed individuals. Two studies [Bos *et al.*, 2012; Theis *et al.*, 2015] have looked at allogrooming from the exposed individuals towards their nestmates and found a decrease in the rate of allogrooming rate. Our observations are in line with these studies. Treated ants reduce their allogrooming towards untreated nestmates, and we further add that they do so equally when they are spore-exposed and sham-exposed. This strategy has been suggested to be generally beneficial to reduce transmission [Theis *et al.*, 2015].

### **(ii) Selfgrooming is increased both by treated ants and by their nestmates**

All ants increased the proportion of time they allocated to selfgrooming (Figure 3.2 C; spore-contaminated [paired-Wilcoxon Test],  $V = 2697$ ,  $p < 0.001$ ; sham-treated  $V = 840$ ,  $p = 0.031$ ; nestmates,  $V = 20610$ ,  $p < 0.001$ ) as compared to the pre-treatment phase. We did not find any difference in the magnitude of this increase between groups (Figure 3.2 C; [LMER]: LR  $\chi^2 = 4,49$ ,  $df = 2$ ,  $p = 0.10$ ).

Selfgrooming, as a behavior which removes infectious particles without incurring the risk of transmission is expected from directly exposed ants, as well as, unexposed nestmates after contact with an exposed individual [Theis *et al.*, 2015]. Elevated selfgrooming after direct exposure was previously reported [Bos *et al.*, 2012; Theis *et al.*, 2015; Reber *et al.*, 2011; Okuno *et al.*, 2012; Yek *et al.*, 2013], yet the expectation of elevated selfgrooming of unexposed individuals was not met until now.

### **(iii) Treated ants immediately increased acidopore selfgrooming**

To complement mechanical removal of the spores social insects can chemically neutralize infectious agents. Ants are known to make use of their poison secretions for disinfection (*e.g.* grooming the opening of their metapleural gland [Fernández-Marín *et al.*, 2006] or the joint opening of the Dufour and poison glands, *i.e.* acidopore

[Tragust *et al.*, 2013]. In particular, poison from the acidopore (at the tip of their abdomen) can be taken up into the mouth and redistributed during allogrooming [Tragust *et al.*, 2013]. We recorded selfgrooming of the acidopore, and analyzed it separately from other types of selfgrooming, given its critical function in sanitary care. We found that after exposure, both spore-contaminated and sham-treated ants increased the time they allocated to grooming their acidopore (Figure 3.2 D; [paired-Wilcoxon Test] spore-contaminated,  $V = 1735$ ,  $p < 0.001$ ; sham-treated,  $V = 738$ ,  $p = 0.012$ ). Furthermore, spore-contaminated ants showed a larger increase in acidopore selfgrooming than sham-treated (Figure 3.2 D; [LMER]: LR  $\chi^2 = 4.21$ ,  $df = 1$ ,  $p = 0.041$ ). On the other hand, nestmates decreased the time invested to acidopore selfgrooming (Figure 3.2 D; [paired-Wilcoxon Test] nestmates,  $V = 68407$ ,  $p < 0.001$ ). This is perhaps unexpected, as nestmates benefit from disinfection as well. This could happen if nestmates give priority first to allogrooming during the time frame we observe, but would anyhow later come back to selfgrooming and disinfection. Extending the time frame of our experiment certainly would shed some light to this matter.

#### **(iv) Pellets are produced by all and the number depends on global spore dose**

Pellets contain the spores (and other detritus) collected while grooming in the infrabuccal pocket (a filtering pouch in the head). The spores are combined with poison secretions in the infrabuccal pocket before being disgorged, and their viability is significantly reduced [Tragust *et al.*, 2013; Fernández-Marín *et al.*, 2006]. The production of pellets has drawn relatively little attention as part of the chain of sanitary behaviors (but see [Fernández-Marín *et al.*, 2006]), perhaps due to the small size of the pellets and the difficulty of observing the expulsion. We recorded (whenever visible) the expulsion of pellets.

Over the duration of the experiment no pellets were produced in our control group (TT), whereas pellets were typically produced in most replicates with contaminated ants (with the exception of one HT and three LT replicates). There was no difference in the proportion of replicates which produced pellets, across experimental groups (Fisher's exact test,  $p = 0.1066$ ; no figure shown). We collected all pellets from each dish and found that the total number of pellets disgorged by the group of ants depends on the global spore dose, with more pellets found in groups with a pair of high-dose

contaminated individuals, the least in groups with a single low-dose contaminated individual and none in dishes with a pair of sham-treated individuals (Figure 3.3 A; [KW test],  $H = 33.08$ ,  $df = 4$ ,  $p < 0.001$ ). There was no significant difference in the number of pellets produced by groups of ants in which the same global spore doses was established, but carried either by a single ant or by two (HT and LL, respectively).

We scored pellet expulsion events, whenever visible. Spore-contaminated ants were seen disgorging 30% of the pellets scored in their group (Figure 3.3 B). A single spore-contaminated ant (*e.g.* H in HT) is thus producing the same percentage of pellets than two spore-contaminated ants (*e.g.* both L in LL). One likely explanation for this is that high-dose contaminated ants can produce more pellets than low-dose contaminated ants. This will be addressed in later sections.

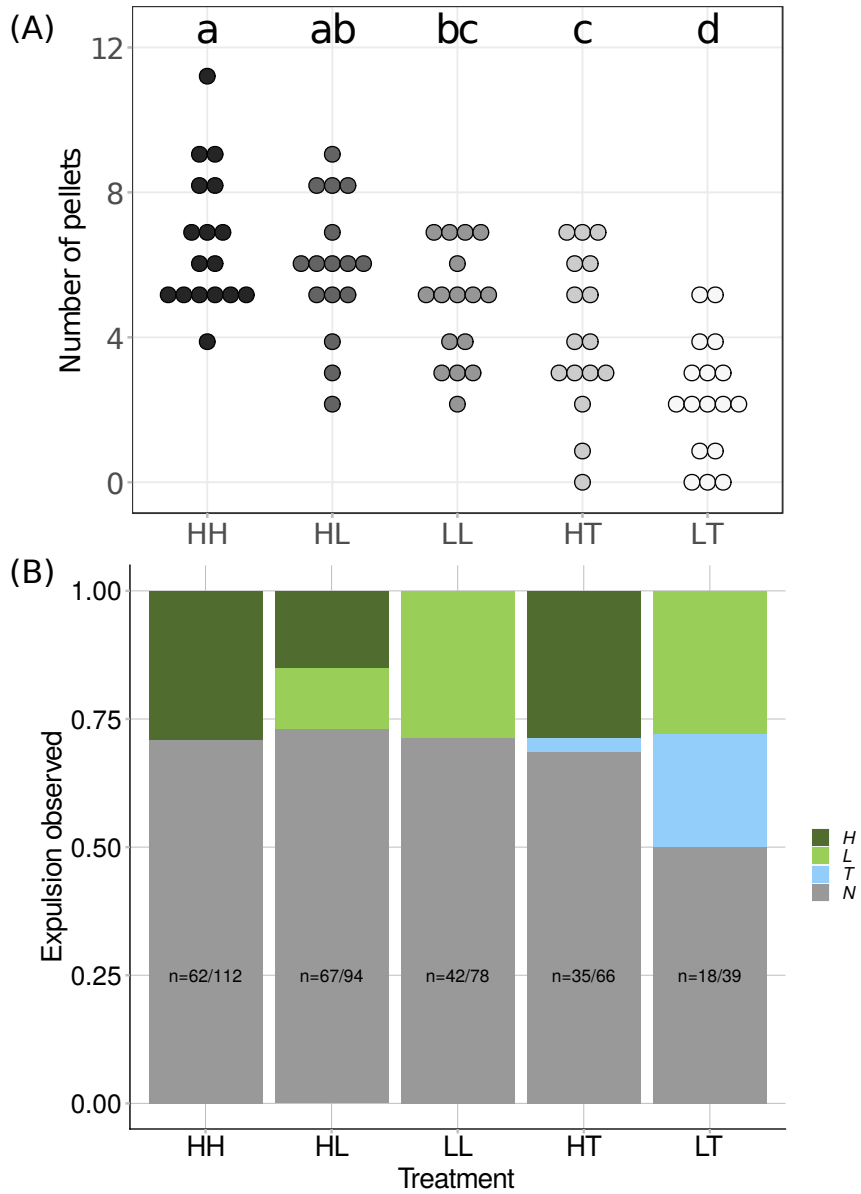


Figure 3.3: Expulsion of pellets. (A) The total number of pellets produced per treatment group, depends on global dose across treatment groups. Letters denote statistical comparisons; groups sharing letters do not differ. (B) Pellets are spit out by both spore-contaminated and non-contaminated individuals. Colors denote the type of ant observed expelling the pellet. The ratio of observed expulsion events / total pellets recovered is also shown.



### 3.3.2 Time-resolved response

Some of the responses that we observe above are localized in time, and now we explore the time-resolved annotations to study the temporal evolution of sanitary behaviors. We first looked at the mean proportion of time allocated to each behaviour by spore-contaminated (S), sham-treated (T) and untreated nestmates (N) with a time-resolution (*i.e.* window size) of three-minutes (Figure 3.4).

#### (i) All behaviors are stationary during pre-exposure

During the observation period previous to exposure, all behaviors are stationary, that is, their mean and variance parameters do not change over time. This observation is relevant to confirm that looking at changes in allocation from pre-exposure baseline (as we did in the previous section) is a valid procedure.

#### (ii) Allogrooming is markedly non-stationary after exposure

After treatment, the allogrooming response – mostly performed by nestmates and received by treated ants – immediately departs from the baseline and reels back to baseline towards the end of the experiment. We first did a coarse-grained exploration of the response, in which we divided the observation period into three equal parts of thirty minutes each. For every ant, we compared its mean allogrooming behaviour during this part (*i.e.* thirty minutes during the post-exposure period), to its mean allogrooming behaviour during the pre-exposure period. We then compared the change (post- minus pre-exposure scores for each ant) across treatment groups. Afterwards, we took a finer-grained, closer look at the first part of the response, which we divided into three phases: Rise (0-3 min) Peak (3-9 min) and Early Fall (9-15 min). (See Figure 3.4 B, where both partitions are depicted)

#### (iii) Allogrooming received depends on spore-presence

After exposure the ants were allowed a few seconds to regain stance, and introduced in quick succession to their group, so that not more than a minute passed between reintroduction and the first recorded behavior. The grooming response (performed by

nestmates and received by treated ants, in Figure 3.4 A-B) peaks very rapidly, within 3 min after reintroduction. The peak of the response lasts only a bit more than 5 minutes before it starts to decay, in an exponential manner. The response trends towards pre-exposure level at the end of the 90 min observation period. Indeed, in the last 30 minutes the grooming performed by the nestmates, no longer differs significantly from pre-exposure scores (Table 3.2).

Spore-contaminated ants receive more grooming than sham-treated, during the first hour after exposure (Figure 3.4 A; Table 3.1). On the other hand, grooming performed by spore-contaminated ants did not differ from sham-treated (Figure 3.4 B; Table 3.2). We further test this observation and its dependence on individual dose and global dose, in a later section (Section 3.3.3).

	First third		Second third		Third third	
	Baseline Comparison paired-Wilcoxon	Pairwise comparisons after Kruskal-Wallis rank sum test $\chi^2 = 171.16$ , df=2, p<0.001	Baseline comparison paired-Wilcoxon	Pairwise comparisons after Kruskal-Wallis rank sum test $\chi^2 = 133.56$ , df=2, p<0.001	Baseline comparison paired-Wilcoxon	Pairwise comparisons after Kruskal-Wallis rank sum test $\chi^2 = 80.78$ , df=2, p<0.001
spore-contaminated	n=131, V=27, p < 0.001	a	V=462, p < 0.001	a	V=1907 p < 0.001	a
sham-treated	n=67, V=34, p < 0.001	b	V=292 p < 0.001	b	V=652 p < 0.01	a
untreated	n=395, V=69383, p < 0.001	c	V=62044 p < 0.001	c	V=57290 p < 0.001	b

Table 3.1: Allogrooming received coarse-grained

#### (iv) Selfgrooming is briefly reduced during peak, but quickly recovers

For simplicity, we considered the same time-partitioning for selfgrooming. Selfgrooming seems to dip below baseline level for all ants during the allogrooming peak, but soon after, exceeds baseline-levels (Figure 3.4 C; Table 3.3). For the first third, we detected no differences between spore-contaminated, sham-treated and untreated nestmates. However, for the second and third period, untreated ants, are self-grooming more than treated ones.

	First third		Second third		Third third	
	Baseline Comparison paired-Wilcoxon	Pairwise comparisons after Kruskal-Wallis rank sum test $\chi^2 = 163.37$ , df=2, p<0.001	Baseline comparison paired-Wilcoxon	Pairwise comparisons after Kruskal-Wallis rank sum test $\chi^2 = 97.81$ , df=2, p<0.001	Baseline comparison paired-Wilcoxon	Pairwise comparisons after Kruskal-Wallis rank sum test $\chi^2 = 18.44$ , df=2, p<0.001
spore-contaminated	V=8187, p < 0.001	a	V=7478 , p < 0.001	a	V=6171 p < 0.001	a
sham-treated	V=2016, p < 0.001	a	V=1805 p < 0.001	a	V=1682 p = 0.001	a
untreated	V=5218, p < 0.001	b	V=21814 p < 0.001	b	V=36882 p = 0.327	b

Table 3.2: Allogrooming performed coarse-grained

	First third		Second third		Third third	
	Baseline Comparison paired-Wilcoxon	Pairwise comparisons after Kruskal-Wallis rank sum test $\chi^2 = 4.59$ , df=2, p=0.10	Baseline comparison paired-Wilcoxon	Pairwise comparisons after Kruskal-Wallis rank sum test $\chi^2 = 8.88$ , df=2, p=0.011	Baseline comparison paired-Wilcoxon	Pairwise comparisons after Kruskal-Wallis rank sum test $\chi^2 = 12.66$ , df=2, p=0.002
spore-contaminated	V=4718, p=0.364	a	V=2248 , p < 0.001	ab	V=131 p < 0.001	a
sham-treated	V=1468, p < 0.05	a	V=792 p < 0.05	a	V=678 < 0.01	a
untreated	V=49688, p < 0.001	a	V=21966 p < 0.001	b	V=15556 p < 0.001	b

Table 3.3: Selfgrooming coarse-grained

### (v) Acidopore selfgrooming is rare and mostly done by treated-ants

Selfgrooming of the acidopore occurs with relatively low frequency (*i.e.* less than 9 seconds per minute) and thus, the average signal appears noisy. Nevertheless, it is evident that throughout the observation period, treated ants increase their acidopore selfgrooming, while nestmates do less of it (Figure 3.2 D and Figure 3.4 D).

	First third		Second third		Third third	
	Baseline Comparison paired-Wilcoxon	Pairwise comparisons after Kruskal-Wallis rank sum test $\chi^2 = 80.01$ , df=2, p<0.001	Baseline comparison paired-Wilcoxon	Pairwise comparisons after Kruskal-Wallis rank sum test $\chi^2 = 83.34$ , df=2, p<0.001	Baseline comparison paired-Wilcoxon	Pairwise comparisons after Kruskal-Wallis rank sum test $\chi^2 = 64.25$ , df=2, p<0.001
spore- contaminated	V=2769, p < 0.001	a	V=1949, p < 0.001	a	V=2235 p < 0.001	a
sham- treated	V=792, p < 0.05	a	V=719 p < 0.01	a	V=1141 p = 0.992	b
untreated	V=70707, p < 0.001	b	V=64365 p < 0.001	b	V=61236 p < 0.001	c

Table 3.4: Acidopore grooming coarse-grained

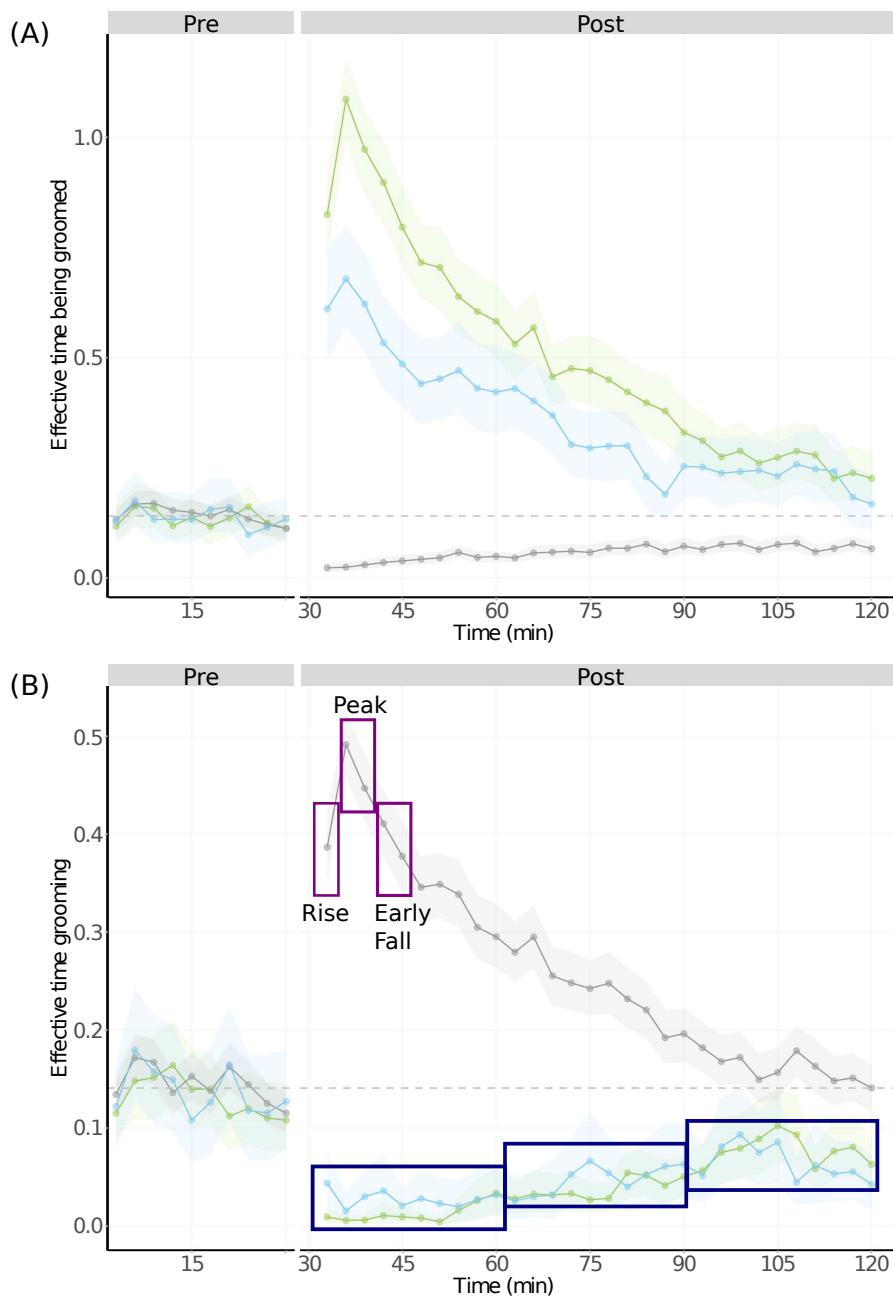


Figure 3.4: Time-resolved behavior before (left) and after (right) treatment. For non overlapping time windows (horizontal axis), the ratio of the total time an ant is (A) performing allogrooming, (B) receiving allogrooming, (C) performing selfgrooming and (D) performing acidopore selfgrooming, over the length of the window (3 minutes), grouped by the treatment of the ant: spore-contaminated (S; green), sham-treated (T; blue) and untreated nestmates (N; grey). We divide the duration of the post treatment observation period into three equally long periods (shown in (B) in dark blue), and identify three periods (shown in (B) in purple), corresponding to the rise, the peak and the early fall of the grooming response. Continued...

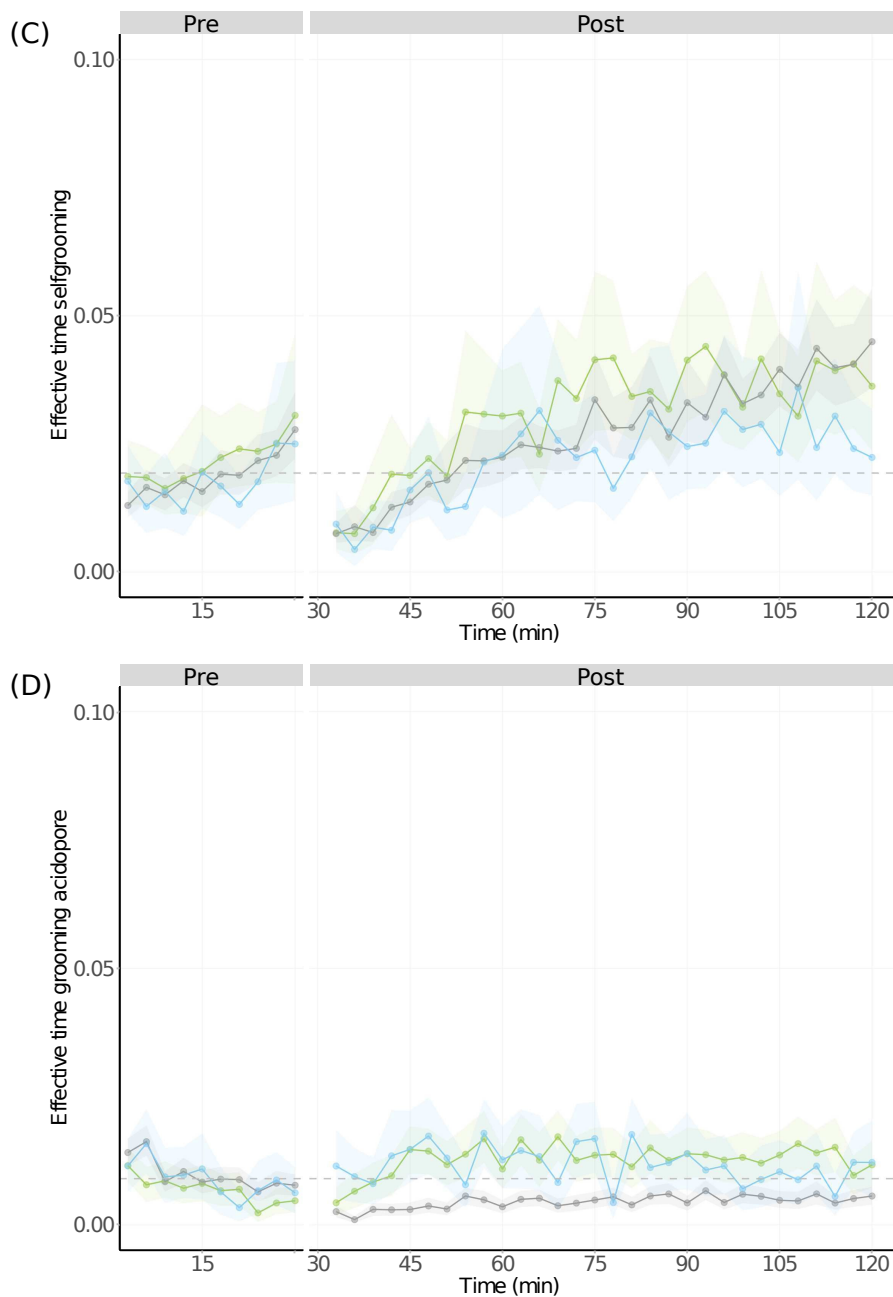


Figure 3.4: (Continued) Effective time is the proportion of time allocated to a given behavior in each window. For selfgrooming and grooming performed, it is simply the proportion of time spent in these states. For grooming received, it is the sum of the time allocated by different ants to the receiver, since one ant can be groomed simultaneously by several ants. The solid lines show the mean effective time grooming, over all ants with a given treatment, per window, and the shaded area the 95% CI of the mean. The dotted line shows the average, over all ants, engaged in each behavior before treatment (*i.e.* the pre-treatment baseline). Statistical comparisons to baseline and between treatment means in Tables 3.1,3.2,3.3 and3.4.

**(vi) Pellet expulsion has a similar time evolution as allogrooming performed**

Not much is known about the production of pellets, except that it is increased after pathogenic exposure [Fernández-Marín *et al.*, 2006]. Pellet expulsion is not a very conspicuous behavior, but we were able to score around half as many events as pellets collected after the experiment. We looked at the timing of these events. The timing distribution of the observed pellet expulsions is similar to that of allogrooming performed by the untreated nestmates, with a fast and sharp rise and an exponential decay. It is slightly shifted to the right, peaking around 15 min after exposure (Figure 3.5 A).

We know the largest part of the pellets were spit by nestmates, so we looked at allogrooming performed by nestmates and timing of pellet expulsion. Nestmates who groom the most in the group (rank = 1 Figure 3.5 B) also spit the most pellets. In particular, we wanted to know how much allogrooming is performed by a nestmate before it produces a pellet. To estimate when grooming for a given pellet begins, we take a look at how much grooming the expelling ant did, between the start of the video and the expulsion of the pellet, then we find the moment in time where the ant had performed half of that grooming (*i.e.* “halftime before pellet” Figure 3.5 C). The amount of time an ant grooms before expelling a pellet varies (Figure 3.5 E), which contrasts with our expectation of a fixed amount of grooming time required to collect spores for a pellet. We think this variation can be determined by the amount of spores present in the groomed ants.

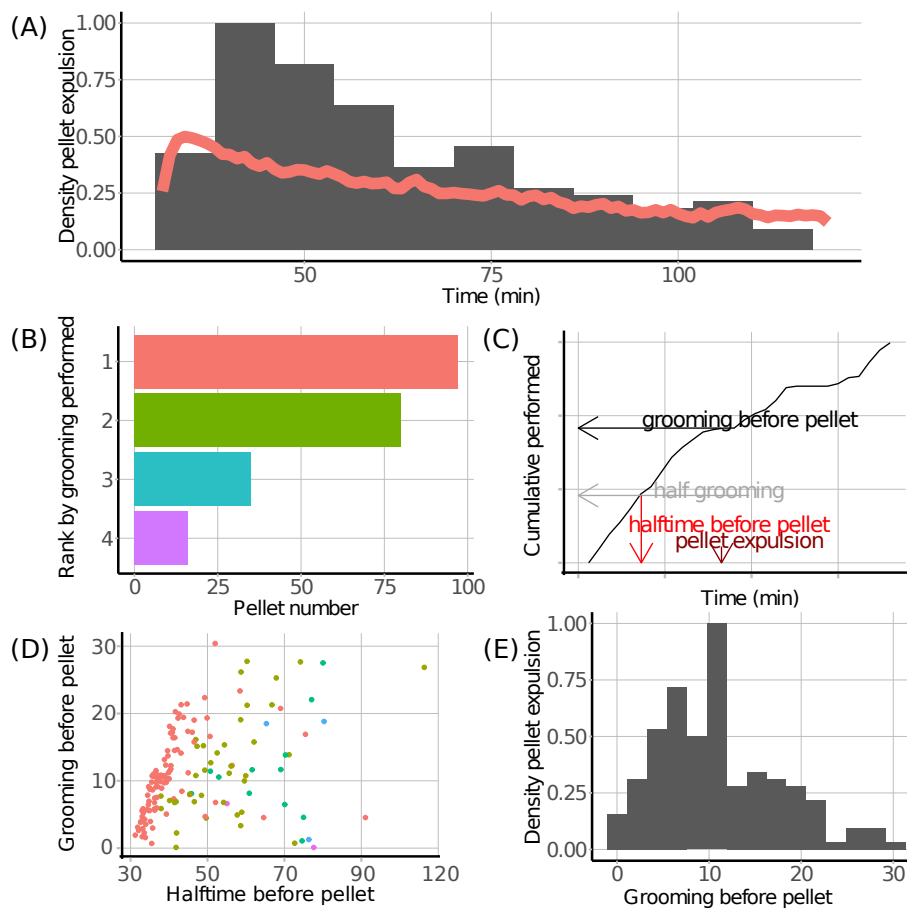


Figure 3.5: Timing of pellet expulsion by nestmates. (A) Distribution in time of expulsion events (grey histogram) compared to nestmate allogrooming response (red line, see Figure 4B) (B) Number of pellets expelled according to grooming rank. Within each dish, the four nestmates are ranked, depending on how much allogrooming they performed. The ants that performed the most grooming in each dish (rank 1) also expelled the most pellets. (C) Halftime before pellet expulsion denotes, for each expulsion event (dark red), the amount of time (bright red) necessary to perform half (light grey) of all the allogrooming performed before the expulsion of the pellet (black). It is a measure of when the allogrooming leading to the expulsion event was performed. The plot is the cumulative allogrooming performed by a randomly chosen nestmate, notice a plateau in allogrooming before expulsion. (D) Amount of allogrooming before each pellet as a function of when it was performed. For each pellet expelled by a nestmate, the amount of allogrooming it performed since its previous expulsion (or the start of observation) was recorded, as was the halftime before that expulsion. Colors denote the first (red), second (green), third (blue) or fourth (purple) pellet expulsion. (E) Amount of allogrooming performed by a nestmate before expelling a pellet.



### 3.3.3 Time-resolved response, a closer look

We look at the very first interaction and then we proceeded to analyze the effects of individual dose (high-dose (H) and low-dose (L) and zero-dose or sham-treated (T), hereafter, often abbreviated for clarity), as well as the effect of global dose. More precisely, we looked at the effect that the treatment of the second ant in the pair has on the response of the first, in other words, the partner dose effect.

#### (i) First interaction is exploratory

We know that spore contaminated ants receive more grooming than sham-treated ants, until both responses go back to baseline. We took a closer look at what happens at the very beginning, to find out whether ants can detect spore-presence from the first interaction, and make a distinction based on individual dose of their interaction partner. For each ant, we looked at the latency to the first allogrooming interaction, the identity of the receiver and the duration. The first allogrooming interaction is not necessarily the first interaction between two ants. For instance, an ant could touch other ants with its antennae (*i.e.* antennation), before it engages in a grooming interaction, potentially recognizing those ants treated by chemical. All ants performed their first observed interaction before six minutes. First, we found that allogrooming another untreated nestmate, at this moment, was infrequent (Figure 3.6 A, missing stats due to problems with model assumptions). Also, the latency to groom a nestmate was higher (Figure 3.6 B) and the duration shorter (Figure 3.6 C [LMER]: LR  $\chi^2 = 19.79$ ,  $df = 3$ ,  $p < 0.001$ ), compared to grooming a treated group member. Thus, nestmates discriminate between untreated and treated individuals, immediately, as the first observed allogrooming interactions are directed towards treated ants rather than untreated nestmates. However, we cannot confirm early discrimination of the pathogen. We conclude that the ants make no immediate discrimination between treated ants. Moreover, we put forth that some “sampling” is needed before nestmates can discriminate the presence of the pathogen, and moreover, get a “global” picture of the pathogen risk.

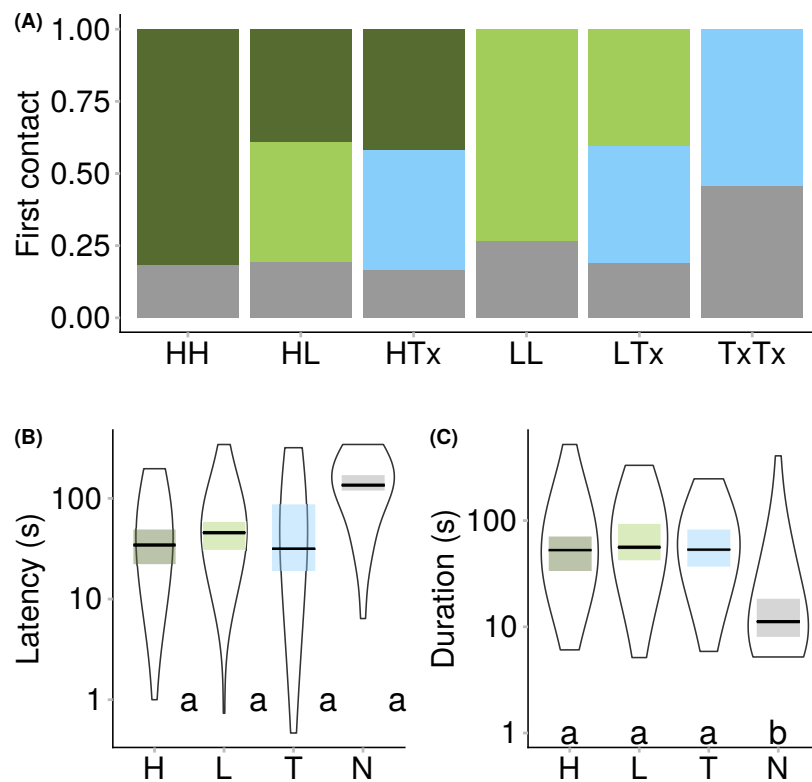


Figure 3.6: First allogrooming interaction. For all nestmates (non-treated individuals), we recorded the recipient of its first allogrooming interaction. (A) Distribution of recipients. Proportion of first allogrooming towards H (dark green), L (light green), sham-treated (blue), or an untreated (grey) ant, grouped by treatment group. (B) Latency. Time to first grooming interaction grouped by recipient treatment. (C) Duration of first grooming interaction, also grouped by recipient treatment (horizontal axis). Shown are the median (black line), 95% CI (shaded boxes), and violin plot outline. Letters denote significant differences between groups after LMER (statistics in text).

### (ii) Allogrooming received depends both on individual and partner dose

We wish to test if nestmates modulate their behavior towards a given infected ant depending on the context, that is, the partner-dose effect. We grouped the ants based on the spore dose given and on their partners dose. We here present the allogrooming response during the peak of the allogrooming response.

At the peak of the grooming response, ants contaminated with a high-dose and paired with sham-treated or low-dose treated (H in HT and HL) are groomed more compared to control treated ants (T in TT). Ants treated with a low-dose and paired with

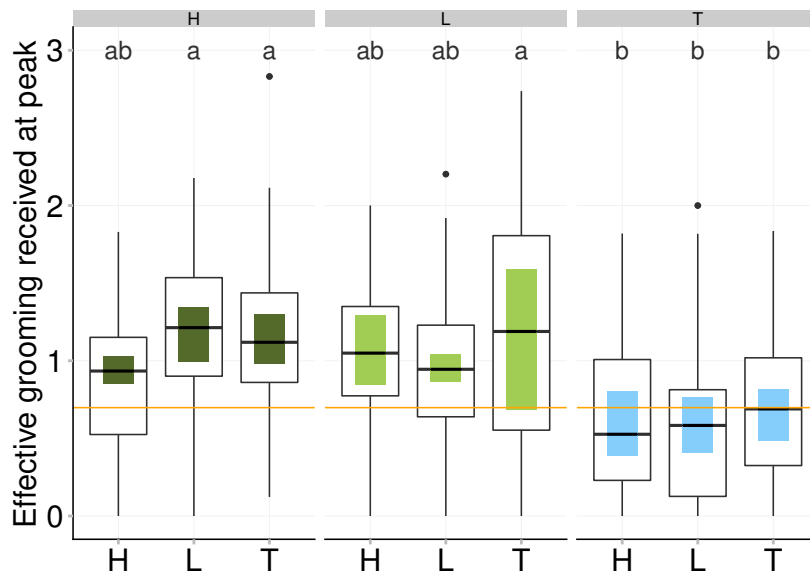


Figure 3.7: Effect of dose given and dose of partner on allogrooming received during peak allogrooming response. Treated ants were grouped by the treatment they received (three panels with grey heading above) and the treatment their partner received (horizontal axis). Data is depicted as boxplots, with shaded boxes for 95% CI around the median. Lettering shows Tukey post hoc comparisons after LMER (statistics in text), groups which do not share letters are significantly different.

sham-treated (L in LT) are also groomed more. Other ants fall in-between (Figure 3.7 [LMER]: LR  $\chi^2 = 32.915$ ,  $df = 8$ ,  $p < 0.001$ , Tukey post hoc comparisons H in HT, H in HL and L in LT vs T in TT,  $p < 0.05$ , all others n.s). We suggest that discrimination is happening and is easier when the contrast between the pair is highest. In other words, when the difference in spore dose given is largest. We further test this preference in the following sections.

### (iii) Instantaneous spore load estimation

We know that spores are effectively removed by allogrooming, thus, the applied spore dose is decreasing with every grooming event. We have a response modulated by a stimulus, which decreases as a result of the response itself. We next explore the predictions of a model where we estimate instantaneous spore load for each exposed individual over time.

We build a spore-decay model to see if the (predicted) instantaneous spore load indeed explains grooming preference throughout the response. Spore load change as a function of selfgrooming and allogrooming received, is best explained using a Michaelis-Menten model. Linear and exponential models were considered, but provided an inferior fit. In such a model, spores( $S$ ) are removed as in Michaelis-Menten kinetics,

$$dS/dt = -vS/(S + K),$$

with constants  $v$  and  $K$ . One can think of an ant as an “enzyme” and spores as the enzyme’s “substrate”. At first, the ant removes spores at a maximum rate  $v$ . The speed of spore reduction is linear. As the spore number is reduced the ant is able to capture less, and the speed of spore removal shrinks exponentially.  $K$ , the dissociation constant gives the transition between the exponential and linear regime. For a number of spores  $S \gg K$ , the equation can be simplified to  $dS/dt \approx -v$ , *i.e.*, linear decay. When  $S \ll K$ ,  $dS/dt \approx -v/KS$ , *i.e.* exponential decay.  $v$  and  $K$  are parameters we fit to experimental data. The parameters are chosen so that the initial distributions of spore loads predicted by the model are as similar as possible to those recovered from exposure controls, as measured by how similar their means and standard deviations are. The stability of these parameter values with respect to the choice of optimization criteria was corroborated by recovering similar values by minimizing the earth movers distance between the distributions.

Below, we compare estimated instantaneous spore loads between pairs of ants. Since all spore load estimations are done using the same model parameters, a sub-optimal fit would lead incorrect estimations, but the distance between two such incorrect estimations would be the same as between two correct ones. Thus, although we have taken great care to do a sensible exploration of the parameter space, the use we are making of the model is tolerant to sub-optimal parameter estimation.

#### **(iv) Implications of the model**

The biological intuition behind this model is that ants remove spores from a contaminated ant at a speed which depends on the number of spores present. When there is plenty of spores they remove at a maximum speed. Speed decreases when spores become more and more difficult to find.

	Experimental	Michaelis-Menten kinetics prediction
median(log(load)) H	12.0078	11.8869
stddev(log(load)) H	0.54688	0.576157
median(log(load)) L	11.4225	11.5039
stddev(log(load)) L	0.57912	0.61598
score	-	0.01301
parameters	-	$v=05.122$ $K=47712.793$

Table 3.5: Spore decay model values. These were found by minimizing, separately for H and L exposure levels, the difference between two distributions of spore loads: that of exposure controls, and that of initial loads estimated using the model.

Ants can remove spores from one another directly by scraping or licking them off with their mouth parts. They can also brush spores from a surface with a stroke of their foreleg [Jander, 1976; Farish, 1972], which they can subsequently clean with their mouth. In both cases, they collect spores and other particulate matter in a flexible filtering pouch inside their mouth, called the infrabuccal pocket [Eisner and Happ, 1962]. We speculate, that ants could be, to some extent, aware of the state of fullness of their infrabuccal pocket. There is room for a positive feedback mechanism – where the ant keeps grooming as long as there are still spores to remove – or a negative feedback – where the ant stops allogrooming to expel a pellet or to continue to groom itself.

#### **(v) Nestmates groom ants with higher instant spore load**

With a model providing the instant spore load per ant at every time point, based on its previous grooming history, see Figure 3.8 for illustration), we can test the hypothesis that the nestmates make a distinction between the two treated ants and preferentially groom individuals currently carrying more spores. We can define preference of the group of nestmates for the ant with a higher load, for each time window. We consider that nestmates ‘choose’ or preferentially groom the treated ant which, we estimate, has a higher spore load in that window, if more than half the grooming time in the window is

allocated to the ant with the higher load, and there are at least 10 seconds of grooming performed towards a treated ant in that window. The 10 second threshold is chosen because no grooming events are smaller than this (duration of a grooming event: min = 10.07, median = 39.7, mean = 57.2, max = 688.6 seconds) and, thus, if a treated ant received less than this grooming in a time window, most of the grooming events are located in an adjacent window. The result is a binary variable, 'nestmates chose higher load or 'do not choose it', per time window. A logistic regression was performed, taking as predictor variable the logarithm of the difference in spore loads.

We found that indeed, nestmates preferentially groom ants with a higher load, with a probability decreasing as the difference in instant spore load between the pair decreases. For a unit increase (or ten-fold increase) in the difference in spore load between treated ants, the probability of grooming the one with higher instant load is given as the Odds Ratio (OR). The OR is highest for spore-contaminated ants paired with sham (*i.e.* HT and LT). This is because ants in these groups are preferentially groomed in the first time windows, when the spore load is highest (see Figure 3.9 A and Table 3.6). We can also visualize the probability for this preference predicted by logistic regression as a function of spore load difference (see Figure 3.9 B).

It must be said, that the difference in spore loads, can reflect the difference in treatment that the ants received (*e.g.* H vs L), but it can also stem from stochastic variation during exposure (*i.e.* the difference in dose between treated ants in HH or LL can largely deviate from zero). Additionally, as one ant receives (both self and allo) grooming for a period of time, the difference between its instantaneous load and that of its partner changes, eventually reversing sign. For this reason, it is not sufficient to study grooming preference, or any other behavior, as a function of the dose the ants were treated with, but instead a model of instantaneous load is very important. Interestingly, the fact that our logistic model predicts a preference for the ant with a higher-dose, in the case of HH suggests that ants really discriminate this differences finely.

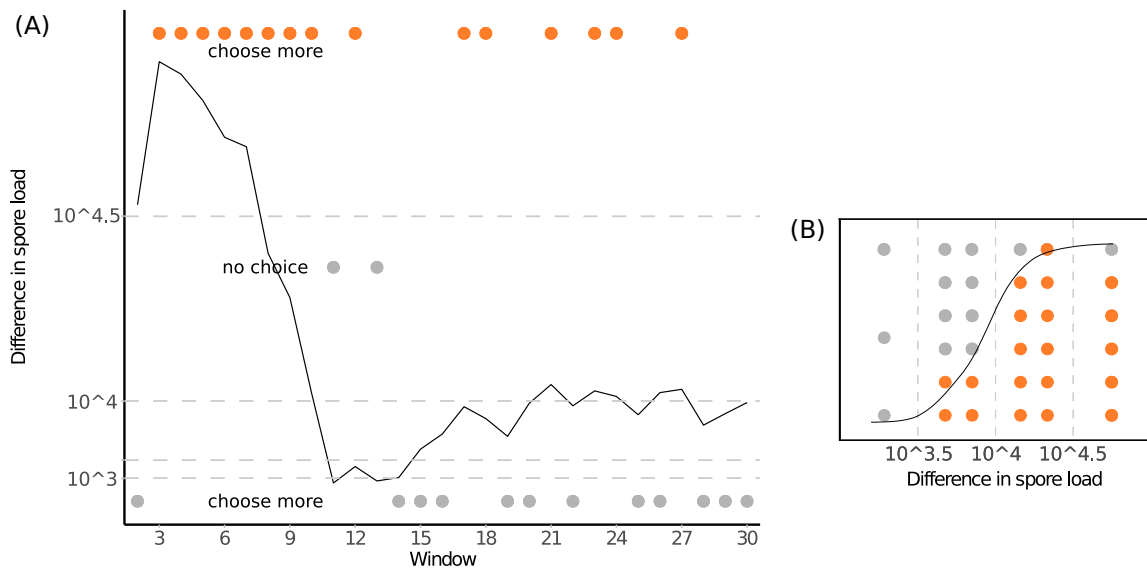


Figure 3.8: Example of grooming choice per window and estimated spore load difference. (A) For each 3 minute time window (horizontal axis) the black line shows the logarithm of the difference in estimated spore loads between the two treated ants. The dots show whether nestmates preferentially groomed the treated ant with higher load (orange, top), chose the one with lower load (gray, bottom) or did not have elements for choice (*i.e.* less than 10 seconds of grooming were performed) (gray, middle). Notice how grooming the ant with higher load diminishes the difference, as spores are removed from it, and, respectively, grooming the ant with smaller load increases the difference. The estimation of instantaneous load was done using a Michaelis-Menten kinetics model (see text). Shown is replicate number 16 from the HL treatment group. (B) For illustration purposes, spore differences were binned into four bins in logarithmic scales (dotted lines in both plots). The number of windows in which the difference in spore load was within a bin and the nestmates preferentially groomed the ant with higher load (orange dots), was fitted with a logistic model.

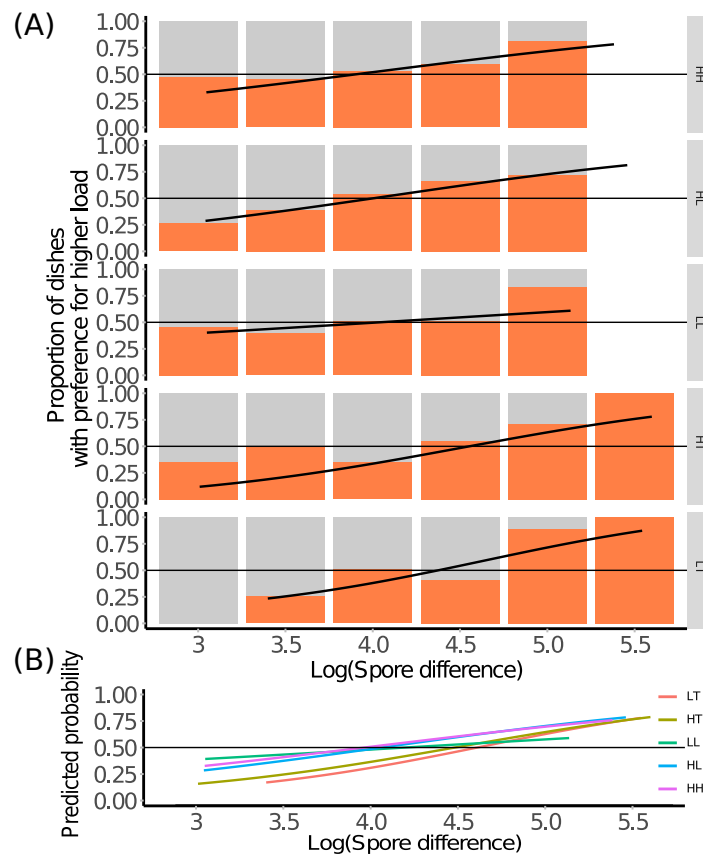


Figure 3.9: Nestmate preference. (A) All 3 minute time windows for all dishes were binned into different ranges of estimated spore-load difference between the two treated ants (x axis). For each bin, the orange bars show the percentage of windows in which the ant with higher spore load was preferentially groomed (see text and Figure 3.8 for details). The dark solid lines show a fit of these points (unbinned) to a logistic model, to predict the probability of the ant with a higher load being preferentially groomed, as a function of the difference in spore loads. The fits for different dish treatments is shown in (B), where it is clear that the probability increases faster in the cases where there is a single treated ant (LT and HT).



Treatment	LOR	OR	$\chi^2$	p	AIC
HH	0.75	2.12	14.8	<0.001	602
HL	0.82	2.27	18.7	<0.001	605
LL	0.39	1.47	2.87	0.09.	600
HT	1.13	3.09	26	<0.001	603
LT	1.37	3.93	37	<0.001	648

Table 3.6: Logistic regression of preference as a function of load difference

### 3.3.4 Outcome of the response in terms of spores

To recall, we exposed two ants per dish to get six treatment groups abbreviated with the combination exposure of the pair as: HH, HL, LL, HT, LT and TT. Low-dose (L) was half of the high-dose (H), by design. Experimentally, there was a considerable deviation from this ratio (H mean 200,478 SEM 3,143, L mean 112,742 SEM 1,428, H / L = 1.78)

We compared the behavior of ants across treatment groups to explore the effect of individual and group (global) dose. In particular, we put to test the hypothesis that the number of spore-contaminated ants, on the condition that the global dose remains the same, can influence the group behavior. Our data reveal that ants preferentially groom individuals contaminated with a higher spore dose, more easily so when the difference in spores is higher. In particular they show this preference earlier, in case the spore-contaminated ant is paired with a sham-treated ant. In essence, even though HT and LL groups have a comparable global dose, the group seems to respond to the individual dose.

In this next section, we assess the consequences of the grooming response, in terms of the number of spores removed from contaminated ants as well as spores transmitted to the nestmates.

#### (i) Spores can circulate through various transmission routes

Spores from the body of a contaminated individual can be collected by selfgrooming in their heads. Specifically, these spores accumulate in a filtering pouch (infrabuccal pockets) where they are mixed with disinfecting secretions, compressed into a pellet and discarded. The spores can be transferred to another ant, either collected by allogrooming or inadvertently transferred during the process. The groomer can, of course, selfgroom and the spores cleaned can be discarded in a pellet, as well.

Spores in pellets and in infrabuccal pouches have reduced germination [Tragust *et al.*, 2013] and pose a relatively negligible risk, as compared to spores remaining on the ants bodies, which hold the potential to infect. A third transmission pathway is shedding or loss to the substrate and inadvertent pickup by a passerby (See Figure 3.10. Spore transmission routes, for a simple depiction of this routes).

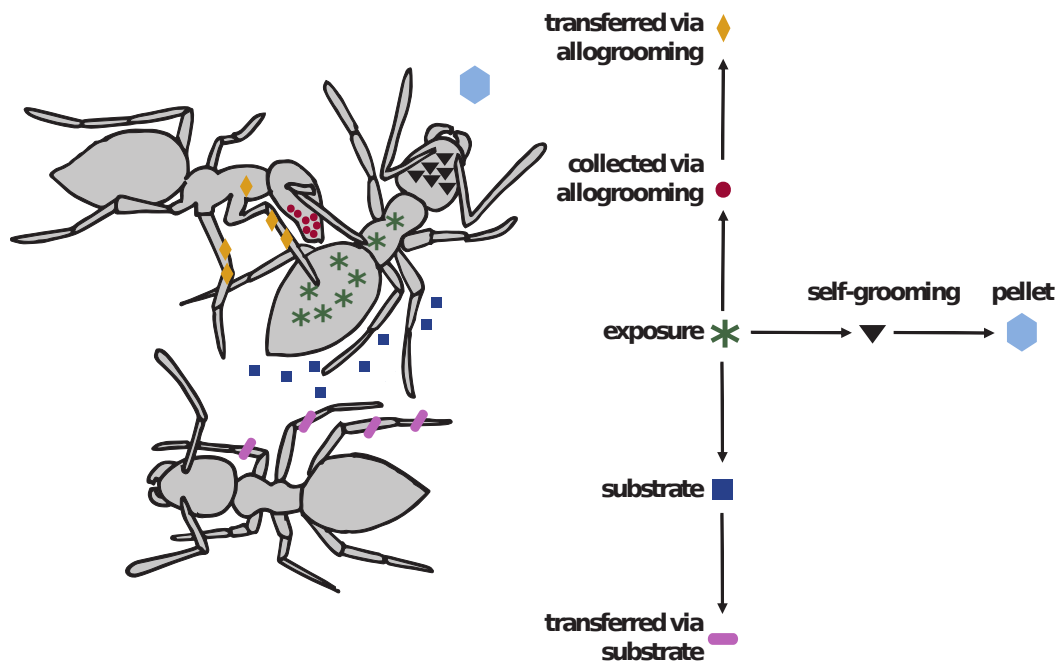


Figure 3.10: Possible routes in which spores move within the system. A treated ant receives spores from exposure. As a result of selfgrooming, the treated ant collects spores into its head, most of which are later expelled in an infrabuccal pellet. When a nestmate grooms the treated ant, it collects spores from it, most of which end up in the its head or in the pellets it expelled. Some, however, can be transferred to the nestmates body. Treated ants also shed spores onto the substrate, where they can also be picked up, *i.e.* indirect transmission.

### (ii) Spores are collected in the head of a contaminated ant by selfgrooming

For contaminated ants, there are two processes by which the spores they were contaminated with, can shift location. On one hand, we anticipated that the spores would accumulate in their head as a result of selfgrooming. On the other, the number of spores remaining on their body can be reduced as a result of both selfgrooming and allogrooming received. As a consequence of these two processes, the ratio of body spores to head spores decreases (*e.g.* reduction on the body and accumulation in the head). While we only have spore measurements for head and body at the end of the experiment, we can compare those to exposure-controls (frozen immediately after exposure and processed identically). Exposure-controls had 5 to 10 times more spores on their body than in their head. We found no difference between dose groups ( $D = 0.16$ ,  $p\text{-value} = 0.80$ , log-transformed variable). Meanwhile, exposed ants (after 90 min

of the experiment) had only 2 to 5 times more spores on their body (Figure 3.11 A). The body to head ratio significantly shifted (Two-sample Kolmogorov-Smirnov Test,  $D = 0.37$ ,  $p < 0.001$ ).

The shift in body to head ratio can be due either to an increase in the spores in the head, or a decrease in the spores on the body. To see how these two processes contributed to the shift, we estimate the number of spores a treated ant must have had in its head and in its body before any interaction and contrast with the final load measured. We estimate the initial number of spores and then assign a portion to the head and a portion to the body, according to the median body to head ratio of the exposure controls. The initial number on a treated ant, is the sum of all the spores of a matching label that were recovered from the dish (*i.e.* from all six ants and pellets). The median body to head ratio of the spore-exposed controls was 7.01, 95% CI (5.86 - 8.59),  $n = 60$ . So for instance, if the total dish eGFP spores measured on a dish was 80,000, we assigned 10,000 to head and 70,000 to body as an initial load for the eGFP-spore contaminated ant (Figure 3.11 A).

By subtracting this initial estimate from the final measured loads, we determine the amount of spores gained or lost in head and on body. The spores gained in the head accumulated there from selfgrooming, and those lost from the body were lost to grooming (both self and allo). The histograms of these differences are presented in Figure 3.11 B, and show that, indeed, treated ants both gain spores in the head, and loose spores from the body, during the 90 minutes of observation period. Both of these processes contribute to a shift in body to head ratio, but most of the shift is due to spores being removed from the body Figure 3.11 B [LMER]: LR  $\chi^2 = 5.52$ ,  $df = 1$ ,  $p = 0.018$ ). This is consistent with the fact that spores can be removed from the body of a treated ant in three ways: by self-grooming, by allo-grooming and by being lost to the environment; while only the first of these leads to an increase in the number of spores in their head.

### **(iii) Spores are collected in the heads of nestmates by allogrooming**

Before we looked at focal individual, now we look at nestmates. Allogrooming has long been known to effectively remove fungal spores [Reber *et al.*, 2011]. Our experiments

show that nestmates collect the spores in their heads, and that the chance of them doing so increases with the amount of allogrooming they performed. We detected spores in the heads of 70-80% of the nestmates. We set to find out if this can be reasonably predicted by allogrooming performed, which would not necessarily be the case, for instance, if they disgorge all spores into pellets. We build a logistic model with a binary variable indicating the presence of spores in the head of nestmates and, as predictors, the total number of spores measured in the replicate group, and nestmate allogrooming rank, based on the allogrooming performed towards spore-contaminated ants. The probability of finding spores in the head of a nestmate increases with global spore dose and is lowest for ants who groomed the least (Logistic regression GLM overall LR  $\chi^2 = 26.59$ , df = 4, p < 0.001; grooming rank LR  $\chi^2 = 6.6291$ , df = 1 p = 0.010; dish load LR  $\chi^2 = 20.4$ , df = 3, p < 0.001).

To better our understanding, we built another model to test whether the amount of spores with a given label, collected by a nestmate, was predicted by time it spent grooming the ant carrying the respectively labelled spores, and the number of them (*i.e.* the dose of the ant being groomed). Indeed, the amount of spores collected by a nestmate is determined by the time it groomed an ant and the dose it had (LMER overall LR  $\chi^2 = 14.95$ , df = 2, p < 0.001; grooming performed LR  $\chi^2 = 4.69$ , df = 1 p = 0.030; dose LR  $\chi^2 = 9.39$ , df = 1, p = 0.002).

#### **(iv) Treated ants also take part in allogrooming their contaminated partner**

With our design with two-labeled spores, we can also look at how many spores are transferred across the treated ants (from now on these spores as referred to as cross-transferred spores). We first examined the cross-transferred spores in the heads of the treated ants and conclude that treated ants indeed collect spores from each other (median 1488, 1stQ 425, 3rdQ 5988), although at least tenfold less than nestmates collect (median 11420, 1stQ 4462, 3rdQ 20340).

We wanted to know when treated ants groom each other *e.g.* whether it depends on their own or their partners dose. We fit a logistic model to predict the probability of finding cross-transferred spores in the head of treated ant. We used the effective time allogrooming the contaminated partner and its given dose (H or L). Cross-transferred

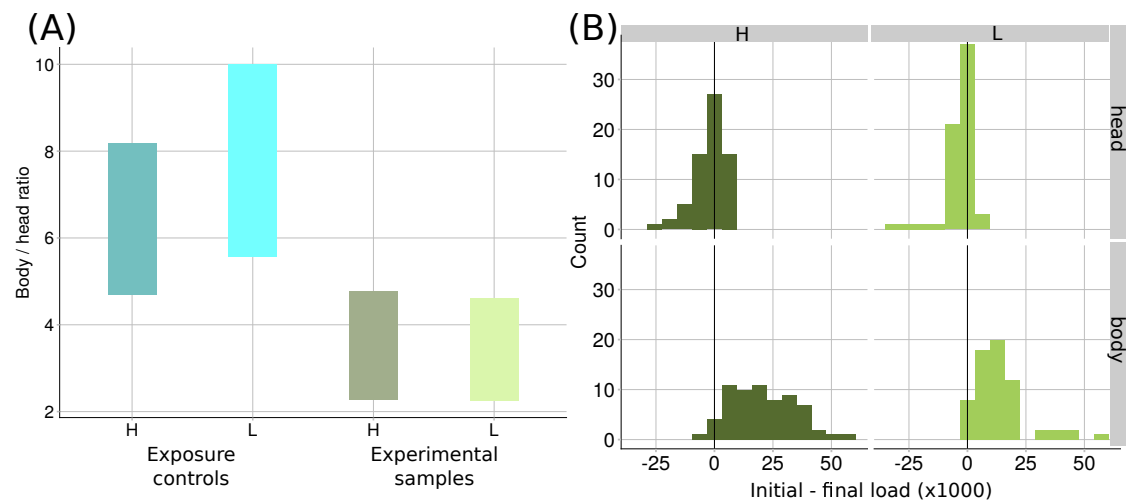


Figure 3.11: Body to head spore load ratio. (A) Body to head ratio in exposure-controls and experimental samples. The vertical axis shows the number of spores on the body over the number of spores in the head, of the same ant, according to treatment dose (vertical axis), either in exposure controls (left) or after 90 minutes observation (right). Mean and confidence intervals (shaded) are shown. (B) Shift with respect to control. A histogram is shown of the difference between the number of spores recovered from either the head (top) or the body (bottom) of an ant, and the estimated number of spores that said ant had in the corresponding body part at the beginning of the experiment. Bins to the right of zero indicate a loss in spores during the 90 minutes of observation, and those to the left a gain in spores. The estimate of initial spore load takes into account the total number of spores with a given label recovered in a dish, and the body/head spore ratio of the exposure controls, as described in the text.

spores were more likely found in the head of ants who allogroomed for longer and even higher for those who groomed a high-dose contaminated partner (Logistic regression GLM overall LR  $\chi^2 = 26.59$ ,  $df = 4$ ,  $p < 0.001$ ; rank LR  $\chi^2 = 6.6291$ ,  $df = 1$   $p = 0.010$ ; dish load LR  $\chi^2 = 20.4$ ,  $df = 3$ ,  $p < 0.001$ ). Nevertheless, ants with cross-transferred spores in their head are not those with spores on their body (Pearson-correlation= -0.08,  $p = 0.256$ ).

We further investigated the spores transferred across treated-ants which end up on the body. These spores are disease relevant, and will be referred to with the term cross-contamination. Since cross-contamination was rare, and the spores relatively few, we used a different approach. We used a probabilistic approach and found that

	HH	HL	LL	HT	LT
Head spores (collection)	14/34	5/16 6/16	3/32	7/15	7/17
Body spores (transmission)	5/34	3/16 3/16	2/32	0/15	1/17

Table 3.7: Spores transferred across treated ants. For each treatment group (in columns) the ratio of replicates in which treated ants had spores from the other treated ant either in their head (top row) or in their body (bottom row). For ants in HL-treated dishes, we distinguish those which were treated with H and had spores from the one treated with L (left), and those which were treated with L and had spores from the one treated with H (right).

the likelihood of cross-contamination is the same across groups (Fisher's exact test  $p = 0.425$ ). Secondly, treated ants are equally likely to get cross-contamination spores from a high-dose contaminated partner than from a low-dose contaminated one (Fisher's exact test  $p = 0.77$ ). Interestingly, 13 out of 98 spore-treated ants, *i.e.* 13%, had spores from the other treated ant on their body, whereas only 1 sham-treated out of 32, *i.e.* 3% had them. It is tempting to conclude that sham-treated individuals acquire less from their treated partner compared to cross-contamination between two spore contaminated partners. Yet, for the sample size and the rarity of contamination, we have not enough power to make this inference (See Table 3.7)

#### **(v) Number of spores packed into pellets across groups and estimated spore content of a pellet**

Another neglected aspect of pellets is simply the amount of spores each of them contains and the total number of spores which a group of ants packs into pellets. This pellet estimates seem relevant, not only if one thinks of pellets as a sink (*i.e.* as spores subtracted from the pathogen infection cycle), but also if one considers that they take time (as presented above) and resources (*i.e.* presumably costly gland secretions [Tragust *et al.*, 2013; Fernández-Marín *et al.*, 2006]) to produce.

We looked at the total number of spores packed into pellets in each dish. The mean number of spores packed in pellets was 7,315 spores and 95% CI [5,651–9,183]. Ants in HH groups packed the largest amount of spores into pellets, with more than 30,000 spores. Comparing across treatment groups, we found a small but significant difference between HH and LT groups (Figure 3.12 A [LM] LR  $\chi^2 = 1.465$ , df = 4, p = 0.032, Tukey post hoc comparisons, BH adj-p-value 0.039, all others n.s.), which had the highest and lowest global dose, respectively.

We pooled the pellets collected before quantification, which means we do not have individual spore measurements per pellet. Nevertheless, we can estimate the average number of spores contained in a pellet by dividing our spore measurement of the pool by the number of pellets pooled (see number of pellets produced per per dish in Figure 3.3 A). A pellet has an estimated 1634 spores, and 95%CI [1,250–2,093], with no significant differences across treatment groups (Figure 3.12 B [LM] LR  $\chi^2 = 0.502$ , df = 4, p = 0.593). The estimate was consistent across groups, which suggests that pellets reach an average size before being disgorged.

**(vi) More spores are removed from high-dose contaminated ants and further more from singly contaminated ants**

As depicted in Figure 3.10, the spores that we applied to an ant at the beginning of the experiment can be transferred to other ants (heads and bodies) and subsequently to pellets, or they can be shed directly to the substrate. In the case of spore-contaminated ants, we can measure the spores ‘remaining’ (*i.e.* those we contaminated them with) and the spores ‘acquired’ (*i.e.* those we did not contaminate them with) All spores are ‘acquired’ if found on sham-treated ants and untreated nestmates. See Method for expanded definitions.

Here we investigate the change, or rather reduction, in the number of spores that an ant initially had (estimated as above, *i.e.* the sum of spores, with the relevant label, on all ants and pellets), and the number of spores remaining. In other words, we look at the difference between the estimated initial load and the final load of the contaminated ants. Differences across treatment groups in the magnitude of spore reduction, can help elucidate the consequences of the behavioral dynamics described above.



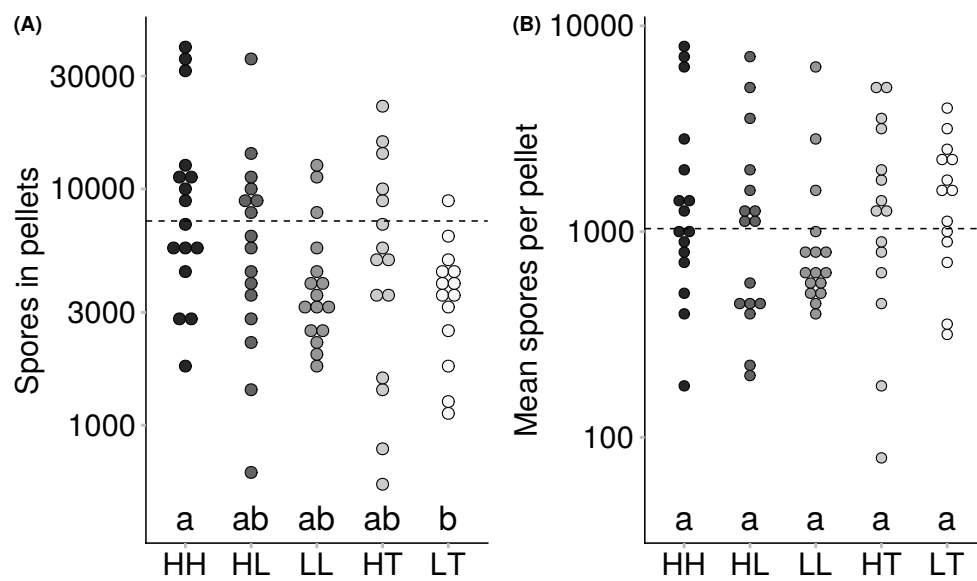


Figure 3.12: Spores in pellets A) Total spores per dish in pellets. The vertical axis shows the total number of spores recovered from all pellets in that replicate group. There is one point per dish. The dotted line shows the overall mean. Lettering shows statistical comparison between groups, groups sharing letters do not differ. B) Average number of spores contained in a pellet. The vertical axis shows the average number of spores a pellet from each dish had. There is one point per dish, and the dotted line shows the overall mean.

We modelled spore reduction for an ant as a function of two predictors, its dose and that of the other ant treated. We found the following. First, spore-treated individuals that carried more spores from the beginning (H) showed a higher reduction in spores than those carrying less (L). Second, spore-treated individuals paired with sham-treated ones (HT and LT) have an even greater reduction in spore load than those paired with other spore-treated ones (Figure 3.13 A: [LMER] full  $\chi^2 = 25.49$ ,  $df = 3$   $p < 0.001$ ; interaction  $\chi^2 = 0.4818$   $df = 2$   $p = 0.786$ ; effect of dose  $\chi^2 = 15.146$ ,  $df = 1$   $p = 9.953e-05$ , effect of partner-dose  $\chi^2 = 11.892$   $df = 2$ ,  $p = 0.003$ ).

The first finding is in accordance to our spore decay model, where the number of spores removed by unit of grooming received is proportional to the number of spores present. The second, is to be expected, since the nestmates (of HT and LT) have only one spore-treated ant on which to focus their grooming.

Now, it is important to notice that the reduction in spores on a spore-contaminated ant is, by our definition, equivalent to the sum of spores acquired from it by all ants, plus the spores found in pellets (of the relevant label). The total amount of spores acquired (in the head) by all ants is not significantly different across treatment groups (Figure 3.13 B, [LM spores acquired by all ~ treatment group]  $SS = 8.77$ ,  $df = 4$ ,  $p = 0.312$ ). The amount of spores expelled in pellets showed a very weak global dose trend, with more spores in pellets for HH compared to LT groups (Figure 3.12 B).

Why is there a larger spore reduction from spore-contaminated ants when they are the only exposed (*i.e.* H in HT and L in LT)? One hypothesis, to discard, is that the extra reduction results from changes in their behavior or that of their nestmates (*e.g.* total time allogrooming and selfgrooming). We modeled grooming behaviors as a function of dose and treatment, including dish as a random effect to deal with pseudoreplication. The spore-contaminated ants paired with sham (H in HT and L in LT) do not receive more allogrooming in total (Figure 3.13 C [LMER]  $\chi^2 = 0.889$ ,  $df = 3$ ,  $p = 0.83$ ), nor perform more selfgrooming (Figure 3.13 D [LMER]  $\chi^2 = 1.463$ ,  $df = 3$ ,  $p = 0.69$ ).

If it is not the amount of allo or selfgrooming, perhaps it could be the timing of these behaviors. We modeled the promptness of grooming behaviors as a function of dose and treatment, including dish as a random effect to deal with pseudoreplication. Neither are they allogroomed earlier (Figure 3.13 E [LMER]  $\chi^2 = 3.584$ ,  $df = 3$ ,  $p = 0.31$ ) nor do they selfgroom earlier (Figure 3.13 F [LMER]  $\chi^2 = 0.385$ ,  $df = 3$ ,  $p =$

0.94). Promptness was computed using the area under the curve of the cumulative sum of the behavior per time window, normalized so that the cumulative sum at the final observation windows is equal to one.

We next investigate whether the total spores acquired on their bodies is different and whether there is potential loss of spores to the environment.

#### **(vii) Loss is highest in treatments with two spore-contaminated ants**

We define loss as the difference between the total number of spores (both labels) measured per dish and the total number of spores applied (See Method for detail). The loss is significantly larger for groups with two spore-contaminated ants (Figure 3.14, Permutation Test based on 9999 Monte-Carlo resamplings  $Z=2.58$ ,  $p = 0.008$ ). This suggests that the more focused attention on spore-treated individuals when they are paired with sham-treated (*i.e.* H in HT and L in LT) may reduce the amount of spores lost to the environment.

#### **(viii) Contamination is highest in groups with two-spore treated ants**

Very few nestmates acquire spores on their bodies. Contamination does not show a global load dependence. Yet, nestmates were more likely to get contaminated in treatment groups with two-contaminated ants (14-19% incidence) compared to groups with a single contaminated target (4-8% incidence). This is backed by a logistic regression of body spore presence as a function of number of ants exposed, with dish as a random factor to account for non-independence of data points within a dish (Figure 3.15 GLMER  $\chi^2 = 6.305$ ,  $df = 1$ ,  $p = 0.012$ ). The number of spores on the body of a nestmate has no correlation to the number of spores it collected in its head (Pearson  $corr = -0.03$ ,  $p = 0.87$ ), which is in contrast with the untested expectations mentioned in literature (*e.g.* [Schmid-Hempel, 1998; Cremer *et al.*, 2007; Theis *et al.*, 2015; Rosengaus and Traniello, 1997; Fefferman *et al.*, 2007]). Hence, allogrooming intensity cannot predict the level of contamination on the body of the groomers (only in their heads, see point (iii) in this section), revealing that transmission to the body surface during the course of allogrooming is unlikely. On the other hand, we find that the rate of contamination is highest in groups with a higher proportion of contaminated and hence

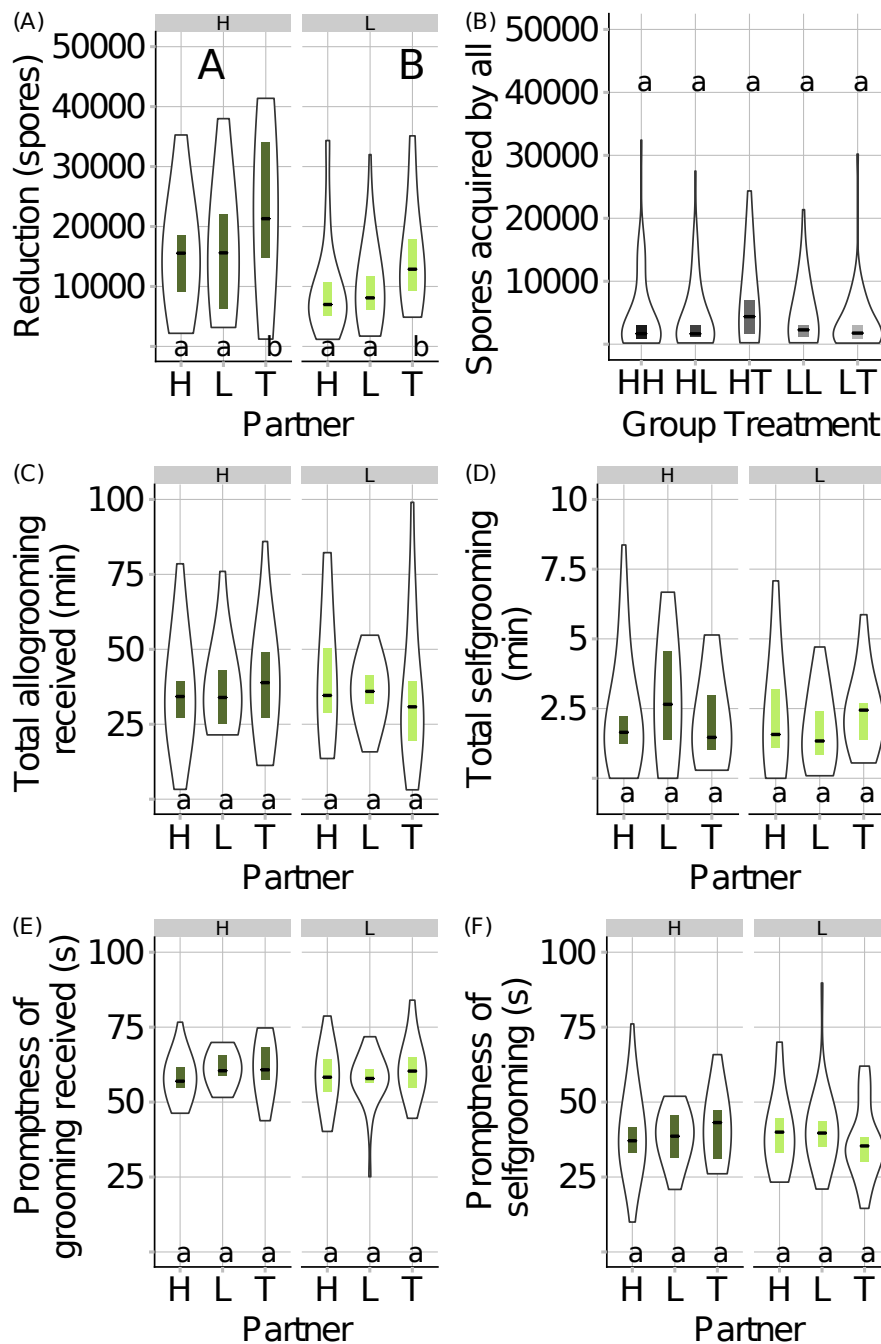


Figure 3.13: Spore reduction and acquisition. A) Spores reduced from spore-treated ants, depending on the treatment they received and their partner. LMER with reduction as a function of dose and partner-dose. Letter for Tukey post hoc comparisons according to dose (upper-case) and partner-dose(lower-case) B) Spores acquired (by all ants) in a dish across treatment groups. Shown is the number acquired into the heads of the ants, but the results also hold if considering the sum of acquired in head and body, since the later is very small.

Figure 3.13 (Continued from previous page): Letters are Tukey post hoc comparisons C) Total allogrooming received and D) Total selfgrooming performed by spore-treated ants, according to treatment and to partner. E) Promptness of allogrooming received and F) Promptness of selfgrooming performed by spore-treated ants, according to treatment and to partner. Promptness is computed as the area under the curve of the cumulative sum of the behavior per time window, normalized so that the cumulative sum at the final observation windows is equal to one.

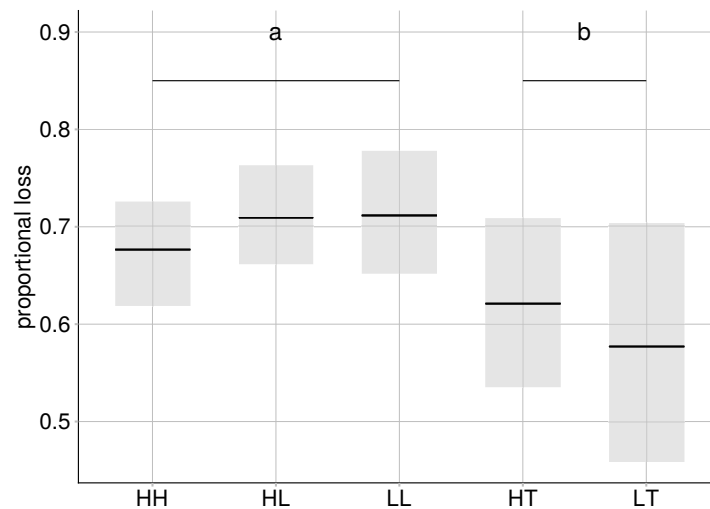


Figure 3.14: Proportional loss estimated with exposure-controls. For each dish, the amount of loss is computed as the ratio of the number of spores measured in all six ants and recovered pellets, over the number of spores originally applied (as per exposure controls). The loss is shown for each treatment group, median and 95% confidence intervals. The letters denote significantly different groups, according to a Permutation Test based on 9999 Monte-Carlo resamplings ( $Z=2.58$ ,  $p = 0.008$ ).

infectious individuals (2/6 instead of 1/6), in which also the loss is highest. Therefore, we formulate a hypothesis whereby nestmates inadvertently pickup spores from the substrate, with a probability proportional to number of spores present on the substrate (*i.e.* the accumulated loss). This working hypothesis, of course, needs experiment validation.

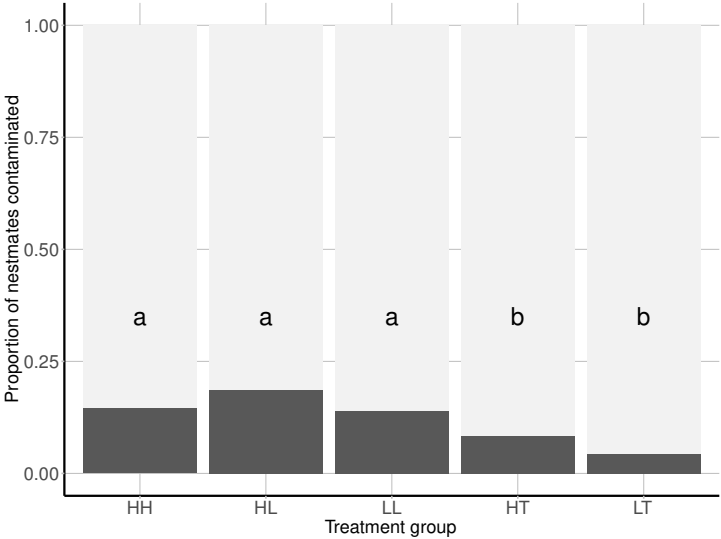


Figure 3.15: Proportion of nestmates contaminated. For each treatment group, the proportion of nestmates with spores on the body at the end of the experiment.

## 3.4 Discussion and Conclusion

### (i) Allogrooming

Allogrooming performed by spore-contaminated ants towards susceptible nestmates is a route for pathogen transmission. Avoiding this route and, in general, self-exclusion from social interactions (*e.g.* leaving the nest when moribund [Bos *et al.*, 2012]) have been posed as adaptive for epidemic control in ant colonies [Theis *et al.*, 2015]. Exposed ants have been reported to distance themselves from brood [Ugelvig and Cremer, 2007] and other nestmates [Stroeymeyt *et al.*, 2018], which implies an overall reduction in their interactions. We confirm the observation [Theis *et al.*, 2015] of reduced allogrooming from infectious to susceptible individuals, but we add, an equivalent reduction in sham-treated ants which suggests that this strategy is prophylactic and not exclusively contingent on pathogen presence. This might constitute a general, less costly, less error-prone strategy. We nevertheless add that it could also simply result from a constraint, namely, that an ant being allogroomed prevents it from allogrooming other ants.

### (ii) Selfgrooming

Selfgrooming is considered to be a generally benevolent strategy in terms of epidemic outcome as it removes spores without risking transmission [Theis *et al.*, 2015]. An increase in selfgrooming is expected to be advantageous both for directly contaminated ants and their nestmates, and thus is expected. We indeed observed a general increase in selfgrooming by both treated and untreated ants. An increase in selfgrooming of spore-contaminated with respect to sham-treated was observed before [Ugelvig and Cremer, 2007], but the observation in nestmates was awaiting confirmation.

Now, selfgrooming has been reported to happen at much higher rates than allogrooming [Theis *et al.*, 2015]. Nevertheless, we find that a smaller proportion of time is allocated to selfgrooming than to allogrooming, both before and after exposure. We believe this inconsistency is due to the fact that behavioral observations in different studies span different intervals of time. Behavioral observations in our study finish ninety minutes after exposure. Thus, we cannot exclude the possibility, that a

late phase of selfgrooming, mainly of spore-contaminated ants, is happening after the allogrooming phase we observed.

### **(iii) Acidopore grooming**

Acidopore grooming has been described as an important component in sanitary care. The acidopore is a structure unique to the family Formicinae located at tip of the abdomen. It gets its name because this aperture is connected to the poison gland, which mostly contains formic acid. It is in fact, jointly connected to the Dufour gland and hindgut. The poison and Dufour gland compounds are known for their use in antipredator defense and trail formation. Given its antimicrobial properties, formic acid, has an additional role in antipathogen defense. *L. neglectus* ants are known to groom the acidopore and take up the secretions into their mouth. The transiently stored compounds are orally applied during sanitary care [Tragust *et al.*, 2013]. Importantly, they also serve to disinfect the spores collected and likely the groomer herself. Also, note that though the use of formic acid is unique to the Formicines, it is likely that poison of other ants is also antimicrobially active and moreover that ants can make use of metapleural gland secretions for disinfection [Fernández-Marín *et al.*, 2006].

Given that the untreated nestmates performed the most allogrooming and produce the most pellets, we expected them to increase acidopore selfgrooming. Unexpectedly, we found increased acidopore selfgrooming from spore-contaminated ants and sham-treated, and a decreased acidopore selfgrooming from nestmates. Now, there is an order in sanitary behaviors where ants transition from grooming to acidopore selfgrooming and finally to pellet spitting. Treated ants produced pellets earlier, possibly depleting the formic acid transiently stored in their mouth; the acidopore selfgrooming we observe is likely replenishing their storage. We cannot exclude the possibility that given longer, nestmates would perform acidopore selfgrooming, as well.

We observed an acidopore selfgrooming response which differed between untreated nestmates and treated ants. Granted that this observation is restricted to the chosen observation period, it could also fall in line with evidence for 'sick signaling' in eusocial insects. Communication about pathogen intrusion is key for any host, including the super-organismic host. In vertebrates, there are cells specialized in patrolling, de-



tecting threats and recruiting a larger cellular response. Besides this, individual cells can signal their own status. Similarly social insects are known to patrol and detect threats [Cremer and Sixt, 2009]. They can also mount complex systemic responses, such as 'fever' [Starks *et al.*, 2000]. Evidence of communication about contaminated or diseased individuals, remains elusive. Signaling from contaminated or diseased individual themselves, 'sick signaling', is still a matter of debate and ongoing experimentation, in particular to determine if any behavioral changes constitute just side effects of contamination which are interpreted by nestmates (cues), or if it is an independently evolved mechanism for signaling contamination. For instance, pathogen-exposed termites have been shown to use vibrational cues to trigger a group response [Rosengaus *et al.*, 1999]. Also, nestmates destroy and disinfect infected brood triggered by cuticular hydrocarbon changes [Pull *et al.*, 2018]. Moreover, wounded ants may signal their status for nestmates to rescue and carry them back to the nest [Frank *et al.*, 2018]. Acidopore grooming, exclusively shown by exposed individuals, needs further confirmation as constituting 'signaling of contamination'.

Given that the acidopore secretion contains both a volatile (formic and acetic acid) and smaller less-volatile (Dufour gland hydrocarbons, used also for pheromone trail marking) fraction [Tragust *et al.*, 2013], acidopore selfgrooming can potentially be used in both short-range (peer-to-peer) and long-range (broadcast) communication, at the same time. If contaminated individuals would apply the secretion unto themselves, the volatile fraction could serve to recruit nestmates (additionally to its active role as disinfectant), while the less-volatile part could be the basis for identifying them as contaminated (in addition to compounds of fungal origin such as octenol (Ugelvig, L.V., unpublished data).

#### **(iv) Overall response dynamics**

The grooming response surges and decays in an exponential fashion towards baseline values within our 90 min observation period after treatment; allogrooming is followed by pellet expulsion. Spore-presence increases the amplitude of the response, in comparison to sham-treatment, but this difference fades away during the last third. By then (60 min after treatment), the grooming performed by nestmates does not differ from their pre-exposure baseline. We seem to be observing a single grooming bout in the

group. The dynamics of this bout are likely to change for different numbers of ants and ratios of contaminated to untreated nestmates. For the bout observed, the nestmates have reached a point where the stimulus is not sufficient to sustain the response. These nestmates might have reached a saturation point for this stimulus. Further work is needed to know if the same ants would take part in subsequent grooming bouts, in other words, to measure what the “refractory” period of an ant is. More experiments, for example, replacing the group of nestmates or the contaminated individuals, are needed to confirm that the stimulus is simply the number of spores. The ants could be chemically imprinting a contaminated nestmate, as they do with larvae (Ugelvig, L.V., unpublished data) We predict that a fresh batch of nestmates will mount another (perhaps of lower amplitude) response. Also, replacing contaminated individuals could elicit a similar response from nestmates after some refractory period. These experiments should take into consideration that germination starts relatively quickly (a couple of hours) after spores first contact the insect cuticle.

#### **(iv) Grooming preference**

Estimating instant spore load, makes it possible to account for two things: 1) the experimental variation in exposure (see Supplement for distribution of spore load in exposure controls) and, more importantly 2) the fluctuating relative difference in spore number between the pair (due to different removal rates). Nestmates preferentially groom those exposed-ants with a larger load. This can be achieved by the group, in several ways. Based on our observations, we delineate one mechanism.

There are several ways that ants may detect spores, one of them is by contact (*i.e.* via a combination of mechanical [Ugelvig and Cremer, 2007] and chemical signals (Ugelvig, L.V., unpublished data) during grooming, which stimulates further grooming. The resulting reduction in spores is the key to a self-regulating mechanism. Let us here note that long-range detection of spores is not sufficient to explain grooming preference or the strong directionality observed.

Our results show that the observed behavioral changes, can occur with no need for an individual to assess the relative spore load of all nestmates, or to be endowed with memory to integrate the global dose. Ants are likely to groom any individual that

they come across with but are more likely to groom for longer so long as they detect spores. There is a moment when they will pause, regardless of the spore load left on the contaminated ants, and that is probably when they reach the capacity of their infrabuccal pocket. They might restart the cycle after expelling a pellet and grooming themselves, until they reach a pathogen detection limit. After this they will go to a steady rate of prophylactic care.

These dynamics, defined in the individual level and without the need for global information, are in line with other descriptions of ant behavior as ensembles of seemingly uncoordinated local behavior from which global patterns, beneficial to the colony, emerge [Solé *et al.*, 1993].

#### **(v) Spores collected by grooming and pellets**

It is now known that social interactions can predict spore load [Stroeymeyt *et al.*, 2018] and it is often assumed that grooming frequency predicts the risk for the groomer to contract disease (in some cases only a low level infection, which provides immune protection [Konrad *et al.*, 2012]). However, the work making these predictions has relied on measures of total spore load of the ants [Stroeymeyt *et al.*, 2018] (but see [Konrad *et al.*, 2012] who measured germination from spores in thorax and abdomen). Here we make a clear distinction between disease-relevant contamination of the body surface and the spores collected in the infrabuccal pocket, which are neutralized and hence, no longer relevant for transmission within the colony.

Doing this distinction, we find that most spores found on non-treated ants are actually found in their heads. Their presence can be predicted by the amount of allogrooming of spore-contaminated individuals which they perform. On the other hand, spores are rarely found on the bodies of nestmates, and when they are, it is in very low amounts. Consistent with this result, we observe that spore-treated individuals also remove spores from their bodies and accumulate them in their heads. In conclusion we have observed and quantified a sanitary behavior that consists of accumulation of spores in the head, where they presumably present less risk.

From the spores in their heads, ants form infrabuccal pellets which they shortly afterwards expel. The amount of spores expelled in a pellets is distributed over two

orders of magnitude, but no difference stems from the pathogen dose in the system where they were expelled. The number pellets expelled, however, is correlated with global spore dose. This suggests that ants collect spores up to a more or less fixed capacity before they expel a pellet and resume grooming.

#### **(vi) Loss to the substrate and spore transmission**

A considerable amount of spores is lost to the substrate. This amount is larger in groups with two spore-contaminated ants, even though a similar quantity of spores is collected and spat into pellets by a similar amount of grooming performed (*i.e.* by self-grooming and allogrooming). In these groups with high loss, transmission to nestmates (*i.e.* spores on their body) is more likely. Further experiments will be needed to confirm that the behavioral response, in particular, the preferential grooming of ants with a higher load, prevents loss and thus transmission to nestmates via the substrate. We did not perform this experiment yet, since we did not foresee the importance of loss. Nevertheless it should be straightforward to quantify spores from the substrate (*e.g.* with fluorescent imaging of the arena), and further, perform experiments to check the viability of these spores (*e.g.* stamping the arena on a cultivation plate) and to estimate the likelihood of inadvertent pick-up (*e.g.* by correlating the trajectories of ants and the spores acquired after walking over arenas with a controlled amount of spores laid). One more interesting aspect to measure would be the decline in the spore viability off-host, since we know that ants disinfect their nest (*e.g.* nest disinfection with formic acid).

Studies of direct pathogen spread over proximity-based interaction networks have started to describe the disease dynamics of ant colonies in unprecedented detail [Sumpster, 2006]. In general, studies of the contact networks of insects have been extremely valuable to test and generate new hypothesis regarding the flow of pathogens [Stroeymeyt *et al.*, 2014], but also of resources and information in complex societies (*e.g.* [Jeanson, 2012; Blonder and Dornhaus, 2011; Pinter-Wollman *et al.*, 2011]). On the other hand, indirect transmission has received comparably less attention in experimental epidemiology [Richardson *et al.*, 2015]. Indirect pathways are able to enhance or decrease spreading, depending on the decay characteristics of the agent in question [Richardson *et al.*, 2015]. Considering indirect pathways is likely to be key to solving the

conundrum posed the simultaneous need of enhanced and decreased transmission in communication networks [Richardson *et al.*, 2015]. In our particular case, considering loss to the environment might explain the sanitary care response or the group which would minimize both, the risk of infection of contaminated individuals and the risk of transmission to nestmates, at the same time.

### **(vii) Importance and Future directions**

Decision making in ants in the context of collective disease defenses has not yet been explored. Our study provides a strong basis to understand the collective properties of the sanitary response. Future work should elucidate the rules that individual ants employ to determine when they switch from one behavior to another (*e.g.* from doing nothing to allogrooming to selfgrooming). By testing several of such rules, including those that reflect the results reported here (*i.e.* grooming preference is proportional to instantaneous load), and comparing the statistics of simulations to those from real data, one can reject the need of each rule or combination therein. Furthermore, one can explore, in simulations, other rules, and see if they lead to behaviors which are statistically consistent with our observations. Many interesting biological hypotheses arise from these approach. For example, one can test the need for ants to have memory of their encounters, and the limits of their pathogen detection and discrimination capabilities. These direction is currently being explored with Katka Bod'ová and Gašper Tkačik.

## **3.5 Method**

We studied the behavioral changes of garden ants upon exposure to an entomopathogenic fungus. All necessary details are described below. For a general summary see Figure 3.1

### **Host and pathogen**

The invasive unicolonial ants (*Lasius neglectus*) were collected in June 2015, from Jena, Germany (N 50° 55.910 E 11° 35.140). The stock colony was housed in six

separate boxes. The experiment was carried out in July 2016, when the colonies were one year old, and had each ca. 20 queens and ca. 8000 workers. We took workers from a single stock colony for the final run of the experiment. We sampled workers from nest chambers which were not shared with queens or brood, in this way we avoided sampling callow or old foragers. The stock colony and experimental groups were kept at constant temperature of 23° C with 75% humidity and a 14/10 light/dark cycle. This is an unprotected ant species, and all experiments and handling were done in accordance with European Law and IST Austria ethical guidelines.

We used conidiospores of a fungal strain *Metarhizium robertsii*, with one of two fluorescent gene labels (*i.e.* eGFP-Ma5275, and mRFP-Ma5275). We cycled them through ants to ensure equal virulence and germination. Prior to the experiment, conidiospores were grown on 6.5% sabaroud dextrose agar at 23° C until sporulation and harvested by suspending them in 0.05% sterile Triton X-100 (Sigma). Germination was determined to be above 95% for both labelled spores in all plates harvested.

## Experimental procedure

To allow for individual behavioral scoring and individual pathogen load estimation, ants were colour-marked (Edding 780 markers) 18-24 hours before observation. Groups of six uniquely marked ants ( $n=18$ ) were placed together in plastered Petri dishes of Ø 45 mm with Ø 50mm glass covers (Edmund Optics), without food and recorded for 30 minutes (*i.e.* Baseline behavior, Figure 3.1). After treatment (more detail below), we allowed only a few seconds, until ants had recovered stance, before we reintroduced them to their dish and recorded a second observation period, of 90 minutes (*i.e.* Treatment-induced behavior, Figure 3.1). After this post-treatment observation period, all dishes were frozen at -80° C, the ants in them hence freeze-killed.

The length of the observation period, the number of ants, and dosages, were chosen based on previous work [Ugelvig and Cremer, 2007] and preliminary runs, to fulfill the following requirements: (1) no pathogen multiplication is happening, (2) grooming interactions happen between all ants, *i.e.* interaction networks are fully connected, (3) transmission happens and is measurable, (4) not too many pellets are disgorged.

Two ants in every dish were randomly assigned to be exposed with a high dose (H), low dose (L), or treated with pathogen-free solution (T), resulting in six treatment combinations (HH, HL, HT, LL, LT, TT). The experiment was designed to disentangle the effects of individual and global dose. To allow for comparison between treatment groups with the same global dose, carried by a single ant or evenly distributed among the pair, we set the high dose to be twice as high as the low dose ( $H=2L$  and thus we can compare HT vs LL with the same global dose).

We used two fluorescently labelled fungi, created from a single strain tagged with one of two single gene labels, created in the lab of Mike Bidochka. Conidiospores (here also referred simply as spores) from the labelled fungi, carry a single plasmid with either eGFP or an mRFP gene. We targeted both genes for simultaneous quantification (see Spore quantification)

The labelled spores used for exposure were randomly assigned, so that the following properties held: i) in case both ants were to be spore-exposed, they would be exposed each to a differently labelled spore, ii) in case a single ant was to be spore-exposed and the other sham-exposed, the spore-exposed ant would be treated with eGFP-labelled spores in 50% of the replicates and with mRFP-labelled spores in the rest. The use of two labels was chosen so that we could infer the origin of the spores collected by or transferred to other ants.

We anticipated that spores would accumulate in the mouth-parts and head as a result of the grooming performed. It is known that spores accumulate in the infrabuccal pocket, where they are mixed with formic acid and other glandular compounds which strongly reduce their germination [Tragust *et al.*, 2013]. They are then physically compacted into a pellet and disgorged. Spores in the head, and pellets, are mostly inactivated and thus no longer able to cause disease. Spores on the rest of the body, best represent disease-relevant transmission, since they still hold the potential to germinate and penetrate into the host. We thus, decapitated the ants (*i.e.* we separated the head from thorax with a scalpel), to separately quantify the spores in the head and on the body (see Spore quantification). Furthermore, we collected from each dish all discarded pellets and pooled them for quantification. All the handling tools (*i.e.* scalpel, pinzers) were thoroughly rinsed with Triton X-100 solution and wiped with optical lense tissue, to avoid contamination between samples.

Using two labelled spores and dissecting the ants, is quite informative. In the case of spore-contaminated ants, we refer to the spores 'remaining', as those we contaminated them with. Spores 'acquired', are spores with a different label to what they were contaminated with. In the case of sham-treated ants and untreated nestmates, all spores are 'acquired', either collected in their heads by allogrooming or picked up, haphazardly, and found on their body. This lets us draw several inferences, for instance, finding eGFP-spores in the head of an mRFP-spore-contaminated ant, implies that treated ants also allogroom one another and we can see how this matches our behavioral observations.

In total, we excluded eight replicates (~7% of the dishes) from all analyses, since we could not ascertain whether contamination or swaps had happened during exposure or in later quantification steps. The replicates excluded were: HL6, HH11, HL11, HT11, LL11, LL16, TT16, HT18.

## Exposure method and controls

We exposed individual ants by gently rolling them over a 0.3 $\mu$ L droplet of a spore or sham suspension with sterile soft forceps. We prepared five aliquots for each suspension and kept them at 4° C. We used new aliquots every day, to minimize changes in spore concentration due to evaporation. This also cut down the risk of contamination.

We prepared two spore concentrations for each labelled spore: a  $1 \times 10^9$  and  $5 \times 10^8$  conidiospores per mL of 0.05 % sterile Triton X-100, a high-dose and half- or low-dose, respectively. Applying 0.3 $\mu$ L of the high-dose suspension to adult worker in this species, constitutes a lethal dose with a killing rate of 50% (or LD50). Sham-treated ants were exposed to sterile Triton X-100 only.

In addition, we produced exposure controls (three replicates) at the beginning of each five experimental day (out of six days). We discarded the samples made on the sixth day, due to abnormally high variation due to experimental mishaps (*i.e.*  $n=15$ ). For the exposure controls, each ant was decapitated and frozen immediately. We used the exposure controls to estimate initial spore load of each ant (see Instant spore load estimation) as well as initial distribution of the spores in the head and on the body. In addition, we estimated the background noise level in spore quantification.



## Spore quantification

Ant samples, pellet samples and control-exposure samples were processed in the same way for spore quantification. In brief, DNA was extracted from the samples and two genes-- eGFP and mRFP-- were simultaneously targeted for amplification. We used a droplet digital PCR (ddPCR), which partitions the sample into thousands of oil droplets. Following PCR, each droplet is read in two fluorescence channels. For each channel, a positive read corresponds to the presence of, with very high (poisson distributed) probability, a single copy a gene. Since each spore carries one plasmid with a single gene copy, we obtain absolute spore counts in the input sample from both labeled spores. Importantly, this technique is equally efficient for live and dead spores (Anna Grasse, establishment work), hence also chemically inactivated spores can be quantified.

Spore quantification was done using the Bio-Rad droplet digital ddPCR system. Prior to this, DNA was extracted from the samples by homogenizing the ant/fungal material in a TissueLyser II (Qiagen) using a mixture of 2.8 mm ceramic (VWR), 1 mm zirconia (BioSpec Products) and 425-600  $\mu\text{m}$  glass beads (Sigma) and 50  $\mu\text{l}$  water. Total DNA was extracted using Qiagen DNeasy96 Blood and Tissue Kit according to the manufacturer's instructions, with a final elution volume of 50  $\mu\text{l}$  Buffer AE.

To perform absolute quantification of the two labelled spores simultaneously, we designed a duplex ddPCR probe assay targeting the mRFP1 and the eGFP gene sequences. Both genes are known to be present as single copies within each fungal spore. Cross-amplification was excluded as well.

For the enzymatic digest of the genomic DNA we used EcoRI and HindIII enzymes (both New England Biolabs). We made sure that the enzymes do not cut within the amplified gene regions. The enzymatic digest was done within the 20  $\mu\text{l}$  1x ddPCR reaction, which comprised the following: 10  $\mu\text{l}$  of 2x ddPCR Supermix for probes (Bio-Rad), 14 pmol of both eGFP primers (forward: 5'-AAGAACGGCATCAAGGTGAA, reverse: 5'-GTGCTCAGGTAGTGGTTGTC; Sigma), 18 pmol of both mRFP1 primers (forward: 5'-CTGTCCCCTCAGTTCCAGTA, reverse: 5'-CCGTCCTCGAAGTTCATCAC; both Sigma), 5 pmol of eGFP probe 5'-[HEX]CAGCTCGCCGACCACTACCAGCAGAAC [BHQ1], 5 pmol of mRFP1 probe 5'-[6FAM]AGCACCCCGCCGACATCCCCG[BHQ1],

both Sigma, 10 U each of EcoRI-HF and HindIII-HF (New England Biolabs), 2.8  $\mu$ l nuclease-free water (Sigma) and 2 $\mu$ l DNA template.

Droplet generation was done using the QX200 droplet generator (Bio-Rad) according to manufacturer's recommendations. Droplets were transferred into a 96-well plate (Eppendorf) for PCR amplification in a T100 Thermal Cycler (Bio-Rad). Cycling conditions were as follows: Enzyme activation for 10 min at 95° C, followed by 40 cycles of 30 sec at 94° C and 1 min at 56° C, followed by enzyme deactivation for 10 min at 98° C. For the entire protocol the ramp rate was set to 2° C/sec.

Following PCR amplification the PCR plate was put into a QX200 droplet reader for the readout of positive and negative droplets. The droplet reader enables detection of fluorescence in two different channels (FAM and HEX). We set the fluorescent amplitude thresholds manually for each channel, using QuantaSoft™ Analysis Pro Software (Bio-Rad). The threshold values selected were 3000 for FAM (reporter in mRFP1 probe) and 2000 for HEX (reporter in eGFP probe). Samples with a total droplet count of less than 10000 were repeated. Raw values are given as copies/20  $\mu$ l well by the software.

Background noise in the quantification of spores was defined as the maximum number of copies read in the non-target channel (i.e reads in FAM channel for eGFP exposure, and reads in HEX channel for mRFP exposure). Values below background noise level (8 copies for mRFP and 12 for eGFP) were not considered (see Supplement). Final values were computed by adjusting raw values by elution volume (2 $\mu$ l of DNA template eluted in 50  $\mu$ l, *i.e.* a factor of 25x) and dilution factor. Samples were run undiluted, and only repeated with a 1:10 dilution when copy number was too high.

From the exposure controls, we recovered roughly two thirds of what was applied, *i.e.* we measured a mean of  $2 \times 10^5$  spores (high-dose control exposure samples, head and body sum), while the exposure droplet contained  $3 \times 10^5$ . This reflects a 60% efficiency. Others have estimated that only 10-15% of the spores applied are expected to ultimately adhere [Cremer *et al.*, 2018]. We confirm this expectation by comparing the number of spores measured from exposure controls to the sum of spores recovered from experimental samples (*i.e.* total spores in ant samples and pellets). Indeed, the proportional loss seems to be quite high and variable (mean 66%, CI 63-70%, sd 16%). We considered this, and use the sum of spores recovered from experimental samples

or the estimated (from controls) spores applied with caution, and specify which when relevant.

## **Recording and behavioral scoring**

We recorded four replicates (*i.e.* petri dishes with a group six ants) at a time in a four camera parallel setup (rolling-shutter cameras from IDS UI-1640LE USB 2.0 CMOS, 18fps, 1024x1024, 1.3MPixel, 1.3 "Aptina Sensor, Rolling-shutter; fixed focal length lense 6MM 1/1.8" f 1.4-f/16 C-mount, Edmund Optics; Streampix software for acquisition).

From the recorded videos, we scored behavior for every ant during both observation periods. We were blind to both group treatment and individual exposure of the ants. We used Solomon Coder © 2017 (by András Péter) to score with frame-based resolution. The behaviors analyzed were a) selfgrooming, b) acidopore selfgrooming, c) allogrooming performed and d) received and, finally, e) pellet disgorgement.

All recordings were done between 8am and 7pm GMT+1, three replicates every day, for a total of six recording days. Twelve additional controls (with no ants treated) were recorded but were not scored or analyzed yet.

## **Instant spore load estimation**

We have experimental spore load measurements at the end of the observation period, as well as an estimate of the spore load at the start. The later we infer from control ants exposed in the same way but freeze-killed immediately and processed together with the experimental samples see Section Spore load quantification. However, we have no spore load estimate throughout the observation period. Here we get an estimate of the spore load on spore-contaminated ants for a series of 3-minute time windows of a 90 minute post-treatment observation period, a total of 30 windows, for each treated individual based on its time-resolved performed and received behaviors.

To this end, we adopt the following assumptions: (i) the measurement of spore load on spore-contaminated ants at the end of the observation period is accurate, (ii) the distribution of initial spore loads from experimental ants contaminated with a given

dose (high or low) resembles the distribution of spore loads from exposure-controls and (iii) The spore load on a given spore-contaminated individual decreases with time with the following dynamics. As individuals selfgroom or receive allogrooming, the spore number is reduced at a rate  $P$  which decreases with spore load, conforming to Michaelis-Menten kinetics (3.1):

$$dP/d\tau = vS/(K + s), \quad (3.1)$$

where  $v$  and  $K$  are parameters to be fit.  $v$  represents the maximum rate of spore decay, and  $K$  is the spore concentration at which  $P = v/2$ .  $P$  is maximum when the spore load,  $S$ , is maximum, and thereafter it decreases with  $\tau$ , the amount of grooming the ant is subject to (both allo- and selfgrooming). The decrease in spore load, we assume, is due to the transfer of spores from the body of the infected individual into the mouth parts of the one performing the grooming.

## Statistical analyses

This section includes necessary details to reproduce all statistical analyses. We first detail the general procedures applied, followed by individual analyses performed in each section, and finally list the statistical packages used.

### General statistical procedures

All logistic regressions were implemented as generalised linear models (GLM) with binomial error terms and logit-link function. To estimate the significance of the predictors, all generalized linear and mixed models (*i.e.* GLM, LMER) were compared to null (intercept only) and reduced models (for models with multiple predictors) using Likelihood Ratio (LR) tests. Significance values were corrected using the Benjamini-Hochberg procedure to protect against false discovery rate, whenever multiple inferences were made. We checked the necessary assumptions of all tests *i.e.* by viewing histograms of data, plotting the distribution of model residuals, testing for unequal variances, testing for the presence of multicollinearity, testing for overdispersion, and assessing models for instability and influential observations.

## Behavioral unit

For all grooming behaviors, we consider the proportion of time allocated to a given behavior-- in an entire observation period (Time-aggregated response) or in each window of the observation period. This unit, which we call effective time, gives a better intuition of the time budget, as opposed to using seconds. For selfgrooming and grooming performed, it is simply the proportion of time spent in these states. For grooming received, it is the sum of the time allocated by different ants to the receiver, since one ant can be groomed simultaneously by several ants. If given for a time window, the effective time exceed one, this means the receiver was groomed by more than one ant for this window of time. Effective time can be easily converted to minutes, for example, given three-minute windows, one needs to multiply effective time by three. One can then think of ant-minutes allocated, similar to the concept of man-hours.

## Time-aggregated response

We analyzed the relative changes in time allocated to each behavior for ants grouped into spore-contaminated (S), sham-treated (T) and untreated (N) categories. We used paired-Wilcoxon signed-rank tests, a non-parametric procedure, to determine whether behavior significantly changes after exposure (*i.e.* pre-exposure vs post-exposure values are paired). To examine all grooming behaviours (allo-, self- and acidopore grooming) and the number of pellets produced, we compared across groups with Kruskal-Wallis rank sum test (KW) test and subsequent post hoc pairwise Mann-Whitney-Wilcoxon (MWW) comparisons, a non parametric alternative. Ants within a dish do not constitute independent observations so, in this case, we dealt with pseudo-replication by collapsing the data by dish (*e.g.* we get a single mean value for all nestmates in the same dish). We used a Fisher's exact test, to compare the number of replicates which produced pellets across groups.

## Time-resolved response

We looked again at relative change in time allocation, this time, splitting the post-treatment period into three thirty-minute partitions, and repeated the statistical ana-

lyses described above (General response).

### **Time-resolved response, a closer look**

We used linear mixed effects regressions (LMER) to test for the effect of treated individual and treated partner dose on each behavior. In this case, we did not collapse the data, but instead included a random intercept for each dish.

For each treatment group, we fit a logistic regression of grooming preference (a binary variable indicating whether or not grooming was performed towards the ant with higher spore load) with spore-load difference as a predictor.

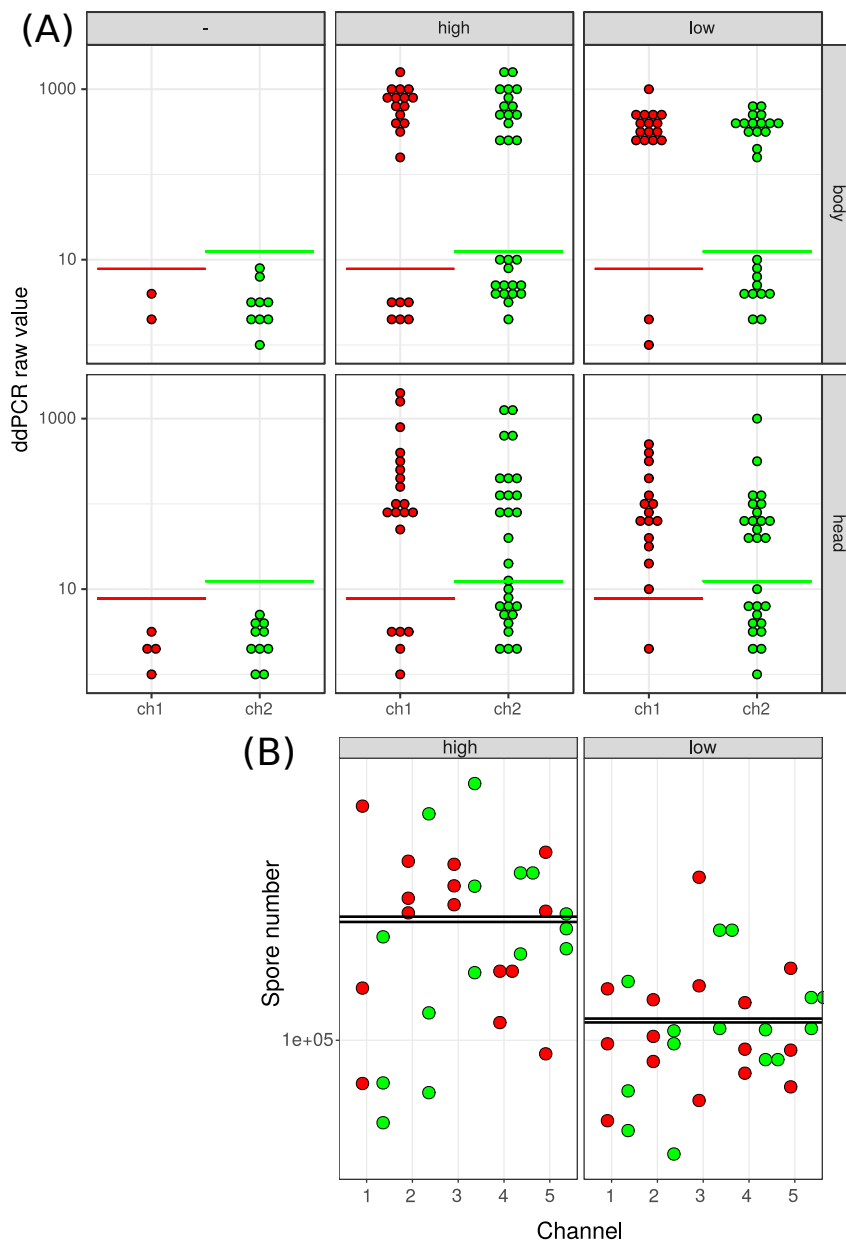
### **Outcome of the response in terms of spores**

We compared the distributions of body to head ratio of control-exposed and experimentally contaminated ants performed a two-sample Kolmogorov-Smirnov test. We also compared between doses using the same test. We tested the contribution of selfgrooming and allogrooming towards the shift in body to spore ratio with a LMER including the behaviors as predictors, and the shift as response variable. We added dish as a random term. We define loss as the ratio between all the spores (both labels) measured in all six ants (body and head) and recovered in pellets, over the number of spores originally applied. These were estimated for each treatment using the median values of the exposure controls.

### **Statistical packages**

All statistical analyses were carried out in R version 3.3.2 [R Core Team, 2013]. We used the packages 'lme4' [Bates *et al.*, 2016] to fit LMER models and 'influence.ME' [Nieuwenhuis *et al.*, 2017] to test all model assumptions. We used the 'multcomp' [Hothorn *et al.*, 2016] package for post hoc comparisons. All graphs were made using the 'ggplot2' package [Wickham *et al.*, 2018].

### 3.6 Supplement



Supplementary figure 3.1: Exposure controls. (A) Raw values from ddPCR for untreated, high and low exposed ant, grouped by body part. Dotted line indicates background noise threshold. (B) Total pore number (head+body) per day. Lines indicates group means. Notice that there is an overlap in the distribution of spore numbers between high and low exposed ants, yet the groups are statistically distinct ([KW test]  $H = 15.98$ ,  $df = 3$ ,  $p = 0.001$ ). Colors indicate fluorescent channel: FAM, mRFP in red and HEX, eGFP in green. See Table S1 for post hoc comparisons.

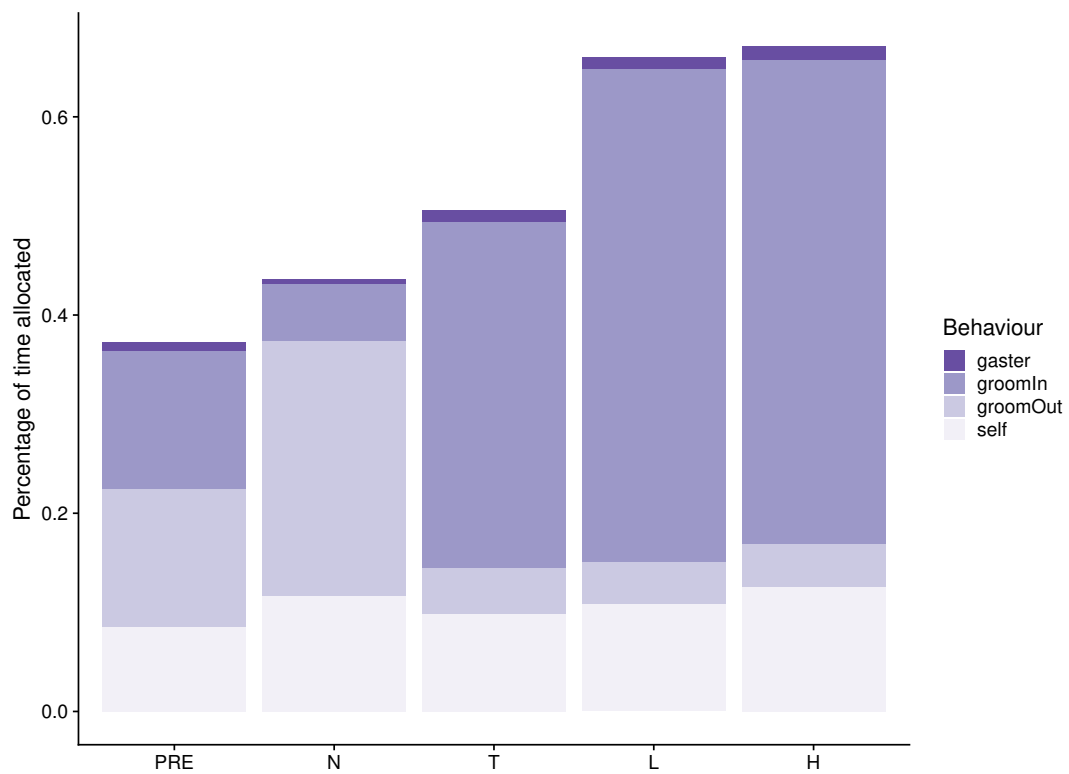
Comparison	H	p value	sig.
high.eGFP - high.mRFP1	-3.80	0.597	n.s
high.eGFP - low.eGFP	16.03	0.008	**
high.eGFP - low.mRFP1	16.16	0.008	**
high.mRFP1 - low.eGFP	19.83	0.002	**
high.mRFP1 - low.mRFP	19.96	0.002	**
low.eGFP - low.mRFP1	0.13	0.98	n.s

Supplementary table 3.1: Comparisons between exposure controls, Kruskal Wallis post hoc comparisons. Grouped by dose and fluorescent channel (*i.e.* spore label). There are no significant differences within dose groups and there are significant between them, as we intended with our design.

Dose	Channel Spore-label	Median	Mean	SD	Group
High	ch1 mRFP1	208 000	201 761	85 128	a
Low	ch1 mRFP1	96 000	111 525	47 119	b
High	ch1 eGFP	181 250	197 435	105 524	a
Low	ch1 eGFP	107 750	112 200	39 745	b

Supplementary table 3.2: Summary statistics for exposure controls, group based on Kruskal Wallis post hoc comparisons (see 3.1). Despite wide variation in exposure, high dose and low dose distributions are statistically distinct, as we intended.





Supplementary figure 3.2: Behavioral budget of all ants before treatment and in the post-treatment period split by treatment (N = nestmate, T = sham, L = low, H = high). Selfgrooming of the acidopore, grooming received, grooming performed and general selfgrooming shown.



## 4 Effect of queen pathogen-contamination on colony development

The experimental design of the work described in this chapter was done together with Christopher D. Pull and Sylvia Cremer. C.D. Pull additionally helped with the experiment setup and colony rearing. The videos were analysed with the use of an image-based tracker developed with Filip Naiser under the supervision of Jiri Matas. We jointly worked on adaptations to optimize ant tracking for this experiment (see Chapter 5). Before submission of the manuscript for publication, we will add results of ongoing experimental work to monitor pathogen load over the course of the experiment, performed with Elisabeth Naderlinger. We would like to thank Adria LeBoeuf, who contributed to the discussion regarding the hormone-based regulation of growth.

### 4.1 Abstract

A mature colony of ants is a collectively organized ensemble where the propensity of each member to perform a set of tasks or to interact with a particular group of individuals can determine the colony's ecological success. The emergence of these group features depends on having reached a particular group size, so what happens until a young colony reaches this stage?

Ant colonies go through vast changes in size and composition from foundation to maturity. Behavioural and morphological transitions also take place; following foundation by a mother queen, the small workers, reared directly by her, take over brood care. Later worker generations acquire a wide array of tasks. In mature colonies, foraging and nest maintenance are performed by specialized groups of workers. During these transitions, colonies face several challenges (*e.g.*: they encounter pathogens, they en-

dure their first winter). The pressure may not always lead to colony extinction, but may have important developmental effects.

Here, we present the results of monitoring colony composition and image-derived proxies of behaviour during colony ontogeny, starting when the first batch of workers emerged and both before and after a period of hibernation. Furthermore, we test whether early exposure of a queen to a pathogen affects the trajectory of a colony.

We find that survival to hibernation is greatly determined by the amount of brood produced immediately before, as well as by the amount of aggregation of workers around the queen. In colonies that were founded by queens which have been exposed to pathogens, growth is reduced with respect to those which have not been exposed. Among such exposed colonies, those which are slow growing have greater odds of surviving hibernation, and tend to recover in numbers afterwards, by growing faster.

These results suggest that the developmental speed of the colonies varies as a means to change the allocation of resources in time, and that this flexibility in growth-rate regulation plays a role in colony survival to pathogen exposure.

## 4.2 Introduction

The individuals of a eusocial insect colony act with such coherence that their functions have for a long time been compared to those of a unitary organism [Wheeler, 1911]. The initiation, growth, reproduction and decline of the colony can be compared to the developmental processes of a multicellular organism. In particular, the division of metazoan cells into germline and soma is mirrored in the separation of insect colonies into reproductive (queens and males) and non-reproductive (sterile workers) individuals [Wheeler, 1911; Boomsma and Gawne, 2018]. This division of labour marks a major, irreversible evolutionary transition from simple sociality to a new form of life – an organism made of organisms – known as the ‘superorganism’ [Boomsma and Gawne, 2018].

An incipient colony is as different from its sexually mature stage, as an embryo is from an adult vertebrate [Tschinkel, 2010]. Typically, a colony is founded by a single reproductive ant, the queen, who leaves her maternal colony to embark on a mass mat-

ing flight with sexuals from other colonies. After mating, the male dies and the queen digs a nest and seals herself underground, never to surface again. This strategy of colony foundation is known as claustral foundation. Without an outside food supply the queen metabolizes her own body tissues to rear her first clutch of workers and to survive her first winter. If successful, the workers will take over all non-reproductive tasks (*e.g.* brood rearing, nest expansion, maintenance, defense and foraging), allowing the queen to focus solely on egg-laying and reproduction. The colony will eventually produce sexuals, usually within 1-2 years of colony initiation, which will leave to start colonies of their own. Most ant species exhibit this mode of reproduction, however, some variants include non-claustral founding, foundation by multiple queens (a.k.a. pleometrosis), attempting to take over an existing colony (a.k.a. social parasitism), and fission or budding of the parent colony (a.k.a. dependent colony founding) [Ward, 2014; Cronin *et al.*, 2013]. These alternative strategies are thought to enhance early colony growth and improve the chances of a colony surviving until it can reproduce (*i.e.* raise sexuals). Put simply, the more workers a colony produces in its early stages, the more able it is to perform behaviours such as brood rearing, nest defense and foraging, which directly impact colony survival and growth of a superorganism.

Like a traditional organism, the growth and development of a superorganism is the result of a complex interplay between signaling and feedback mechanisms, and is influenced by environmental factors [Yang, 2007]. Relatively few studies have focused on the early development of insect colonies and the factors that affect growth. Notably, the consequences of pathogen exposure on colony development remain largely unexplored in ants (but see [Calleri II *et al.*, 2006; Calleri II *et al.*, 2007] for work on termites).

There is more to development than just growth. Individuals in a colony vary in quality throughout development. For instance, the first workers of a claustral queen are smaller than those produced in later stages. It has been suggested that these small workers (also called nanitics or minims) are fast and cheaply produced [Peeters and Ito, 2015] and yet they can be more efficient at brood rearing and live longer [Kramer *et al.*, 2016; Porter and Tschinkel, 1986]. Nanitics are gradually replaced by 'normal' sized workers, which can either be of strikingly different proportions and sizes (*i.e.* polymorphic) or have limited variation (*i.e.* monomorphic species).

In addition to the metabolic resources of the queen, body size is conditioned upon many factors. These include, but are certainly not limited to, larval nutrition, the social environment, and the abiotic environment of the colony. At the same time, body size will influence resource utilization (*e.g.* larger workers carry more) and mediate resistance to stress (*e.g.* desiccation, temperature, pathogens).(recently reviewed by [Trible and Kronauer, 2017; Wills *et al.*, 2018]).

As the brood transitions through larval and pupal stages to adulthood, workers need to attend the colony's changing needs. As the colony grows, foraging becomes more frequent and efficient, whereas brood is handled more systematically. Nanitics get replaced by larger workers who each perform specialized behaviours and colony dynamics altogether change.

Development does not happen in isolation. Ant colonies, will face many challenges early in their development and recurrently thereafter, including seasonality of temperature (*i.e.* cold, drought, lack of food) and pathogen contamination (*e.g.* the pathogens a queen encounters, on her path from mother colony to her own nest, and pathogens imported by foragers).

When incipient colonies face their first winter, they can go into a reduced metabolic state, called diapause. Diapause in ants can be studied at the individual level and at the colony level [Elena B. Lopatina, 2018]. The capacity for diapause can be facultative (*e.g.* middle stage larvae), always present (*e.g.* queen) or absent (*e.g.* eggs, first instar larvae, pre-pupae and pupae) at the level of the individual, while it is inevitable at the colony level, for most temperate and boreal species. Diapause can be triggered by environmental (*e.g.* temperature, photoperiod) and social (*e.g.* worker interaction) conditions (reviewed in [Elena B. Lopatina, 2018]). At the individual level it is generally assumed that overwintering affects ants in the same way it affects any other insect, in terms of energy resources, water content and immune defence. Despite a wealth of literature on overwintering strategies in animals, relatively little attention has been devoted to the study of overwintering in ant colonies [Haatanen *et al.*, 2015]. Overwintering is most crucial in developing colonies, before the colony excavates deeper and escapes extreme temperature changes.

The response of ant colonies to pathogens has been investigated under many different scenarios [Stroeymeyt *et al.*, 2014]. Yet, as far as we know, only one study

[Bordoni, 2017] was performed to investigate the long term effects of pathogen exposure. In this study [Bordoni, 2017], queens were exposed shortly before the end of hibernation to a high-dose (LD50) of a fungal entomopathogen (genus *Metarhizium*), and monitored for one year. The authors report high mortality of the pathogen-exposed colonies, but no developmental effect on the surviving colonies after a year.

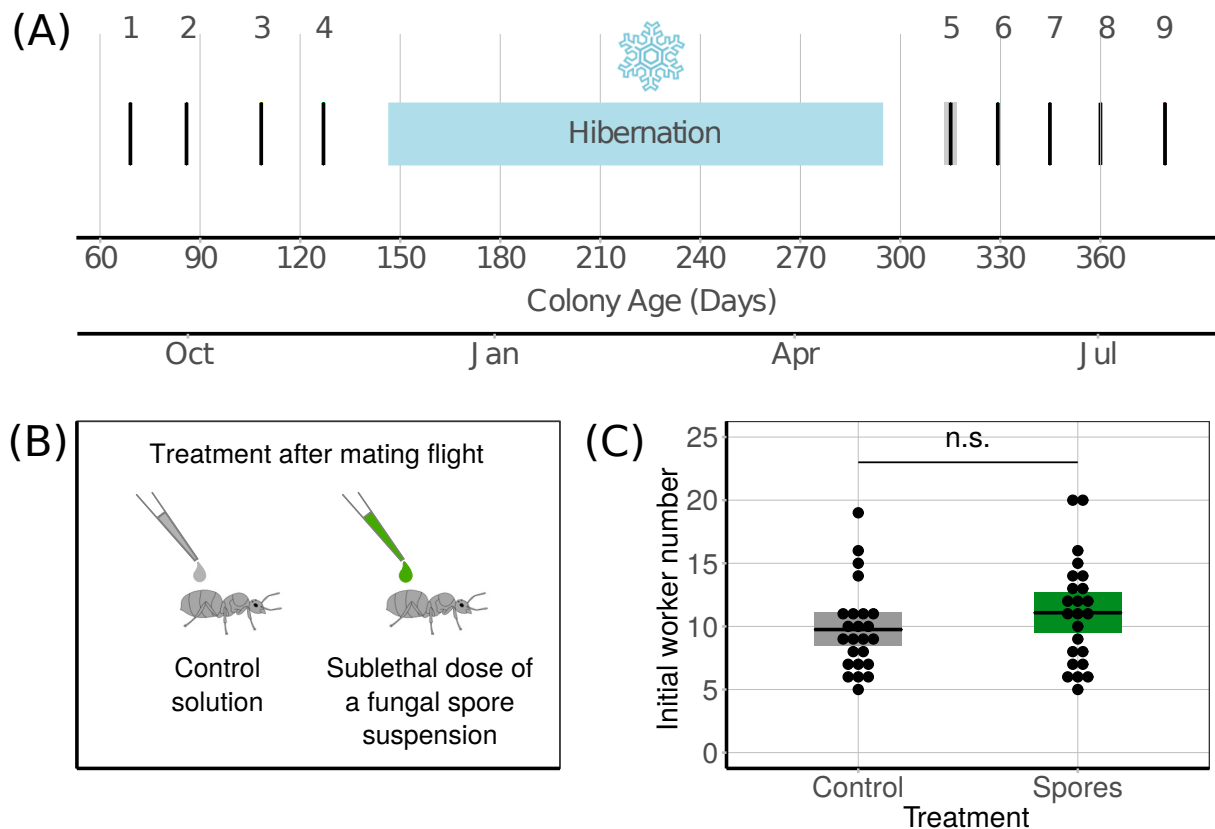


Figure 4.1: Experimental design. (A) Sampling. Forty eight queens and their incipient colonies were observed at approx. 2.5 week intervals, except during hibernation, for one year, totalling nine observation periods. (B) Treatments. Half of the queens were exposed to a sub-lethal dose of a fungal pathogen, whilst the other half were treated with a pathogen-free control solution within a week after mating flight. (C) Worker number at the start of the observation period. Observations started nine weeks after flight, when all pupae from the first batch had hatched. The number of initial workers was not significantly different between treatment groups.

Given that queens are likely to face a low level exposure during mating flight and this challenge will be closely followed by winter here we examine the consequences of such trials for queen and the development of her colony. We exposed queens directly after a mating flight to a (sub-lethal, LD2) conidiospore solution or a control solution

of a fungal pathogen and reared them under controlled conditions for a year, including a controlled (4° C) winter pause. We used the common black garden ant, *Lasius niger*, which is a claustral, monogyne, monomorphic species, with a single annually periodic and reproductive event, which means that all colonies reached winter at the same age. We used a generalist entomopathogenic fungus, *Metarhizium brunneum*, which is broadly distributed and naturally infects *Lasius niger* queens. We filmed three hour sessions every two and a half weeks on average, before and after the colonies overwintered (Figure 4.1). We monitored colony size and composition and measured overwintering survival. In addition, we extracted image-derived measures of activity, foraging, aggregation, and worker size-distribution.

## 4.3 Results and Discussion

### Growth

#### (i) Pathogen exposure slows colony growth before winter diapause

On average, colonies increased in size exponentially before and after overwintering, halting their growth during the simulated winter conditions (Figure 4.2 A). For each colony, we examined growth (measured as number of workers) during pre-diapause and post-diapause periods, separately. To estimate the growth rate ( $\beta$ ) we fit a linear regression of the log-transformed number of workers on colony age (i.e days after mating flight). This is equivalent to rearranging an exponential growth equation  $y = y_0 e^{\beta x}$  into  $\ln(y) = \ln(y_0) + \beta t$ , where  $y$  is the number of ant workers and  $t$  is the colony age. Ant colony growth is thought to be approximately logistic, but the maximum size is usually not reached within the first two years (e.g. [Tschinkel, 1998; Cole, 2009]), thus an exponential fit is suitable here. Colonies from pathogen-exposed queens, on average, grew at slower rates than control colonies during pre-diapause (Figure 4.2 B MWW  $W = 402$ ,  $p = 0.018$ ). However, growth rate was not significantly different between treatments after diapause (Figure 4.2 C MWW  $W = 128$ ,  $p = 0.789$ ). One possibility leading to a decrease in growth before diapause is that colonies had a different starting point. If contaminated queens reared a smaller first batch of brood, the subsequently smaller colonies would likely also rear a smaller number of larvae to



adulthood, resulting in slower growth compared to control colonies. We were able to rule this out since the number of workers was similar for both treatment groups at the start of the study (Figure 4.1 C MWW  $W = 228.5$ ,  $p = 0.221$ ; mean  $\pm$  SD number of workers: spore contaminated =  $11.08 \pm 4.2$ ; control =  $9.77 \pm 3.4$  workers).

To gain a better understanding of colony growth and the effect of queen spore exposure, we used a linear mixed effects analysis to model worker number (log - transformed), with treatment and colony age as predictors (Figure 4.3 A [LMER]: LR  $\chi^2 = 78.53$ ,  $df = 3$ ,  $p < 0.001$ ). This approach allowed us to introduce a different starting point (random intercept), as well as a differing rate of growth (random slope) per colony, which conveyed that the more workers a colony started with, the more it could produce. Model fit was improved by inclusion of an interaction term between treatment and colony age, indicating that the effect of treatment differed for different values of colony age (treatment\*age interaction  $\chi^2 = 6.6$ ,  $df = 1$ ,  $p = 0.010$ ). In particular, colonies from spore-exposed queens grew more slowly over time before overwintering, compared to controls. The negative effect of the pathogen seems stronger at observation periods three and four, which corresponds to periods when pupae started eclosing as adults. In contrast, colony growth seemed unaffected by pathogen exposure after winter (Figure 4.3 B [LMER]: LR  $\chi^2 = 52.46$ ,  $df = 2$ ,  $p < 0.001$ ; interaction LR  $\chi^2 = 0.45$ ,  $df = 1$ ,  $p = 0.49$ ; effect of age, LR  $\chi^2 = 51.85$ ,  $df = 1$ ,  $p < 0.001$ ; effect of treatment LR  $\chi^2 = 0.41$ ,  $df = 1$ ,  $p = 0.51$ );).

Overall, sub-lethal exposure to *Metarhizium* appears to take a toll on initial colony growth. Immune defense and reproduction have been known to trade-off in several insect species (review, [Schwenke *et al.*, 2017]), including *L. niger* ant queens [Pull *et al.*, 2013]. The delayed negative effect of the pathogen might seem surprising, but this may be due to the timing of egg laying and infection. Queens started laying eggs immediately after they were housed, whilst the pathogen takes approximately 48 hours to germinate and penetrate the host cuticle. The first batch of eggs was likely laid before the queen was infected, but an infection was possibly harboured by the queens whilst they lay a second batch and thus we see a delayed effect. There are several possibilities for the disappearance of the pathogen effect after hibernation: (a) the colonies that suffered most from exposure did not survive overwintering, (b) the pathogen was cleared before or during hibernation or (c) once the colony had grown

(A)

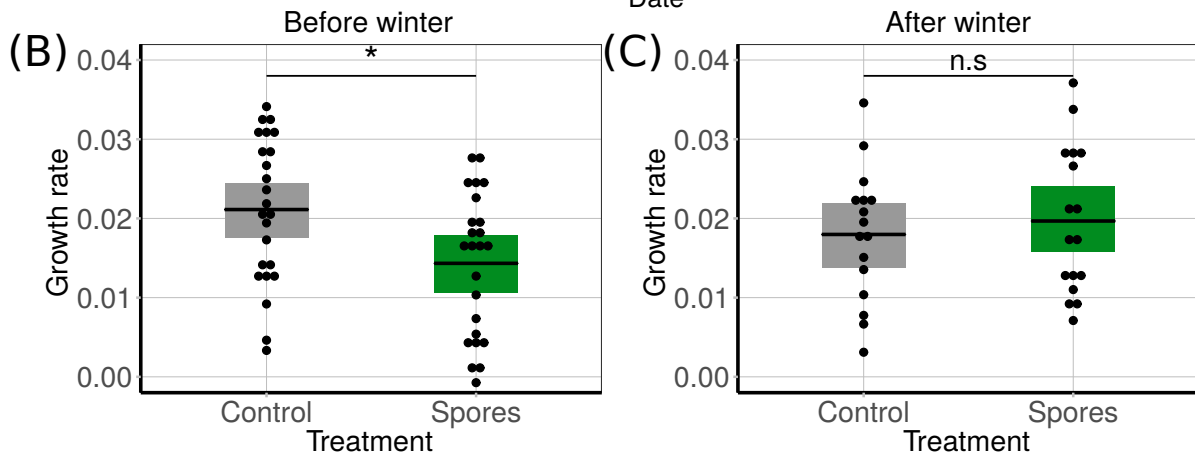
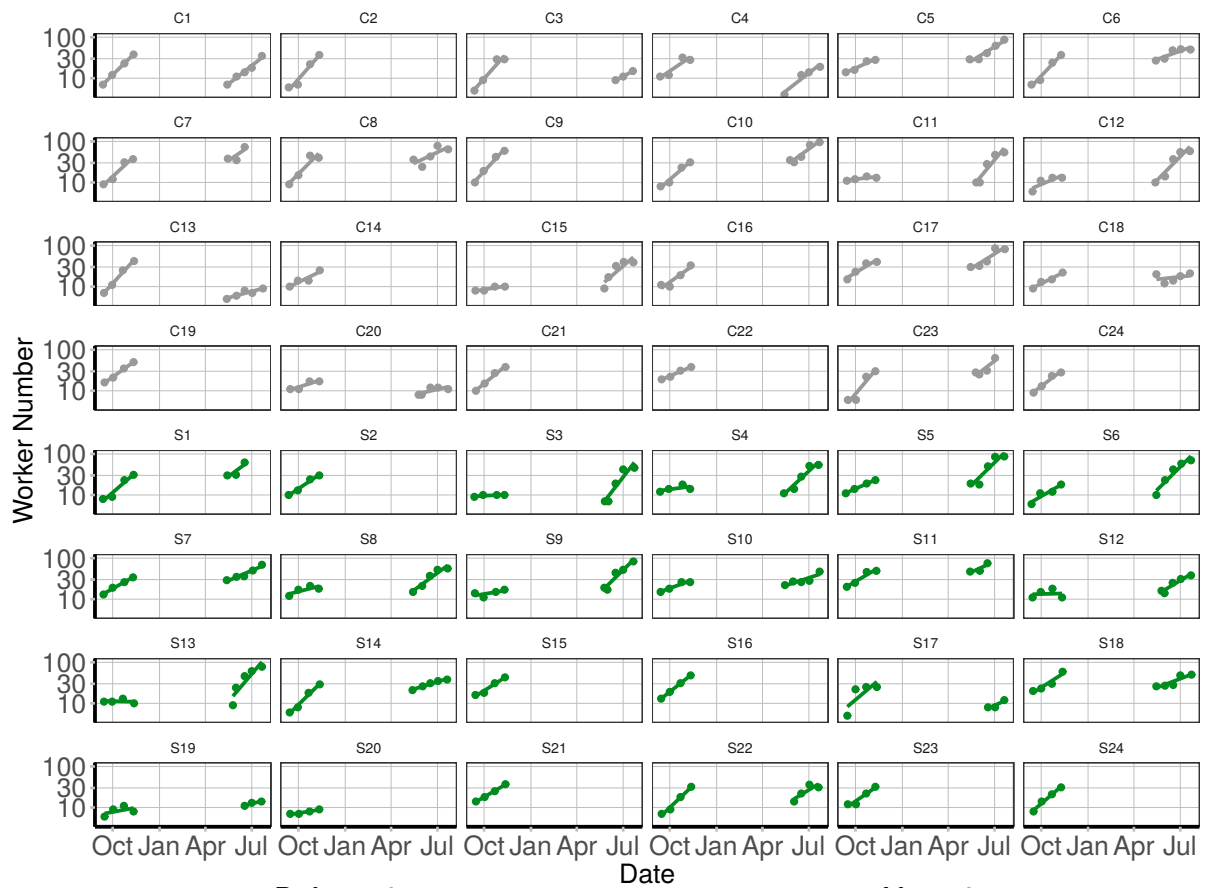


Figure 4.2: Individual colony growth trajectories (A) Number of workers as a function of time. Note the scale is logarithmic indicating an exponential growth. Scale for worker number is natural-logarithmic, time units are days after mating flight (*i.e.* colony age), but shown as months in they year. (B) Exponential growth rate  $\beta$  is slower for the colonies of spore-contaminated queens before hibernation compared to control colonies, (C) but equal after winter conditions.

beyond a critical size, brood rearing success is independent of the number of workers, and so growth rate can recover. We know that queens can sustain infections for a while before clearing them ([Pull *et al.*, 2013]). We are currently running experiments to monitor pathogen clearance, to tease apart the possible scenarios. In the following sections we explore the link between overwintering survival, colony size and pathogen contamination.

### **(ii) Slow growth increases overwintering survival odds for pathogen-exposed colonies**

The variation in colony size increases with time: before diapause, the interquartile range almost tripled for both treatment groups (Figure 4.3 C [LM]: LR  $\chi^2 = 18.74$ ,  $df = 1$ ,  $p = 0.007$ , treatment had no effect and was removed from the model). After diapause, the interquartile range increased tenfold in the controls and fivefold in spore-exposed (Figure 4.3 D [LM]: LR  $\chi^2 = 15.47$ ,  $df = 2$ ,  $p = 0.003$ , effect of time LR  $\chi^2 = 19.76$ ,  $df = 1$ ,  $p = 0.003$ ; effect of treatment LR  $\chi^2 = 11.18$ ,  $df = 1$ ,  $p = 0.012$ ). At the end of the experiment, the largest colony was ten times larger than the smallest (*i.e.* 96/9, largest/smallest). It was clear that some colonies had entered an exponential growth phase whilst others remained small (Figure 4.3). For simplicity, and to maintain a balanced design, we divided up colonies based on their growth rate before winter diapause, such that the half that grew slower and the half that grew faster than the median growth rate, respectively for each treatment group, were split in two groups. The same grouping is kept for the data after hibernation. Colonies which grew faster before hibernation stagnated afterwards, whereas slow growing colonies sped up and recovered (Figure 4.4 A-B). The fast growing colonies were equally large in both treatments, but the slow growing pathogen-challenged colonies were much smaller than the control colonies, shortly before hibernation (Figure 4.4 C [GLMER]: LR  $\chi^2 = 31.53$ ,  $df = 3$ ,  $p < 0.001$ ; interaction LR  $\chi^2 = 4.21$ ,  $df = 1$ ,  $p = 0.04$ ; Tukey post hoc comparisons  $p < 0.05$ ). At the end of the experiment (T9), the size of the colonies did not significantly differ across groups (Figure 4.4 D [GLMER]: LR  $\chi^2 = 3.91$ ,  $df = 3$ ,  $p = 0.27$ ). We did not measure pathogen load in the colonies, since our method to quantify low amount of fungal material is destructive. Consequently, we are unable to explain whether the very slow growth of some contaminated colonies was linked with pathogen load or the continuing presence of an infection. Nevertheless, if there was an effect of infection on

colony growth rate, it is likely to manifest and impact on overwintering survival. That is, if some spore challenged colonies grow slow due to heavier infection, we could expect them to be less likely to survive winter diapause.

Almost a third of all the colonies did not survive overwintering (15/48), but there was no difference in survival between treatments. Knowing that pathogen treatment slows growth for exposed colonies, but it is not directly associated with higher mortality, we wanted to know whether the opposite was true (*i.e.* slow growth leads to greater survival). Indeed, growing slow increased the probability of survival more likely for colonies of pathogen-contaminated queens (Table 4.1 Fisher's one-sided test  $p = 0.034$  OR 9.9), while there was no association for control colonies (Table 1, Fisher's one-sided test n.s OR 1). Growth rate in the presence of a pathogen becomes important for survival. How the deceleration effect is brought about by the pathogen, by the exposed queen or by the colony, merits further research.

Colonies from spore-exposed queens				Colonies from sham-exposed queens			
Growth mode before diapause	Survive	Fail	Total	Growth mode before diapause	Survive	Fail	Total
Slow	11	1	12	Slow	8	4	12
Fast	6	6	12	Fast	8	4	12
Total	17	7	24	Total	16	8	24

Table 4.1: Growth mode before diapause and survival

Colonies from spore-exposed queens				Colonies from sham-exposed queens			
Growth mode		After diapause		Growth mode		After diapause	
		Slow	Fast			Slow	Fast
Before diapause	Slow	4	7	Before diapause	Slow	4	4
	Fast	5	1		Fast	4	4

Table 4.2: Growth before and after diapause for surviving colonies

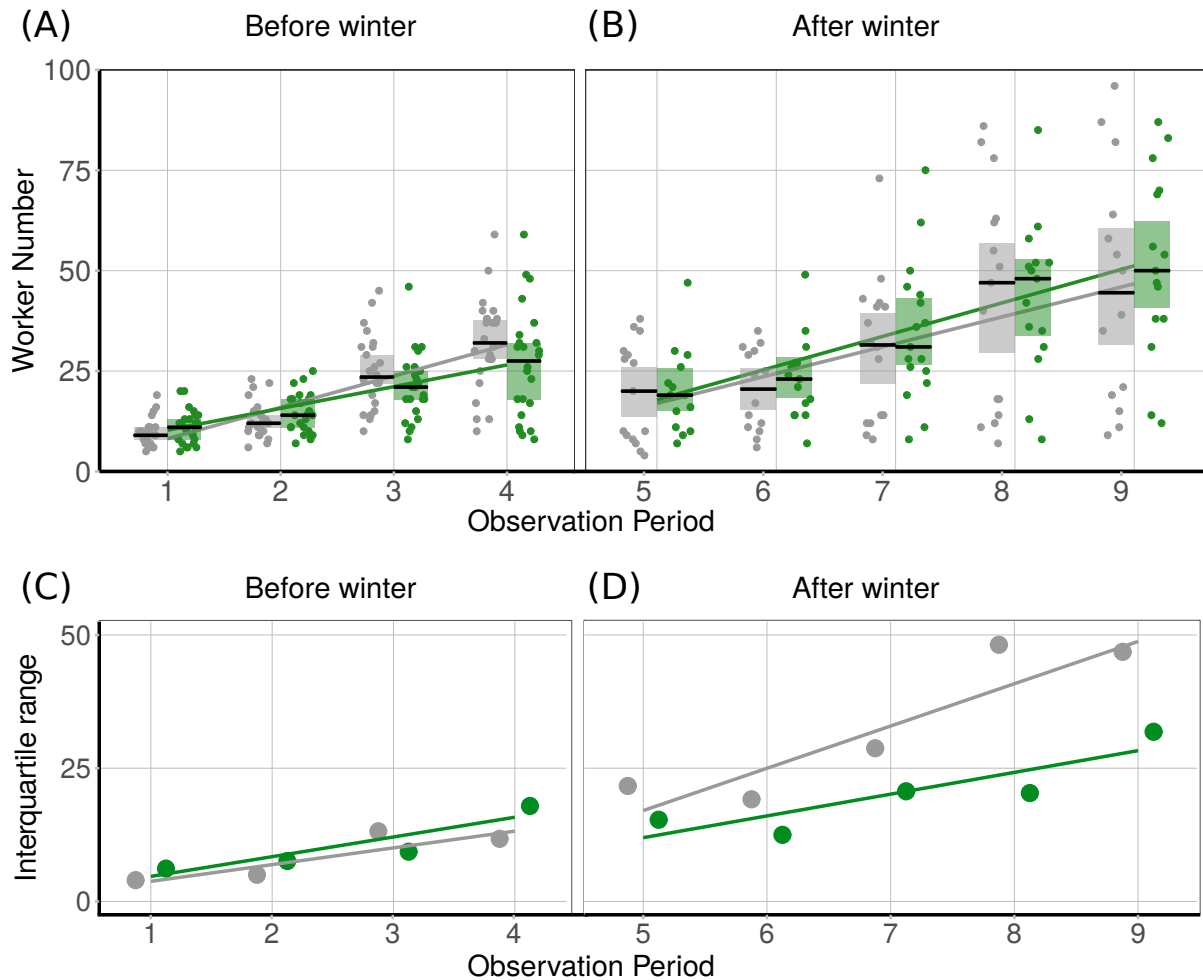


Figure 4.3: Colony growth (A) Number of worker in each colony before and (B) after hibernation. Median and confidence intervals are shown and data is grouped by treatment and observation period. Colonies from fungus contaminated queens grow slower than control colonies, the largest worker number difference is noticeable during the third and fourth observation periods, which correspond to times when pupae eclose. Notice that as colonies grow, the dispersion of worker number values increases. This is because some colonies stay small while others multiply fast. (C) Worker number variation before and (D) after hibernation. Data corresponds to the interquartile ranges of the worker number values for each treatment, in every observation period. As colonies grow, the variation in colony size increases. Statistics in text.

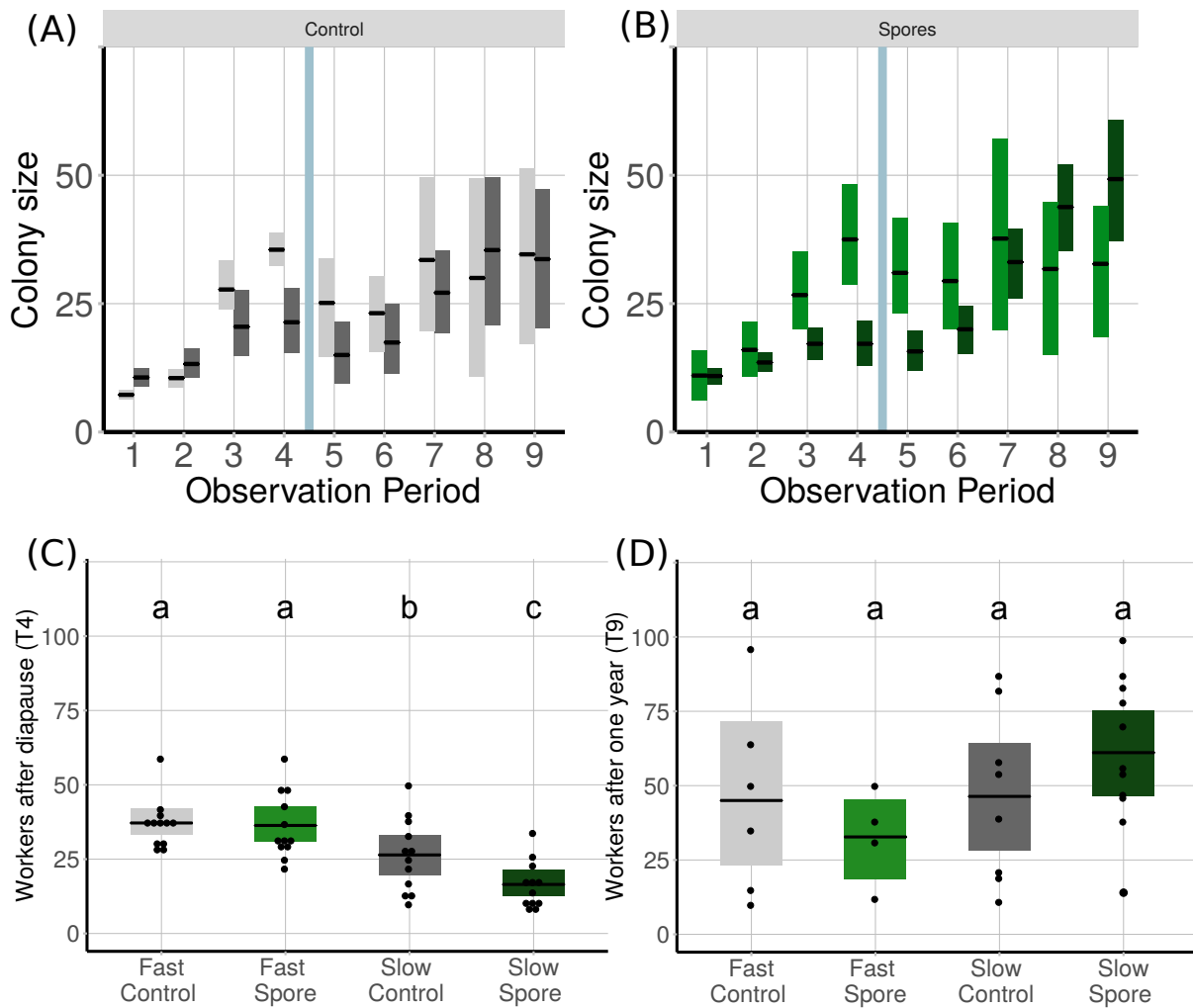


Figure 4.4: Colony size split by growth mode. (A) Worker number in colonies from queens treated with control or (B) spore solution. Mean and confidence intervals are shown and data is grouped by observation period and by growth mode: light hues correspond to fast growing colonies, dark hues, to slow growing colonies. The blue bars show when winter was simulated. Initially fast growing colonies grew slowly after hibernation and *vice versa*. (C) Worker number shortly before hibernation (fourth observation period) and (D) at the end of the experiment (ninth observation period). Data is grouped by growth mode and treatment. Letters denote significantly different groups (Tukey posthoc comparisons after GLMER,  $\alpha < 0.05$  after BH adjustment). Slow-growing colonies from spore-contaminated queens were much smaller than slow-growing control colonies, before hibernation.

### **(iii) Growth before winter diapause determines growth after winter diapause for spore-exposed colonies**

For all surviving colonies, we determined a growth modality for the whole period after overwintering, in the same manner as for the period before winter. Several pathogen challenged colonies that grew slowly were able to accelerate growth after diapause. All colonies from spore-exposed queens that had grown rapidly before diapause had slower growth rates afterwards, except for one fast growing colony, which maintained a high growth rate but died before the end of the experiment (*i.e.* colony S1). We tested the hypothesis that no modulation, *i.e.* growing fast before hibernation, would have a cost for the colonies that survived. There is a marginally significant association between growth mode before and after diapause (Table 4.2 Fisher's one-sided test  $p = 0.088$  OR 0.13). We repeated the test excluding colony S1, which survived overwintering but died before the end of the experiment. (Fisher's one-sided test  $p = 0.028$ , OR between 0 and 0.76, 95%CI). For colonies from sham-exposed queens, colony growth before diapause clearly did not determine colony growth afterwards (Table 4.2 Fisher's one-sided test  $p = 0.69$  OR 1). This result, admittedly only weakly supported by the statistics, suggests that modulating colony growth rate before hibernation has an impact after hibernation, when a pathogen is present. Modulating colony growth could be an adaptive response to pathogens in incipient colonies. Connected to this idea, modulation of colony pace [Buechel and Schmid-Hempel, 2016] has been reported as a defence mechanism against disease in mature colonies of many social insects (see Chapter 2).

## **Brood production**

We compared brood production between colonies of pathogen exposed and control queens, before and after diapause. We first analysed the relationship between brood numbers and growth rate. Afterwards we analysed the link between brood and overwintering failure.

### **(i) Slow growing pathogen-exposed colonies produced less brood**

The number of brood produced by the queens changed throughout the duration of the experiment. Moreover, production was different for queens depending on their

treatment and the colony growth rate (*i.e.* slow or fast growth mode). Slow growing spore-exposed colonies produced the smallest amount of larvae (Figure 4.5 A [NB]: LR  $s = 21.80$ ,  $df = 3$ ,  $p < 0.001$ ; interaction  $s = 4.65$ ,  $p = 0.032$ ) and pupae before hibernation (Figure 4.5 C [NB]: LR  $s = 21.80$ ,  $df = 3$ ,  $p < 0.001$ ; interaction  $s = 4.65$ ,  $p = 0.032$ ). In particular, these colonies had significantly less larvae in the first period (Figure 4.5 B [KW test]:  $H = 12.65$ ,  $df = 3$ ,  $p = 0.005$ ), and significantly less pupae during the second period of observation (Figure 4.5 D [KW test]:  $H = 21.17$ ,  $df = 3$ ,  $p < 0.001$ ). Brood production was similar otherwise, including after hibernation (see Supplement for all comparisons). The differences in brood production help to explain the slower growth of pathogen challenged colonies, since there was essentially no worker death in the colonies before winter.

We also analyzed the production of early brood (*i.e.* egg clutch and first instar larvae), which is interesting, as it presumably represents a smaller investment for the colonies, compared to production of pupae and larvae at later stages. Eggs can be viable and develop or merely represent a food source (*e.g.* trophic eggs or cannibalism), and thus do not necessarily correlate with colony growth. We observed that the percentage of colonies presenting early brood fluctuated in time. The number of time points in which colonies had early brood did not differ between slow and fast colonies, or between treatments (Figure 4.5 E [NB]: LR  $s = 0.77$ ,  $df = 3$ , ns). Interestingly, fast-growing pathogen-exposed colonies had early brood shortly before overwintering (Figure 4.5 F, no statistics). These colonies, as we will later detail, were the least likely to survive overwintering.

#### **(ii) Colonies with less brood and workers had a better chance of surviving overwintering**

We compared the total amount of brood produced before winter, between colonies that survived overwintering and those that failed. We further split up the analysis by brood type. Colonies that produced more workers, pupae, larvae and early brood were less likely to survive, independently of the queen treatment. (Figure 4.6 A-D [KW test]: workers,  $H = 5.78$ ,  $df = 1$ ,  $p = 0.016$ , pupae,  $H = 11.46$ ,  $df = 1$ ,  $p < 0.001$ , larvae,  $H = 9.8$ ,  $df = 1$ ,  $p = 0.001$ , early brood =  $6.8$ ,  $df = 1$ ,  $p = 0.009$ ).

To better understand how the composition of the colony before hibernation is predictive of overwintering survival we explored a set of models. For each observation



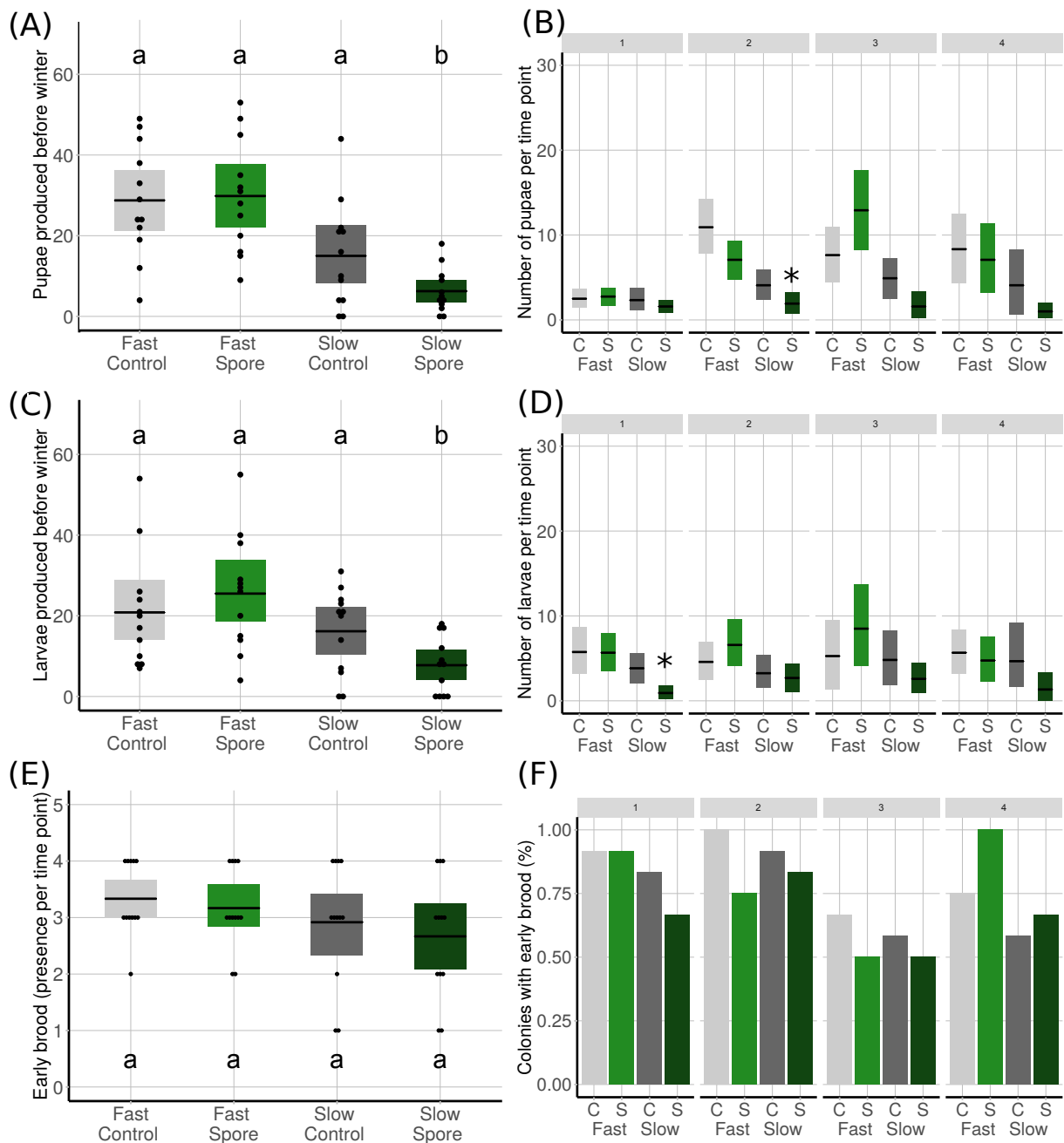


Figure 4.5: Brood production before hibernation. Total brood produced (left) (A) Total number of pupae (A), larvae (C) and (E) observation periods with early brood present. Letters denote significantly different groups (pairwise post hoc comparisons after Negative Binomial regression, significance threshold = 0.05). (B,D,F right) Brood produced per time period. Asterisk denote a significantly different group according to a Kruskal Wallis test with pairwise comparison and BH correction. Everywhere we show the mean and confidence intervals of data grouped by treatment (spore = greens, control = grays) and growth mode (light hues = fast, dark = slow).

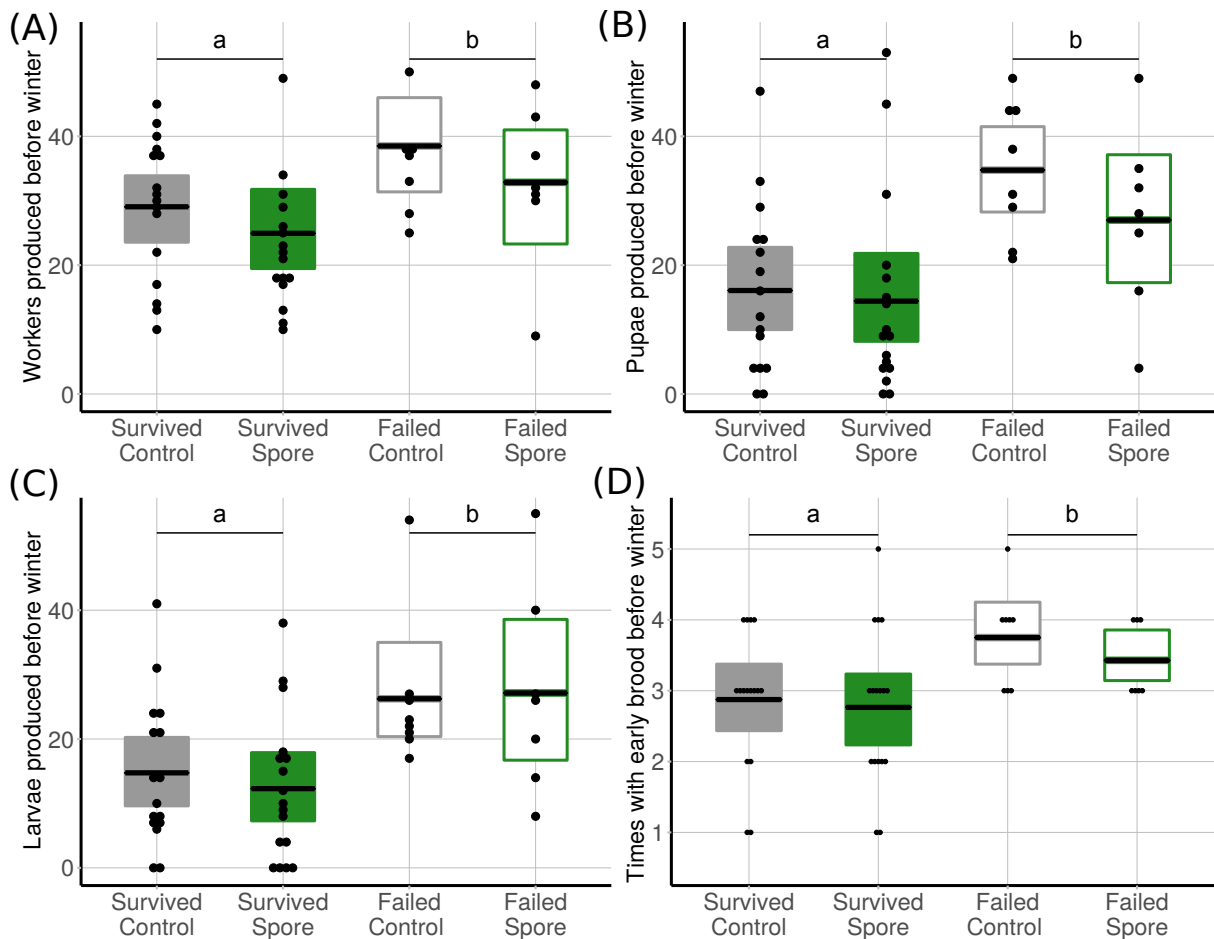


Figure 4.6: Brood production and overwintering outcome. (A) Total workers (B), pupae, (C) larvae and (D) number of observations (out of four) in which early brood was produced, before hibernation in colonies grouped by treatment and outcome. Mean and confidence intervals shown (spore = greens, control = grays) and growth mode (light hues = fast, dark = slow). Letters denote difference between groups which survived and groups which failed hibernation, there were no differences between treatments (KW with pairwise comparison and BH correction).

period, we fit a logistic regression of overwintering survival, with the total number of pupae and late larvae and the presence of early brood produced before hibernation, as predictors. We looked at how well the composition per time point predicted survival (Table 4.3). The brood composition seems to be the most predictive shortly before the colonies were put into controlled winter conditions, during northern-hemisphere winter. We conclude this based on the Akaike Information Criterion (AIC), an estimator widely used for statistical inference. Simply put, AIC scores a model considering how well it fits the data (based on likelihood estimation) and penalizing for model complexity. In this case all models have the same number of parameters, it's the data used which changes, *i.e.* we use data for one observation period at a time. Conversely, the number of brood items in any category, has no predictive power at the first time point sampled.

## Behaviour

Ants in a colony express many behaviours simultaneously that are expected to change with growth and development (*e.g.* a focus on brood care in spring). Moreover, early disease exposure may alter the response thresholds of ants in a plastic and adaptive manner. To get a proxy of colony behaviour we focused on the following measurements: (1) proportion of ants near the queen (2) mean distance of the ants to the queen, (3) proportion of ants active (exhibiting locomotion), (4) mean distance between active ants, (5) mean distance to the closest ant and (6) effective time foraging. We first investigated whether colony behaviour predicts overwintering survival, then we look at the change in colony behaviour after diapause.

Even though proportions of ants, distances averaged over a number of ants, and effective (*per capita*) time foraging are, by definition, relative to colony size, the relationship is not necessarily linear. Hence, we look at the change of each variable with respect to colony size.

### **(i) Aggregation around the queen and worker activity were predictive of survival**

Workers from colonies that survived overwintering had a smaller average distance to the queen, during the pre-hibernation period, than those which failed, irrespective of the treatment of the queen (Figure 4.7, Table 4.4 Proportion near queen, and Mean

Observation period	Model	$\chi^2$	df	p	BH adj-p	sig	Residual deviance	AIC
1	Full	6.48	3	<0.001	<0.001	n.s	53.14 df = 44	61.14
2	Full	13.75	3	0.003	0.006	**	51.16 df = 47	59.16
	Pupae	6.87	1	0.008	0.010	*		
	Larvae	12.11	1	<0.001	<0.001	***		
	Early brood	0.78	1	0.375	0.375	n.s		
3	Full	17.86	3	<0.001	<0.001	***	38.67 df = 42	46.67
	Pupae	6.25	1	0.012	0.014	*		
	Larvae	7.03	1	0.008	0.010	*		
	Early brood	13.13	1	<0.001	<0.001	***		
4	Full	24.18	3	<0.001	<0.001	***	35.44 df = 44	43.44
	Pupae	8.60	1	0.003	0.006	**		
	Larvae	4.86	1	0.027	0.029	*		
	Early brood	7.86	1	0.005	0.009	**		

Table 4.3: Overwintering survival predicted by colony composition at each time point

distance to queen). Accordingly, a smaller proportion was active, i.e fewer exceeded the speed threshold we set to determine motion (Figure 4.7, Table 4.4, Proportion of ants active). Aggregation between workers, and foraging activity were not predictive of overwintering survival (Figure 4.8, Table 4.4, Mean distance between active ants, Mean distance to closest, Effective time foraging).

### (ii) Group behaviour changes after hibernation

Aggregation and activity fluctuate across time points, irrespective of treatment. On average, the proportion of ants near the queen decreases after hibernation, as the ants become more active and leave the vicinity of the queen. This is visible both in the increased average distance to the queen and between workers. Although we do see

some scouts before hibernation, foraging becomes commonplace only after hibernation (See Table 4.5 and the third column of Figure 4.7).

LMER with queen treatment and overwintering outcome as predictors and colony ID as a random intercept		$\chi^2$	df	p	sig
Proportion near queen	treat+outcome	15.20	2	<0.001	***
	interaction	0.82	1	0.365	n.s
	treatment	3.07	1	0.079	n.s
	outcome	12.42	1	<0.001	***
Mean distance to queen	treat+outcome	10.63	2	0.005	**
	interaction	0.84	1	0.359	n.s
	treat	2.42	1	0.119	n.s
	outcome	8.25	1	0.004	**
Proportion of ants active	treat+outcome	11.23	2	0.004	**
	interaction	1.16	1	0.280	n.s
	treat	1.10	1	0.293	n.s
	outcome	10.08	1	0.001	**
Mean distance between active ants	treat*outcome	3.03	3	0.387	n.s
Mean distance to closest	treat*outcome	3.62	3	0.305	n.s
Effective time foraging (KW)	treat*outcome	1.95	3	0.582	n.s

Table 4.4: Aggregation and activity before diapause

Paired-Wilcoxon Test	V	p	sig
Proportion near queen	483	<0.001	***
Mean distance to queen	59	<0.001	***
Proportion of ants active	26	<0.001	***
Mean distance between active ants	115	0.002	**
Mean distance to closest	141	0.012	*
Effective time foraging	20	<0.001	***

Table 4.5: Mean aggregation and activity compared before and after diapause

**(iii) Aggregation and activity features were weakly dependent on colony size**

Colony size ranges from 5 to 99 workers throughout the experiment. The features

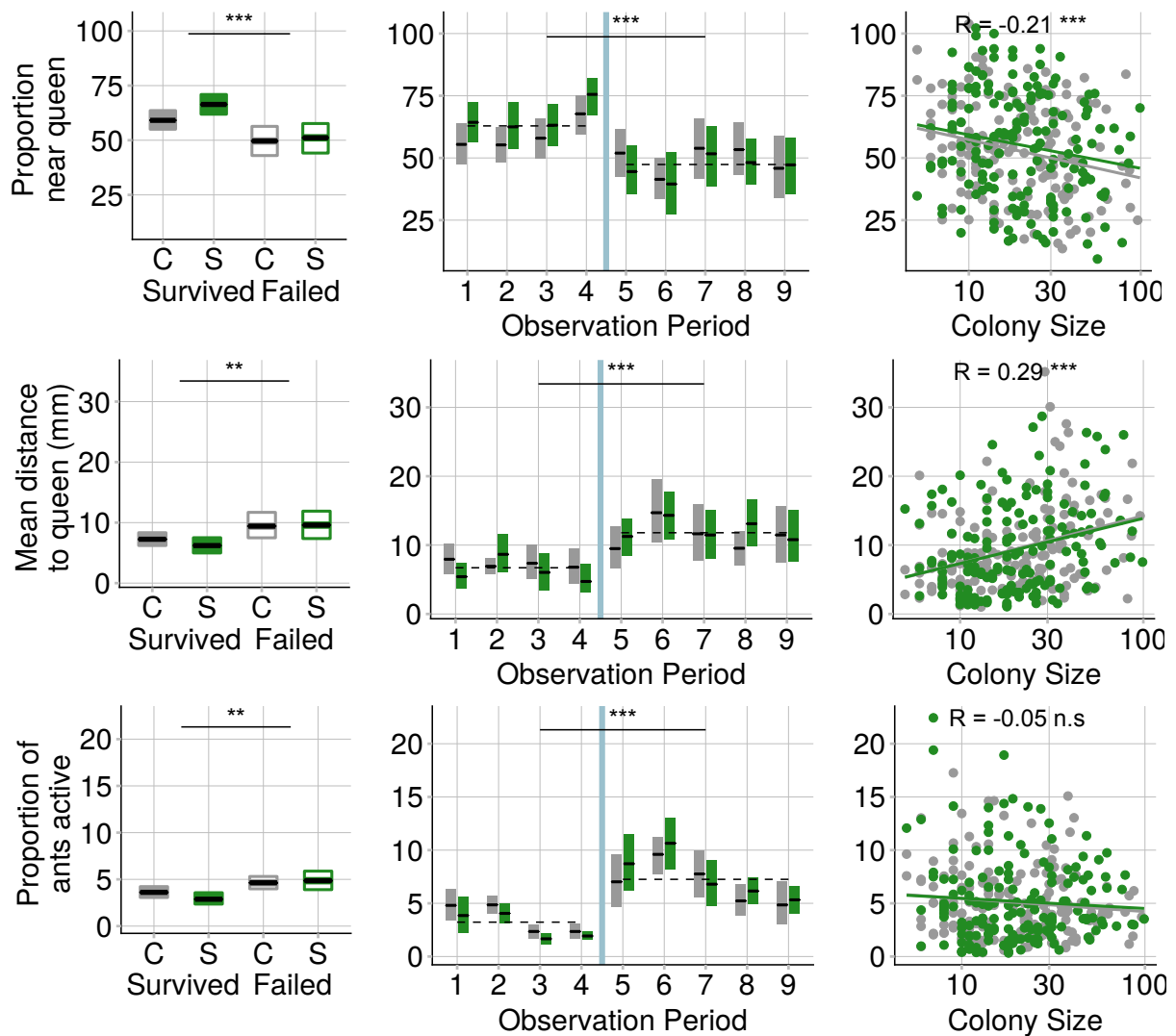
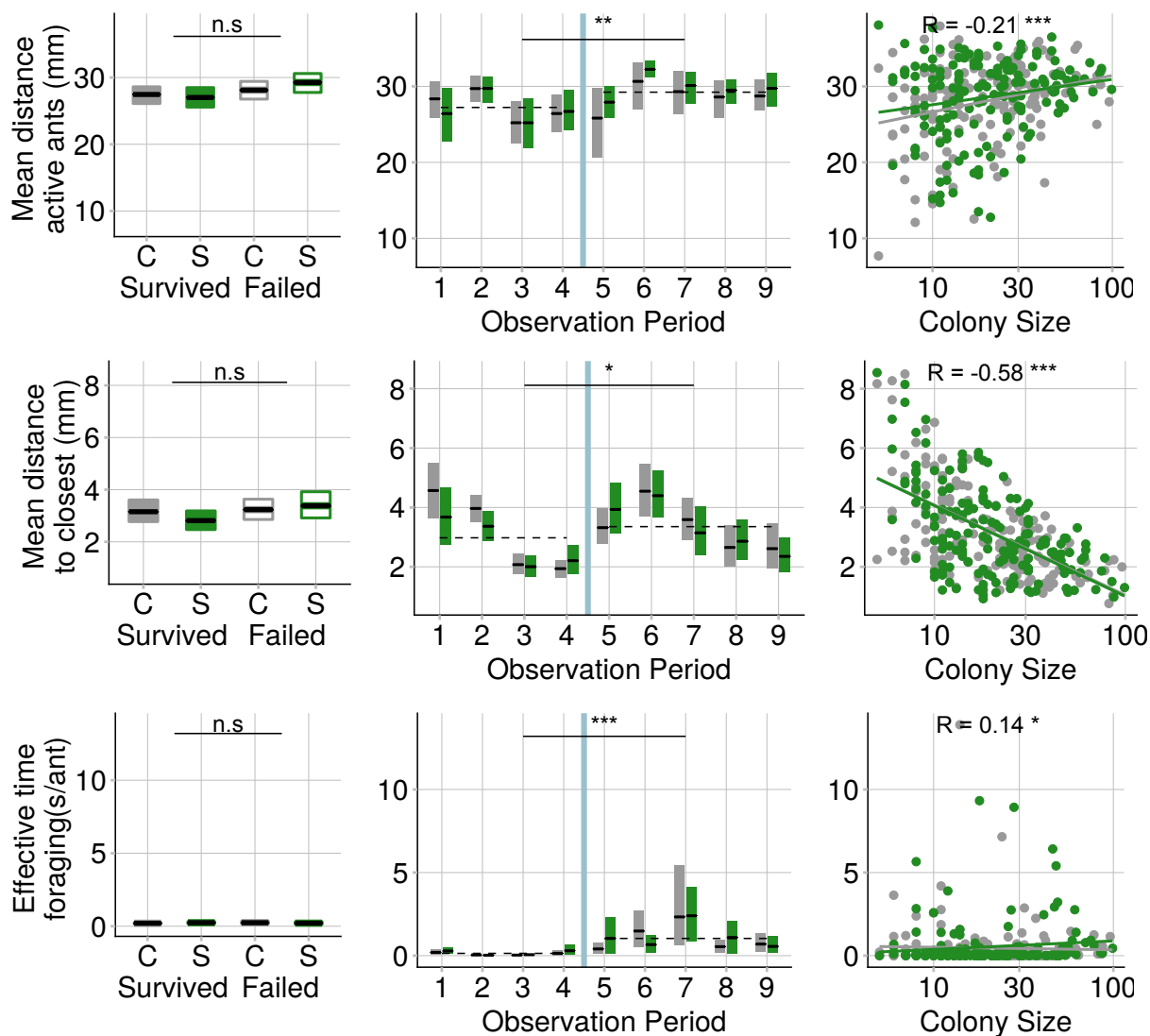


Figure 4.7: Colony behaviour. Each row corresponds to one behavioural variable. The first column shows the mean and confidence interval of the values before diapause in colonies grouped by treatment and overwintering outcome. Asterisks denote significance of the survived/failed factor in the models predicting the variables on the y-axes as a function of treatment and survival (See statistics in Table 4.4). The second column shows the mean and CI for each observation period. Asterisks denote significant change after winter compared to values before winter (See statistics in Table 4.5). The third column shows a scatter of the values against colony size, together with a linear regression, with  $R$  and significance level indicated (but See statistics in Table 4.6). Not significant ( $p > 0.5$ ) is denoted by n.s, while significance level is denoted by asterisks as follows,  $p < 0.01$  \*,  $p < 0.001$  \*\* and  $p < 0.0001$  \*\*\*.



Colony behaviour (Continued). Each row corresponds to one behavioural variable. The first column shows the mean and confidence interval of the values before diapause in colonies grouped by treatment and overwintering outcome (See statistics in Table 4.4). The second column shows the mean and CI for each observation period. Asterisks denote significance change after winter compared to values before (See statistics in Table 4.5). The third column shows a scatter of the values against colony size, together with a linear regression, with R and significance level indicated (but See statistics in Table 4.6). Not significant ( $p > 0.5$ ) is denoted by n.s, while significance level is denoted by asterisks as follows,  $p < 0.01$  \*,  $p < 0.001$  \*\* and  $p < 0.0001$  \*\*\*.

computed (means and proportions) should be independent of colony size if the relationship between these variables and colony size were linear. To check if the variables are roughly linear with respect to colony size for both treatments, we used linear mixed models with each variable as a response and colony size and treatment as predictors, specifying time and colony identity as random effects, to deal with non-independence of the observations. In addition we computed a Spearman correlation, from which one can directly interpret the strength of the association (See Table 4.6 and the third column of Figure 4.7).

Whilst treatment had no effect, the responses changed weakly with colony size. In particular, workers were slightly less likely to be near the queen when the colony size was larger (Figure 4.7, Table 4.6 Proportion near queen and Mean distance to queen) and more likely to be closer to other workers (Mean distance to closest). The proportion of active ants and the foraging activity did not significantly change with colony size (Figure 4.7, Table 4.6 Proportion of ants active, Effective time foraging).

The spatial patterns of individuals are linked to their social interactions. In our study species (*L. niger*) brood-tending ants gather in large stable clusters, whilst food-gathering ants aggregate in short-lived small clusters [Depickère *et al.*, 2004]. Functional segregation into behavioural clusters (*i.e.* foragers and nurses) and the stability and strength of these clusters, can have serious implications for a colony. For instance, the social structure of *L. niger* has been shown to have transmission inhibiting properties, which are further enhanced adaptively, as the colony responds to the presence of a pathogen [Jander, 1976; Stroeymeyt *et al.*, 2014]. Aggregation patterns in these examples are quantified directly by monitoring individuals and their interactions. The imaging techniques implemented to do so have improved considerably in the past decade and continue to achieve greater precision, efficiency and usability (See Chapter 5).

We measured aggregation of workers in three ways, with respect to the queen, with respect to each other (closest ant), and between active ants. We categorized those ants which stay close to the queen, those (active) which move, and those which forage. We directly measured foraging activity as the time of overlap with a delimited food source. These measurements together provide a unique and, previously, uncharacterized view of colony behaviour during early development .



LMER with queen treatment and colony size as predictors and colony ID and colony age, as random effects		$\chi^2$	df	p	sig	Spearman correlation $\rho$ and BH adjusted p-value
Proportion near queen	treat*size	14.681	2	<0.001	***	r = -0.21 p <0.001
	interaction	0.396	1	0.529	n.s	
	treat	0.563	1	0.453	n.s	
	colony size	24.13	2	<0.001	***	
Mean distance to queen	treat+size	27.40	2	<0.001	***	r = 0.29 p <0.001
	interaction	0.005	1	0.944	n.s	
	treat	0.786	1	0.375	n.s	
	colony size	26.94	1	<0.001	***	
Proportion of ants active	treat*size	0.130	3	0.988	n.s	r = -0.05 p = n.s
Mean distance between active	treat+size	24.121	2	<0.001	***	r = -0.21 p <0.001
	interaction	1.237	1	0.266	n.s	
	treat	0.615	1	0.443	n.s	
	colony size	23.444	1	<0.001	***	
Mean distance to closest	treat+size	78.56	2	<0.001	***	r = -0.58 p <0.001
	interaction	0.49	1	0.482	n.s	
	treat	0.12	1	0.727	n.s	
	colony size	78.40	1	<0.001	***	
Effective time foraging	treat*size	4.88	3	0.180	n.s	r = 0.14 p = 0.014

Table 4.6: Aggregation and activity relationship to colony size

## Worker size

An increase in worker body size is expected, as small nanitic workers are joined or replaced by larger workers. To detect this transition and test whether the pathogen had an effect on its timing, we estimated worker size distribution from each video. We did so by sampling the area values of single ant detections from the image-segmented frames of the videos (See Methods and Chapter 5 for more detail). Morphometric head width measures are certainly more stable than body area. Comparison between area and head width measures in our experiment should be done to validate our results.

Before winter diapause, worker size fluctuates without any discernible trend (Fig-

ure 4.8 [LMER]: LR  $\chi^2 = 0.004$ , df = 1, p = 0.99). After winter diapause, worker size was small but steadily increasing (Figure 4.8 [LMER]: LR  $\chi^2 = 56.69$ , df = 1, p < 0.001). We did not detect any effect of treatment in worker size before or after diapause. We detected, by means of image processing, an overall increase in worker size, confirming previous observations based on measuring ant morphometrics [W.R. Tschinkel, 1993]. In the case of tropical fire ants, most of the change in worker size occurred over the course of six months [W.R. Tschinkel, 1993]. In contrast, for *L. niger* we observed little change in the four months observed before hibernation, and consistent growth only thereafter.

We speculate that the transition from nanitic to full sized workers, could be delayed in all temperate species, compared to tropical species. One reason for this delay could be a constraint in colony development, for example, if the colony needs to reach a certain metabolic threshold before the brood can start developing into ordinary workers, rather than nanitics. In fact, there is evidence of such a threshold (75-200 individuals) above which nanitics engage in cooperative foraging, and the colony starts producing normal sized workers [Deacon, 2013]. This is consistent with our observations that foraging only occurs after diapause.

A second possibility, is that delaying the production of full-sized workers is an adaptation to overwintering, for instance if nanitics were better suited to withstand the winter conditions. Because nanitics are smaller, they presumably need less metabolic reserves to sustain them over winter. Nanitics have been shown to survive longer than foragers [Kramer *et al.*, 2016], but the comparison is controversial given that foragers engage in more risky activities (*e.g.* risk of encountering pathogen while foraging [Cremer *et al.*, 2007]). An increased overwintering survival of nanitics could manifest as either death of normal sized ants, production of nanitics during the winter, or a combination of both. In any case, a decrease of median worker size would be observed. In this experiment, indeed we detect a considerable drop in median worker size after diapause, that is, the median of the size distribution is significantly smaller in time point five compared to time point four (Figure 4.8 [LMER]: LR  $\chi^2 = 21.154$ , df = 1, p < 0.001). The salient drop in size, given that there is no significant reduction in colony size (4.3) suggests that during winter, workers produced were particularly tiny. We did not find differences in worker size distribution between colonies which survived and those which

failed, neither with respect to treatment and growth mode. Nevertheless, we suggest a more systematic comparison between nanitics and full sized workers, which measures survival, physiological performance and size over different winter scenarios (*i.e.* a wider range of temperatures and starvation lengths).

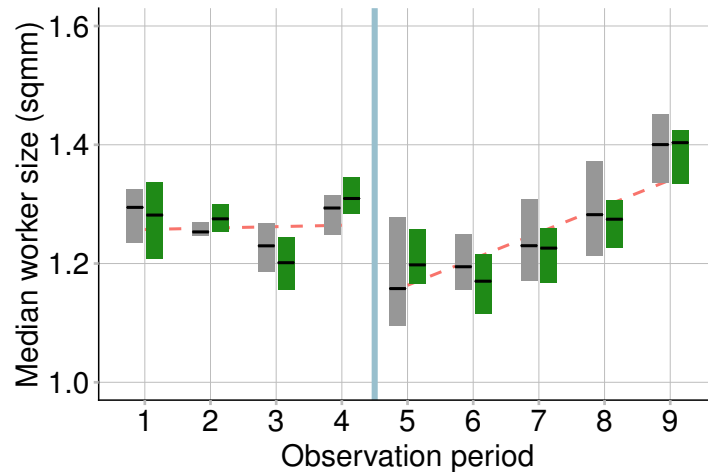


Figure 4.8: Worker size change in time. Mean and confidence intervals of worker size measured as area (in square millimeters) per observation period, and grouped by treatment. An LMER was fit for the median worker size before and after hibernation, with treatment as film batch as predictors. Treatment had no significant effect. So the models without treatment as a predictor are shown as dotted red lines.

## 4.4 Conclusion

In summary, pathogen contamination of the queen can slow down colony growth. Contrary to what we expected, fast growth in pathogen-exposed colonies leads to an increased susceptibility to overwintering failure. Moreover, growth rate before diapause will affect growth rate after diapause. Hence, modulating colony growth in the presence of a pathogen could be an adaptive trait.

The composition of the colony shortly before hibernation had the best predictive power for overwintering survival but, colony growth modulation is bound to happen much earlier.

We do not know whether the queen or the workers are responsible for the growth deceleration. We also do not know by which mechanism this happens. We can draw from

the existing literature to formulate a hypothesis. There is an interesting link between reproduction, immunity and hibernation.

In insects, the juvenile hormone (JH) stimulates vitellogenesis (*i.e.* leading to egg production) and suppresses immunocompetence [Schwenke *et al.*, 2017]. In ants, a synthetic analogue of JH is known to suppress both vitellogenesis and immunocompetence [Pamminger *et al.*, 2016]. The decoupling of JH and vitellogenesis would explain how queens can survive for impressively long periods while maintaining a high yield of brood throughout, escaping the reproduction-survival trade-off.

The levels of JH steeply decline at particular moments in the haemolymph of sub-adult insects, allowing them to transition to the next stage [Hiruma and Kaneko, 2013]. During winter diapause, JH halts larval growth. The molecular pathway which leads to lipid accumulation, also leads to JH synthesis. In ants, JH can be fed to larvae by the workers [Leboeuf *et al.*, 2016] and possibly also by the queen. In this way, in addition to modulation by environmental cues, the schedule of brood development can be adjusted by the colony.

On one hand, the colony should use JH to halt larval development, since pupae do not survive the winter. On the other hand, a queen under pathogen stress should not produce JH since it would suppress her own immunocompetence.

The overwintering survival of a colony depends on its particular state (*i.e.* size and composition) at the time winter strikes it. The colonies which did not survive had grown large in worker and brood numbers when they were forced into diapause. We hypothesize that these colonies produced a large amount of JH, either as a measure to slow down larval development or as a byproduct of the lipid pathways triggered during diapause. The large metabolic expenditure combined with the immune suppression caused by JH, is likely responsible for the reduced survival of larger colonies in this experiment.

Overwintering survival is also predicted by the pattern of aggregation around the queen (*i.e.* proportion of ants near queen and mean distance to queen) and the proportion of active ants. We believe that these patterns of aggregation are related to colony size. Larger colonies produce a large amount of brood, and as the number of brood items increases, it becomes more likely that a second brood pile is formed. The workers move between brood piles to care for the brood. This phenomenon simul-

taneously explains more active ants, further away from the queen, in larger colonies, which also tend to fail overwintering. This does not exclude that ants which aggregate closely near the queen, could be providing care which makes these colonies more likely to survive.

We thus have an experimentally malleable developmental system, which can be easily and cheaply reared and monitored in the long term, and combined with physiological measurements, is likely to shed light on many interesting questions from evolutionary biology and ecology, and perhaps also, at least by analogy, to developmental biology. For instance, the delayed growth observed in pathogen challenged colonies warrants comparison to the little-understood embryonic diapause, *i.e.* an obligate or facultative, quiescent stage in blastocysts, which synchronizes development with more favourable conditions in many species [Renfree and Fenelon, 2017].

The early development of a colony is a collective phenomenon of dynamic optimization. Incipient colonies do not simply need to maximize growth, as this may be too costly once resources have just been invested in immunity. The timing of any decision is crucial when the cost of overwintering is steep. In this work we have shown that a sub-lethal pathogen contamination during colony founding, can have a large impact on the developmental trajectory of a colony. Pathogen challenged queens can grow slowly and survive the winter, or grow fast and risk overwintering failure. When they survive, the growth mode before hibernation will impact their growth afterwards.

It is increasingly possible to move beyond colony size to describe a social insect colony. The composition (*i.e.* worker and brood categories), and behavior (*i.e.* aggregation and activity patterns) of the group can add crucial information. From an evolutionary point of view, early colony development is key to understanding the evolution of eusociality, by identifying the times when selective pressure is highest, and the traits upon which it acts. The strategies of the superorganism to face developmental challenges, should inform and benefit from comparison to other social systems, including multicellular organisms.

## 4.5 Method

### Collection and exposure

We collected *Lasius niger* queens during mating flights on campus, at IST Austria, on July 5, 2014. The queens had mated and shed their wings. Five days after collection, we exposed individual queens, by holding them with sterile soft forceps, and smearing a 0.5ul droplet of a conidiospore suspension or a sham solution onto their thorax. The fungal suspension was prepared from sporulating agar plates (6.5% Sabaroud dextrose) of *Metarhizium brunneum*, Ma275 KVL 03-143 and adjusted to a concentration of  $2 \times 10^4$  spores per mL of 0.05% sterile Triton X-100 (Sigma). The germination of the spores was >95% for all plates used, and the killing rate for the dose applied to queens of this species was LD-2, determined during preliminary studies. Sham-treated ants were exposed to sterile Triton X-100.

### Rearing and overwintering

After exposure, we transferred the queens to individual clear plastic vials (height= 3 cm,  $\varnothing = 2$  cm) with a plastered base as substrate. They were maintained in a climate controlled room, at 23 °C and 70% humidity, and the plaster was kept moist. As *L. niger* queens do not forage (*i.e.* they are claustral founders), we did not provide food before the first workers had eclosed from pupae.

Once the first batch of workers had emerged, we housed 48 colonies, 24 spore-exposed and 24 control-treated, in plastic petri dishes (height= 3 cm,  $\varnothing = 9$  cm) with 1/2 division. Half the dish had plastered-flooring, and half was left bare. The ants could freely move across, but the plastered half was generally preferred by the queens and the unplastered part is where we placed the food. This arrangement served to keep the plate cleaner. A vial with sucrose solution (25%, in a cotton-plugged tube) and minced cockroach (*Blaptica dubia*) were provided and replaced weekly.

All colonies were moved into simulated winter conditions (4 °C), starting 130 days after they were collected, and for a period of 20 weeks (mid-November to mid-April). Afterwards, the colonies were returned the climate-controlled room at 23 °C and 70% humidity.

## Filming and colony counts

We started filming all colonies five weeks after the mating flight (Sept 12, 2014), when the first batch of workers had emerged (average number of workers =  $10 \pm 3$ , no difference between treatments). Colonies were filmed inside the climate-controlled room every  $2.55 \pm 0.36$  weeks for three hours each, except during the overwintering period. Filming was carried out between 7am and 8pm GMT+1 and filming order was randomized. We stopped the experiment one year after the queens' mating flight (July 20, 2015).

Briefly before filming, food and large debris were removed from the plate, and honey was offered as foraging stimulus. A honey droplet was sandwiched between plastic and a piece of paper-towel cut into a triangle and placed in the unplastered area, to help clearly delineate a foraging arena. After recording, we replaced the honey with sucrose solution and minced cockroaches.

Approximately, a thousand hours of video were recorded (more than 18TB produced), for 337 projects, one per colony per time point. We focused on the colonies which survived for the duration of the whole experiment (29/48 colonies). But we also looked at colonies that did not make it through winter (19/48).

We recorded four colonies at a time, two controls and two spore-exposed, in a parallel setup (rolling-shutter cameras from IDS UI-1640LE USB 2.0 CMOS, at 15fps before overwintering and 18fps after overwintering, 1024x1024, 1.3MPixel, 1.3" Aptina Sensor, rolling-shutter; fixed focal length lense 6MM 1/1.8" f 1.4-f/16 C-mount, Edmund Optics; Streampix software for acquisition).

From still images extracted from each video, we manually counted the number of workers, pupae and larvae (2nd and 3rd instar) and noted down the presence of eggs and small (1st instar) larvae. We made no distinction between new brood items and brood present at two consecutive time points. Nevertheless, after 2.5 weeks we expected most brood to have transitioned to the next stage, since development from egg to adult approximately takes 6 weeks, with 2 weeks between each of four stages. Nevertheless, developmental time is a plastic trait which can vary with colony parameters, such as colony size, and thus we cannot discard that some brood is double-counted in consecutive time points.

## Image analysis and feature extraction

Each video was processed with FERDA, a general multi-object tracking software, implemented in Python and adapted specifically to solve the complex task of detecting ants in our setup. (see Chapter 5). The ants are detected across different backgrounds (*e.g.* plastered area adopted as a nest, or unplastered area with food). The foreground (a number of similarly sized ants, running alone or interacting closely with each other around a larger ant queen) has to be discerned from a difficult background (with non-static brood items and detritus). The size, shape, orientation and color are features (image moments) which alone, are usually not sufficient to classify foreground from background. More sophisticated pattern descriptors computed from image moments were also not sufficient for our task. FERDA provides a tool for training a background/foreground, pixel-based, supervised (Random Forest) classifier, efficiently using a large set of features. The classifier outputs, for each pixel in each frame, a probability of belonging to the foreground. The MSER method ([Matas *et al.*, 2004]) is applied to the corresponding matrix of probabilities as follows. The probabilities are thresholded with a series of threshold values, and connected regions of the frame which remain above many of said values are considered to be ant detections (foreground objects). Detections in consecutive frames can be assigned the same identity when they fulfill certain criteria, and a sequence of detections with the same identity constitute a trajectory. The output contains a list of trajectories and for each frame in a trajectory: 1) a position, 2) a contour and 3) area of a detection (in pixels).

This process has two steps. The first step requires user interaction and is done from a desktop computer. In this step, we delimit the arena, constrain the number of detections (*i.e.* the number of ants to search for) and generate a training set for the foreground/background classifier from a random set of frames. The second step requires computing power to classify all regions and assign them to trajectories. Each project was processed as a set of parallel tasks. Each task has access to a small part of a video (100 frames). The results for each task are written as separate files. The process was executed on an High Performance computing Cluster at IST Austria.

The videos have two qualities that made them particularly challenging for image analysis and so required cleaning steps. On one hand, ants had a somewhat wide



range of coloration. That is because ants which recently eclose have little cuticle pigmentation, which darkens as they age. The range of cuticle coloration closely resembles that of other elements found in the nest (*e.g.* faeces, food bits that are placed by the ants near the brood, small holes dug on the plaster, shadows). These elements are sometimes incorrectly classified as ants and assigned to trajectories. We refer to the trajectories made up from these elements as spurious tracklets.

On the other hand, the ants tend to lay immobile and very close to each other, for long periods of time. These groups of ants, and their shadow, are often classified as a single detection. The trajectories which consist of multiple ants are referred to as multiple tracklets. The queen is usually found closely surrounded by workers, that is, one of the multiple tracklets contains the queen, and we refer to it as queen tracklet.

Even though the videos present these problems, there are many detections which are accurate and correspond to single ants. The majority of these detections belong to ants which are far away from each other and moving. We call these trajectories single tracklets.

We wrote Matlab scripts to determine whether tracklets contained multiple ants - with or without a queen- single ants or spurious detections. We filtered spurious tracklets and inferred the number of ants inside multiple tracklets, to generate features which were comparable across time points and across colonies. Below we describe the cleaning, supervised annotation, and feature extraction steps in detail.

The output of the processing done by FERDA on the HPC cluster, is a series of files containing trajectories for small parts of the video. The series of files that correspond to a video need to be accessible by all post-processing scripts. Given the large size of the data, it is not possible to simply load all trajectories to memory at once. To handle the data, we implemented a trajectory manager as a Matlab class. An object of this class contains, for instance, information on which trajectories exist at any given frame. Importantly, it loads trajectories from files into memory as they are required.

The criteria to label single tracklets, were: a velocity larger than 1mm per frame and mean area smaller than 1.8mm<sup>2</sup> with standard deviation, across frames, of less than 1.3 mm<sup>2</sup>. This step required no user intervention. The first step that requires input prompts the user to adjust the arena bounds, mark the foraging area and input the number of ants in the video. Next, a frame with a large number of detections is shown,

where the user selects spurious detections. The selected detections, and detections outside the arena boundary, are labelled as spurious. The position and contour of labelled spurious tracklets is used to detect reappearing spurious detections. If the centroids of all detection in a tracklet are contained within the contour of a previously labelled spurious detection, the tracklet is labelled spurious, as well.

Then, the user is presented with the first frame of the video, to select the queen detection. The corresponding tracklet is labelled queen tracklet. The first frame after the end of the queen tracklet is shown for the user to select the queen detection, and in this way the user is prompted to label ten consecutive queen tracklets. From these manually annotated queen tracklets, we infer the mean size and displacement of the queen detection. The following queens tracklets are labelled automatically as such, when they are similar sized and have a relatively small displacement with respect to the last queen detection. Otherwise, the user is again requested to select the queen tracklet. At this point, the user can also select additional spurious detections, that could have gone undetected by the process mentioned above. Annotation of queen tracklets and spurious tracklets is done at once, to save user time, as well as to avoid the costly access to trajectories and video.

The final step requires user input to select an intensity threshold which correctly segments pixels inside a multiple tracklet. With the selected value, the image inside the contour of a multiple tracklet is thresholded to estimate the number of ants inside of it as function of the area whose intensity is below the threshold. This estimation is done using a linear model previously adjusted by hand, after manually annotating multiple detections with counts. The model is  $count = round(0.0027 \text{ area\_after\_thresholding } K + 0.54)$ , where  $K$  is the quotient between mean area of the single tracklets of the video with which the model was adjusted, and the mean area of the single tracklets in the video being processed. To find the threshold, the user is presented with frames thresholded by different intensity values and with estimated counts, according to the linear model. The user chooses the frame in which the estimate best matches the number of ants presented. In summary, after user interaction, we end up with supervised classification of each trajectory, as well a the best suited threshold value to get counts inside multiple tracklets.

Another round of processing is done in the HPC cluster, consisting of two steps

per video frame. First, the user-selected threshold is applied to detections in multiple tracklets and the model estimates the number of ants contained inside them. Second, a number of features based on position and speed of all ants, is computed, namely:

- Number/fraction of active ants (number)
- Average speed of active ants (mm / s)
- Average speed of all ants (mm / s)
- Average pairwise distance between all workers (mm)
- Average pairwise distance between all active workers (mm)
- Average distance between each worker and the queen (mm)
- Average distance between a worker and the next closest worker (mm)
- Number/fraction of ants inside the foraging area (number / sqmm)
- Number and size of the ants estimated inside each detection (number / sqmm)

## Statistical analyses

**General statistical procedures.** To estimate the significance of the predictors, all generalized linear and mixed models (*i.e.* LMER, LM, GLMER, GLM) were compared to null (intercept only) and reduced models (for models with multiple predictors) using Likelihood Ratio (LR) test [Bolker *et al.*, 2008]. All significance values were corrected using the Benjamini-Hochberg procedure ( $\alpha = 0.05$ ) to protect against false discovery rate when multiple inferences were made [Benjamini and Hochberg, 1995]. We checked the necessary assumptions of all tests *i.e.* by viewing histograms of data, plotting the distribution of model residuals, testing for unequal variances, testing for the presence of multicollinearity, testing for over-dispersion, and assessing models for instability and influential observations. Specific details for each analysis are described below.

**Growth.** To compare the worker number between treatment groups, at the start of the experiment, we used a Mann-Whitney-U test or Mann-Whitney-Wilcoxon test

(MWW), a non-parametric procedure for independent samples. We used Paired-Wilcoxon signed-rank tests to compare the growth rate  $\beta$  between treatment groups before and after overwintering.

Colony growth was further analyzed with a general linear modeling framework [Bolker *et al.*, 2008]. We specified a linear mixed effects regression (LMER) with worker number (log-transformed) as a response, and as predictors, treatment (categorical), colony age (numerical), and their interaction. To handle the non-independence coming from repeated observation, we included a random intercept and slope for each colony [Bolker *et al.*, 2008].

To determine whether the variation in size across colonies increases with time, we modeled the interquartile range of worker number per observation period as a linear function of observation period and treatment. We assessed the significance of each predictor and reduce the model accordingly. The linear models (LM) were fit separately for observations before and after the simulated winter.

The colony size shortly before hibernation was compared across colonies, grouped by treatment and growth rate, using a general(ised) linear model (GLM) with Poisson error terms for count data and logit-link function. Specifically, worker number during the fourth observation period, was modeled as a function of treatment (*i.e.* categorical, spore contaminated or control) and growth (*i.e.* categorical, slow or fast growth, detailed in main text). The same was repeated for colony size at the end of the experiment, *i.e.* worker number of colonies at the final (ninth) observation period.

The associations between growth mode and survival were tested (separately for pathogen contaminated and control colonies), with a one-sided Fisher's exact test. Based on the knowledge that there was no survival differences between treatment groups, and that treatment slowed colony growth, we concluded that slow growth does not lead to reduced survival. We thus tested whether the opposite was true, using a one-sided hypothesis, namely, that growth mode is negatively associated with mortality (*i.e.* slow growth leads to a reduced mortality whereas fast growth results in an increased mortality). Finally, we evaluated the association between growth mode before diapause and growth mode after diapause with one-side Fisher's exact tests.

**Brood production.** We compared the total number of pupae produced by the colonies before hibernation (*i.e.* the sum across observation periods), using a negative

binomial regression (NB), with treatment and colony growth mode, and their interaction, as predictors. We used the same procedure for the total number of larvae and for the sum of observation periods where early brood was present (*i.e.* discrete range from zero to four). Differences between groups at each time point were evaluated with a Kruskal-Wallis test (KW) and the Benjamini-Hochberg procedure was performed to control for Type I error (*i.e.* false positives) arising from multiple testing.

We compared the total brood produced by colonies grouped into four categories (*i.e.* treatment by overwintering outcome) using a Kruskal-Wallis test.

To assess the power that colony composition had per time point to predict overwintering survival we built a logistic model. For each time point, we fit a logistic regression with overwintering outcome of each colony (*i.e.* survived or failed) and each of the brood categories (*i.e.* pupae, larvae and early brood) as predictors. Since the number of worker ants is strongly correlated to the number of pupae and late larvae, we excluded this predictor from the model to avoid multicollinearity (Pearson correlations: worker-pupae  $cor = 0.30$ ,  $t = 5.7$ ,  $df = 330$ ,  $p < 0.001$ , worker-larvae  $cor = 0.34$ ,  $t = 6.73$ ,  $df = 330$ ,  $p < 0.001$ , pupae-larvae  $cor = 0.15$ ,  $t = 2.90$ ,  $df = 330$ ,  $p < 0.003$ ).

**Behaviour.** We estimated aggregation and activity values (*i.e.* proportion near queen, mean distance to queen, proportion of ants active, mean distances between active ants, mean distance to closest ant and effective foraging time) using image processing (See Image analyses and feature extraction in this section). We obtained these values with a frequency of 3Hz. For all of these analyses the data for each time point (3 hours) was collapsed into a single mean value. The behavioural features were compared across colonies grouped by treatment and overwintering outcome, using a LMER with these grouping variables as predictors, and colony ID as a random effect to account for repeated measures. Aggregated values were compared before and after hibernation with a Paired-Wilcoxon test. Finally, each variable was regressed against colony size (and treatment which had no effect), using and LMER with queen treatment and colony size as predictors, and specifying for each colony a random intercept and slope. A simple Spearman correlation between each variable and colony size was also computed.

**Worker size.** A worker size distribution for each colony was obtained from all the area of detections that corresponded to single ants (See image analysis and feature

extraction in this section). The median value of the distribution was compared across colonies before and after diapause, using an LMER with median of the worker size for each colony as a response, and treatment and film batch as predictors.

**Statistical packages.** All statistical analyses were carried out in R version 3.3.2 [R Core Team, 2013]. We used the packages ‘lme4’ [Bates *et al.*, 2016] to fit LMER models, ‘influence.ME’ [Nieuwenhuis *et al.*, 2017] to test the assumptions and to obtain p values. All graphs were made using the ‘ggplot2’ package [Wickham *et al.*, 2018]. For Kruskal-Wallis (KW) tests and subsequent post hoc comparisons we used the ‘agricolae’ package [de Mendiburu, 2016] and ‘multcomp’ [Hothorn *et al.*, 2016]. For Wilcoxon tests we used ‘MASS’ [Venables and Ripley, 2002] and for data handling ‘dplyr’ [Wickham *et al.*, 2017].

**Missing and incomplete data.** For the period after hibernation we have missing values at time points where we did not record the colony. First, when the queen did not survive overwintering, we did not continue to observe the colony. Second, when the queen survived but less than five workers survived with her, we continued recordings only when the colony had recovered above this size threshold (*i.e.* C3,S17,S19,S22). Third, some colonies survived and multiplied but died before the end of the experiment for unknown reasons (*i.e.* C21,C7,S1,S11). Some videos were lost due to software and disc failures (See Supplementary table 4.1). Our models can handle missing data and thus no replicates were excluded from our analyses.

## 4.6 Supplement

Control																							
1	2	3	4	5	6	7	8	9	10	11	12	13	14	15	16	17	18	19	20	21	22	23	24
Blue	Blue	Blue	Blue	Blue	Blue	Blue	Blue	Blue	Blue	Blue	Blue	Blue	Blue	Blue	Blue	Blue	Blue	Blue	Blue	Blue	Blue	Blue	Blue
Blue	Blue	Blue	Blue	Blue	Blue	Blue	Blue	Blue	Blue	Blue	Blue	Blue	Blue	Black	Blue	Blue	Blue	Blue	Blue	Blue	Blue	Blue	Black
Blue	White	Black	Black	Blue	Blue	Blue	Blue	White	Blue	Blue	Blue	Blue	Blue	Blue	White	Blue	Blue	White	Blue	White	White	Blue	White
Blue	White	Black	Black	Blue	Blue	Red	Blue	White	Blue	Blue	Blue	Blue	Blue	Blue	White	Blue	Blue	White	Blue	White	White	Blue	White
Blue	White	Blue	Blue	Blue	Black	Red	Blue	White	Black	Black	Blue	Blue	White	Blue	Blue	Black	Blue	White	Blue	White	White	Blue	White
Blue	White	Blue	Blue	Blue	Blue	White	Blue	White	Blue	Blue	Blue	Blue	White	Red	Blue	Blue	Blue	White	Blue	White	White	Blue	White
Blue	White	Blue	Blue	Blue	Blue	White	Blue	White	Blue	Blue	Blue	Blue	White	Blue	White	Blue	Blue	White	Blue	White	White	Blue	White

Spore																							
1	2	3	4	5	6	7	8	9	10	11	12	13	14	15	16	17	18	19	20	21	22	23	24
Green	Green	Green	Green	Green	Green	Green	Green	Green	Green	Green	Green	Green	Green	Green	Green	Green	Green	Green	Green	Green	Green	Green	Green
Green	Green	Green	Green	Green	Green	Green	Green	Green	Green	Green	Green	Green	Green	Green	Green	Green	Green	Green	Green	Green	Green	Green	Green
Green	Green	Green	Green	Green	Green	Green	Green	Green	Green	Green	Green	Green	Green	Green	Green	Green	Green	Green	Green	Green	Green	Green	Green
Green	White	Green	Green	Green	Green	Green	Green	Green	Green	Green	Green	Green	Green	White	White	Black	Green	Black	White	White	Green	White	White
Green	White	Green	Green	Green	Green	Green	Green	Green	Green	Green	Green	Green	Green	White	White	Black	Green	Black	White	White	Green	White	White
Green	White	Green	Black	Green	Green	Black	Black	Green	Black	Green	Black	Green	Green	White	White	Green	Green	Green	White	White	Black	White	White
White	White	Green	Green	Green	Green	Green	Red	Green	Green	White	Green	Green	Green	White	White	Green	Green	Green	White	White	Green	White	White
White	White	Green	Green	Green	Green	Green	Green	Red	Green	White	Green	Green	Green	White	White	Green	Green	Green	White	White	Green	White	White

Supplementary table 4.1: Data overview. Complete projects are shown in color. In white, project missing due to colony death. In gray, video missing due to technical failure in acquisition or storage, or when colonies not filmed since they were too small (*i.e.* under five workers) after hibernation. For these, we have information on worker number. Incomplete projects shown in red, correspond to projects for which video exists, brood was counted as well, but image analysis failed (*e.g.* video corrupt, readable but not possible to process).

Time	Predictors for number of pupae	LR stat.	df	p	signif.
1	Treatment * Growth	2.25	3	0.52	n.s
2	Treatment + Growth	23.85	2	<0.001	***
	Treatment	7.71	1	0.005	**
	Growth	19.46	1	<0.001	***
3	Treatment * growth	13.95	3	0.003	**
	Interaction	5.08	1	0.024	*
	Treatment + growth	7.68	2	0.021	*
4	Treatment	2.40	1	0.12	n.s
	Growth	6.90	1	0.008	**

	Control		Spore				
Time	Fast	Slow	Fast	Slow	$\chi^2$	p	signif.
1	a	a	a	a	2.79	0.424	n.s.
2	a	ab	b	c	21.127	<0.001	***
3	a	ab	bc	c	15.33	0.0015	**
4	a	ab	bc	c	10.60	0.014	*

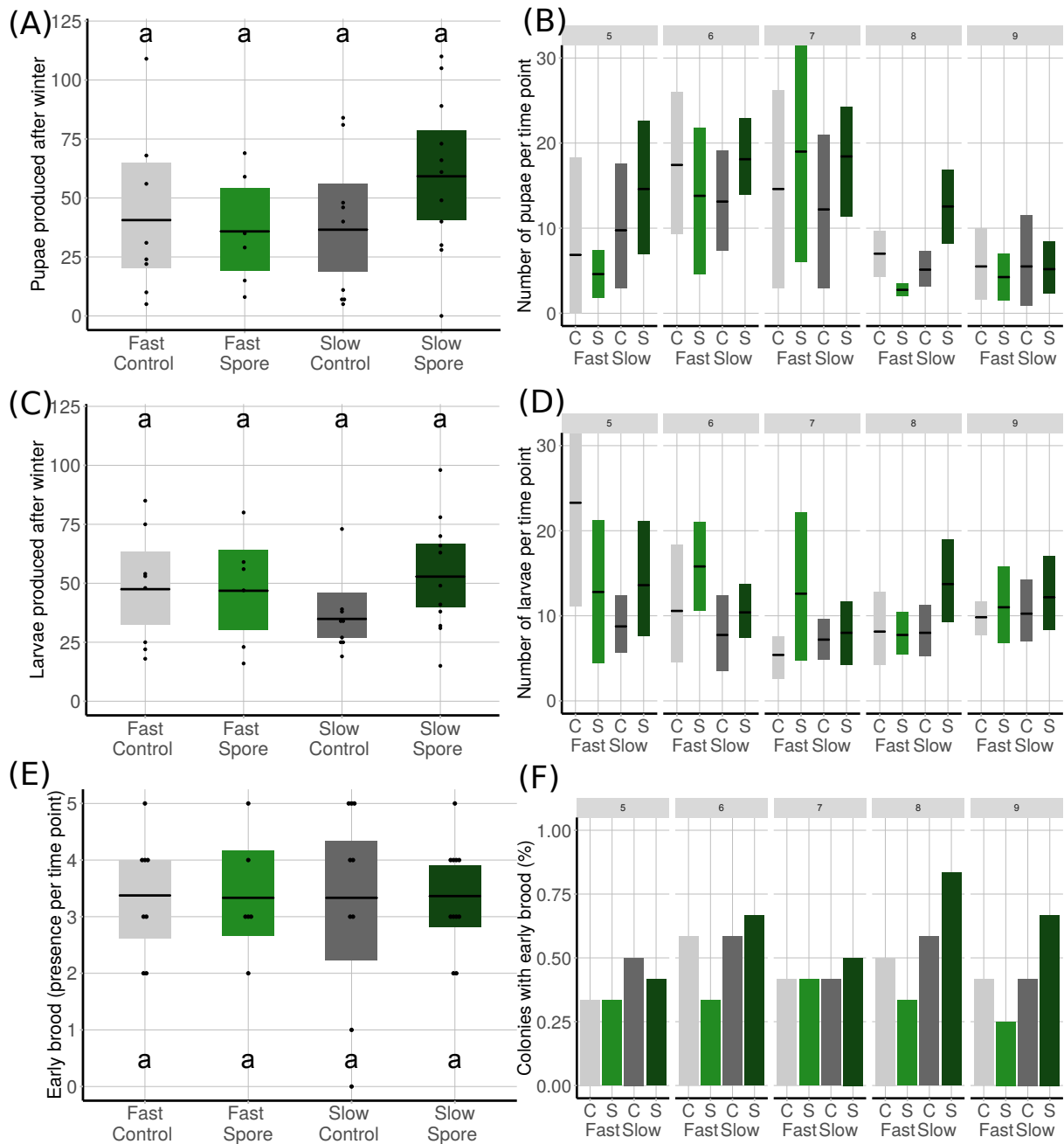
Supplementary table 4.2: Number of pupae as a function of treatment and growth. For each time point, we fit a negative-binomial regression between the number of pupae and two predictors: Treatment (control exposure and sham-exposure of the queen) and Growth (slow and fast growth before hibernation). We tested the interaction between the predictors, and when it was not significant we estimated the effect of each predictor. Group differences were tested with Kruskal-Wallis test and post hoc comparisons.



Time	Predictors for number of larvae	LR stat.	df	p	signif.
1	Treatment * Growth	14.01	3	0.003	**
	Interaction	4.69	1	0.030	*
2	Treatment * Growth	24.89	2	<0.001	***
	Interaction	4.24	1	0.039	*
3	Treatment * Growth	24.60	2	<0.001	***
	Interaction	16.10	1	<0.001	***
4	Treatment * Growth	27.79	2	<0.001	***
	Interaction	11.15	1	<0.001	***

	Control		Spore				
Time	Fast	Slow	Fast	Slow	$\chi^2$	p	signif.
1	a	a	a	b	12.65	0.005	**
2	a	a	a	a	6.263	0.090	n.s.
3	a	a	a	a	3.569	0.311	n.s.
4	a	a	a	a	7.559	0.560	n.s.

Supplementary table 4.3: Number of larvae as a function of treatment and growth. For each time point, we fit a negative-binomial regression between the number of larvae and two predictors: Treatment (control exposure and sham-exposure of the queen) and Growth (slow and fast growth before hibernation). We tested the interaction between the predictors, and when it was not significant we estimated the effect of each predictor. Group differences were tested with Kruskal-Wallis test and post hoc comparisons.



Supplementary figure 4.1: Brood production after hibernation. Total brood produced (left) (A) Total number of pupae (A), larvae (C) and (E) observation periods with early brood present. Letters denote significantly different groups (pairwise posthoc comparisons after NB, significance threshold = 0.05). (B,D,F right ) Brood produced per time period. Asterisk denote a significantly different group after KW with pairwise comparison and BH correction. Everywhere we show the mean and confidence intervals of data grouped by treatment (spore = greens, control = grays) and growth mode (light hues = fast, dark = slow).

## 5 Computational analysis of behavior

The work presented in this chapter results from two collaborations. It is presented in two sections. The first, describes the development of Ferda, a project to build an image-based tracker, which started in 2013 and is ongoing. The main developer of Ferda is Filip Naiser, who obtained his Diploma Thesis in 2014 [Naiser, 2014] and Master Thesis in 2017 [Naiser, 2017], working on this project under the supervision of Jiri Matas, both affiliated to the Center of Machine Perception in Prague. The second section, describes a deep neural network approach to behavioral classification, and includes preliminary results. This was mainly implemented by Christoph Sommer, staff scientist for Image Analysis at IST Austria. My contributions to each project are stated in the text and summarized at the end of each section.

### 5.1 Abstract

Advances in imaging technologies and image processing have undoubtedly pushed forward most fields of science, and behavioral biology is no exception. Imaging methods extend the spatial and temporal scale at which behaviors can be studied. It is increasingly possible to study behaviors that are naturally invisible to the human eye or that are not easily perceived in real time. Image processing automates, to some extent, the process of extracting behaviorally meaningful measurements from images.

To extract meaningful quantities that capture behavior, one needs, to define what one means by behavior. The behavior of an animal can be described based on its structure, measured by its consequences or delineated in relation to certain features in the environment or other individuals [Martin and Bateson, 2007]. For instance, while

observing a foraging ant one can examine aspects of its tripod gait, the amount of food retrieved or the trajectory between the nest and a food source. The descriptions span multiple scales and choosing the level that will shed light onto a particular biological question may be a challenge [Berman, 2018].

From a sequence of images it is possible to extract behaviorally meaningful measurements at different scales. An animal can be described as a single point moving through space, but a richer description can be achieved by incorporating additional points, *e.g.* the position of its limbs. Similarly, social interactions can be described based on the distance between two or more animals or making use of their posture relative to each other. All of these measurements can be interpreted as a description of the state of an animal or group of animals.

Given a description of states, the task of behavioral annotation can be translated into a classification task. Classification can be achieved by different methods which range from rules defined by a user to rules inferred automatically (*i.e.* machine learning). A class can also be inferred bypassing the description of states, from a raw image (*i.e.* image-based deep learning).

Each step of the way can be automatized. Yet, humans have not been completely surpassed by computers in many tasks, for example, keeping identity during occlusion or recognition of behavioral patterns. These challenges still inspire the computer vision scientists and hurdle behavioral biologists.

In this chapter, I will describe an image-based tracking software (Ferda) developed in collaboration with Filip Naiser and Jiri Matas, to tackle the challenges posed by our behavioral studies on ants, while keeping flexibility to address the general challenges in the field. I will also describe the preliminary results of a second, ongoing, collaboration with Christoph Sommer, which aims to classify ant behaviors using a deep neural network approach, training on our manually annotated and motion-feature enriched behavioral datasets.

# Tracking multiple animals

## 5.2 Introduction and approach

Image-based tracking is on the rise in behavioral research. Monitoring single animals is becoming a staple across the field, from toxicological studies to neuroscience. Tracking multiple animals, however, still remains difficult. In the last years, a number of software solutions have been developed, which taken together, address many requirements in behavioral research. Nevertheless, finding amongst them, the right tool for a particular research endeavour, is not straightforward. For instance, many software solutions are very limited in the number of individuals they can follow (*e.g.* Cadabra, Miceprofiler, 3DTraker, Flydra, GroupHousedScan, Motr). These usually require either multiple camera setups or very high-resolution images. Some are not limited in the number of targets but are only suitable when maintaining identity is not a requisite (*e.g.* GroupScan, Multitrack). A few perform well on many animals, but only on similarly sized animals of a given shape (*e.g.* Multiworm, Zebrazoom). Some were developed for use within a specific platform, require a commercial license or the source code is not open for customization (*e.g.* EthoVision, Phenotracker). (See [Dell *et al.*, 2014], Table S1 for a comparison of the software mentioned, and references therein).

Additional requirements include i) tracking multiple interacting animals of different shapes and sizes (*e.g.* predator and prey, parent offspring) ii) observing them in different levels of detail (from their location on the image to the precise position of their limbs) iv) disentangling sequences in which individuals come into close contact or even occlude each other, v) working with imaging setups that are compatible with the subjects (*e.g.* optimizing the setup can be unfeasible or impractical) and (vi) handling the processing of hundreds of hours of video recordings, to name a few. These demands, of course, depend on the experiment at hand and the research questions.

Perhaps the most ambitious demand is that an image-based tracker keeps track of the animals individually throughout the experiment. The problem of keeping identities of objects which minimally or significantly occlude each other, does not have a generic solution in computer vision. In animal experiments, this can be non crucial (*e.g.* when an animal cross each other) or rather be a central part of the research (*e.g.* when an-

imals engage in a certain interaction). In the absence of correct identities, the output of a tracker can be quite informative (*e.g.* to compute the spatial distribution of individuals or their average motion statistics). When identity is essential, there are plenty and diverse strategies to attempt to retrieve it.

There are two multi-platform, open-source projects, that fulfill a wide range of user needs: Ctrax and idTracker (See Table 5.1 for a quick comparison of these and our proposed solution).

	Computer environment	Image requirements	Output	Multiple targets	Identity method
Ctrax 2009	Python, Matlab	Constant and uncluttered background	2D trajectories, orientation	similar sized and elliptical, 15 pixel resolution	Solve crosses
idTracker 2014	Matlab	Good contrast between animals and background	2D trajectories, orientation	wide range of sizes and shapes, 150 pixel resolution	Fingerprint
Ferda	Python	Can deal with cluttered background	2D trajectories, orientation, contour (from which pose can be estimated)	wide range of sizes and shapes, 150 pixel resolution	Solve crosses, fingerprint

Table 5.1: Comparison between our tracker and two state of the art solutions

Ctrax, published in 2009, is a freely available and widely used tracker [Branson *et al.*, 2009]. Animals are detected by thresholding a gray-scale-image from which centroids are identified and connected across frames. When animals cross or overlap, a function fits ellipses to the animals inside the over-segmented region, dividing it. The method works well to track similarly sized individuals moving across a constant, uncluttered background. The researchers made available tools to manually correct wrongly assigned identities, and, furthermore, tools to compute features from these trajectories and train a behavioral classifier [Kabra *et al.*, 2013].

ID tracker, published in 2014, recognizes the major issue which poses the propagation of wrong identities (*i.e.* once a trajectory is wrongly assigned, the error persists throughout the experiment) [Pérez-escudero *et al.*, 2014]. Cleverly, this algorithm focused on identity recognition, based on ‘fingerprint’ computed for each animal. This fingerprint consists of a two-dimensional histogram of distances between, and sum of intensities of, each pair of pixels that, after segmentation, are deemed to belong to

the animal. This fingerprint is translation, rotation and reflection invariant, and, the authors claim, obtaining a large enough set of them for a single animal, can also capture posture invariance. In the original paper they report test cases in two species of fish, ants, flies and mice, where identification is achieved performing better than by human observers. The initialization of these fingerprints is done on video segments in which the expected number of animals can be told apart, mostly because they are far away from each other. Once the prototypical histograms have been computed for each individual, the rest of the frames which are not so clear are identified using a nearest-neighbor classifier. Earlier this month (February 2019), an update was published [Romero-ferrero *et al.*, 2018], which identifies animals touching or crossing using an approach similar to ours.

Of these two approaches, only Ctrax existed at the beginning of this project and we found it had the following limitations. **(1) Handling large data.** There was a need to significantly reduce video file sizes. Sub-sampling the resolution decreased the quality with the result that the number of interactions which could not be resolved, increased. Cutting the length of the videos and processing by parts was an option, but the processing could not be parallelized. Furthermore, the output was written to be used with Matlab tools, which limited further the amount of data which could be processed efficiently. **(2) Setup requirements.** The output consisted of too many tracklets to feasibly correct by hand, after several optimizing attempts to get the right image quality. **(3) Parameters.** The amount of parameters needed was large and not reusable, which made creating a uniform protocol difficult and time consuming. **(4) Posture.** Orientation was not well preserved for interacting ants, when they were properly segmented. Multiple detections were fitted with ellipses which frequently did not correspond to ants. **(5) Segmentation.** The segmentation was not suitable to detect differently sized individuals (*e.g.* queen ant and workers), which was needed in one of our setups.

Given these limitations, we embarked in developing Ferda, our own tracking software. We did so keeping in mind the following principles of good software design: Good software is portable, efficient, structural, flexible, general, readable and well-documented.

**Portable.** Cross-platform portability in software (or the ability to run on different operating systems) is the norm and already a canon for many programming languages, such as Python. This means today one doesn't have to think about platform differences between operating systems, nearly as much, as one decade ago. Nevertheless, programming languages are not completely OS-agnostic and software development still requires testing and solving for incompatibilities. Ferda was done using open-source libraries, available for the different platforms that we used: MacOS X, Linux on a desktop, Linux on HPC cluster and Windows. I was involved in testing the deployment on both the Linux platforms.

**Efficient.** Efficiency in the usage of processing and memory resources is always critical. Ferda uses parallel computing in three ways: 1) multicore processing, 2) GPU processing for machine learning algorithms and 3) optionally distributed computing in an HPC cluster. I was involved in designing the parallelization strategy and I developed the scripts necessary to distribute the computations into two different HPC clusters (one with GPUs and CPUs and another with only CPUs) and reintegrate the results.

**Structured.** To develop a program the task must be broken into subtasks, which are developed independently. A structural code is easier to read, test and document. Ferda was designed in such a way that each of the processing steps is performed by a standalone or almost independent module. For some of these steps, several alternative modules have been developed and can be easily interchanged (*e.g.* image segmentation).

**Flexible and general.** The biggest challenge in our field is the slight variations that each experimental setup or research question brings. For example, software which is written rigidly for certain image format (RGB, fluorescent), individual class specifications (fixed number vs variable number of classes), arena specifications (*e.g.* multiple arenas and their shapes), etc are rendered unusable for different scenarios. While there are pre-processing workarounds, this single hurdle will likely deter many researchers from using this software, and even from using this type of approach. A program should be flexible to handle most changes without having to rewrite. Ferda is written in a way that it is relatively simple to add



different segmentation algorithm, arena specs, etc. Therefore, although Ferda is written for a particular task, it should work for similar tasks of the same domain.

**Readable and well documented.** An effort for readability was made so that I could modify, test and debug parts of the code that I was using. An object-oriented approach and structure were implemented. Documentation is one of the most important components of good software. As the end user, I have been contributing to the documentation, mainly proofreading and expanding where necessary.

We wanted our software to tackle two tasks, to generate two types of dataset. One dataset requires the highest level of precision in identity assignment, where we limit the number of ants to a small group in a simple background. The other requires less precision in id-assignment, but deals with a large number of ants in a more complex setup and comprises a larger volume of raw data. The datasets are described in more detail below. The tasks stem from the experiments described in Chapter 3 and Chapter 4 and we summarize them in Table 5.2. Handling both tasks with a single piece of software, demanded the generality and flexibility missing from other approaches, which we aimed to provide.

**High precision dataset** . In each sequence a group of six uniquely color-marked ants (*Lasius neglectus*) moving across a simple background is recorded. The general idea is to observe individual behavioral sequences and link them to a measured group outcome. In particular, we want to know if the grooming interactions between individuals determine pathogen transmission (See Chapter 3 for detail). For this reason, identity assignment is extremely relevant throughout the sequence. This type of dataset with maximum amount of individual detail is quite useful to approach questions that have to do with animal personality, hierarchies, and questions where individual traits are the focus. As stated, we limited the number of targets in this dataset, yet we designed the software to be able to deal with a larger number of targets with equally high precision, at some reasonable cost in terms of efficiency.

**Low precision dataset** . In each sequence a single colony of ants (*Lasius niger*) is monitored. The colony consists of one queen and a fixed number of workers,

Description	The immediate response of a small group of ants to a pathogen-exposed group member	Long term monitoring of colony development after queen sub-lethal exposure
Experiment magnitude	2 hours per sequence 108 sequences 18fps, 1024x1024 216 hours in total 2TB of video	3 hours per sequence 337 sequences 15-18fps, 1024x1024 1011 hours in total 18TB of video
Number of individuals	6	6-99
Size of individuals	Similarly sized workers	Similarly sized workers and a considerably larger queen
Arena	Ø 45 mm relatively homogeneous and contrasting background (white plaster)	Ø 90 mm half nest (white plaster) and half foraging arena (plastic over white paper) food, debris and brood items
Task	Keep or recover ID of all individuals, especially the pathogen-exposed individual throughout the sequence	Obtain long enough trajectories that allow to study the aggregation of workers around the queen. Individual ID is not crucial to maintain throughout. Reliable segmentation is important in such a complex background. Detections should be allowed to vary in size, contain one or more ants and/or the queen

Table 5.2: Summary of two tracking tasks and relevant specifications

ranging from 6 to 99. They move across a complex background where brood and detritus are visible. The arena is divided into two parts: one half is plastered and preferred by the ants as a nest, the other unplastered half is where we place food. The plastered part is initially white and even and offers good contrast against the dark ants. In later time periods, the plaster is smudged and small holes are bored by the ants, which sometimes can look quite similar in shape and size to workers, making their detection more challenging. Detections vary in size, specifically, the queen can be much larger (ten times) than a single worker. Detections vary in appearance. It is expected that the first workers reared by a queen are smaller and are gradually replaced by larger workers. Newly hatched workers are lighter in color. Thus, worker size and color variation is small but not negligible. Detections vary in behavior as well. For example, the queen can move much faster than the workers. In some sequences, workers will cluster around the queen and stay relatively motionless, while in other sequences, they will venture out exploring and performing foraging trips. In this experiment, positional information with loss of individual identity is used to gather group motion and aggregation statist-

ics. In particular, quantifying aggregation around the queen and foraging trips are of interest (See Chapter 4). In general, getting positional information for different classes of detections is essential, considering that most ecological interactions happen between individuals which differ in size, appearance and behavior (*e.g.* asymmetric competition, predation, parasitism or mutualism).

## 5.3 Method

Ferda is our general tracking solution to the tasks outlined above. A brief summary of the workflow is given in the next paragraphs (See [Naiser, 2014; Naiser, 2017] for a complete description). Ferda was first implemented (in Python 2.7) in [Naiser, 2014] as a multi-object tracker with a function to resolve interactions. The problem was initially represented as a graph, with detections in each frame for nodes, connected between consecutive frames by edges, with a weight (or cost) given by three scores. The first two scores are based on the distance and rotation of the observed detection from one predicted by a simple movement model. The third is an “ant likeness” score, which is determined by the area and major axis length of the detection, and is proportional to the probability, estimated from manually labeled observations, that a detection with said dimensions is labeled as an ant. The first two scores have been used by other trackers (*e.g.* Ctrax), while the third score (ant-likeness) was introduced in this work. Assignment between two consecutive frames was performed by selecting the set of edges between nodes with the smallest sum of weights, also allowing for two nodes to be assigned to the same detection, or to none, which is necessary to cope with detections corresponding to multiple ants (*e.g.* when two ants cross or overlap) or to none (*e.g.* spurious). In the case where a detection contained more than one ant, the position of each ant within was estimated. This was done by iteratively rotating and translating the contour of the individual ants until their union corresponded best with the contour of the detection. The estimation of the position of ants within multiple detections is a problem that is not entirely solved.

On two test datasets which I prepared, the first version of Ferda showed a larger ratio of correctly classified objects compared to other trackers, which were state of the art, at the time (*e.g.* idTracker, Ctrax). In a dataset provided by the developers of idTracker,

this version of Ferda was unable to detect some ants, but our tracker maintained identity without a single mismatch. Although our tracker fared well in comparison to the other trackers, many issues were identified. The main challenge, which remains, is the estimation of positions during an interaction. Position estimation can be used for automated behavioral annotation, which is a primary drive for using quantitative image analysis in behavioral ecology.

With the first version, no function for identity recognition had been implemented, which meant that every mismatch error (wrong assignment of detections between frames) would be propagated to the following frames. Although, these could be verified and corrected by the user, it requires a massive labour investment. The next version of the software [Naiser, 2017] incorporated ID recognition.

In its second iteration of development, several major improvements were made. In particular, more semi-automatic processes were introduced, as well as more sophisticated classification techniques. These are aimed at coping with the very varied and complicated scenarios encountered during image classification, while simultaneously leveraging the large amounts of training data that result from even small investments in manual annotation.

The overall approach of this second Ferda shares two steps with the first version: First images are segmented into regions, then regions in successive frames are identified as belonging to the same ant. Two new steps are then introduced. In the first, detections are classified to determine whether they contain, zero, one, or more ants. In the second and final step, the identity of sequences of consecutive frames is determined. Below, each of these steps is described, in more detail, but the reader is referred to [Naiser, 2017] for details in the implementation.

**Image segmentation.** Image segmentation, the attempt to identify pixels that belong to an ant, is performed using a statistical classifier of the Random Forest type. We opted for this approach as we had learned, from the previous version, that directly using threshold or MSER-based segmentation requires the user to tune several parameters for which it is difficult to acquire intuition. Furthermore, the parameters used for one video are usually not useful for the next. Selecting, instead, a machine learning based approach allows the user to simply select positive and

negative examples of what constitutes an ant, and the classifier automatically derives criteria to apply to the rest of the frames. In this case, the classifier uses a representation of pixels that considers information regarding their intensity in each of three channels, that of their neighboring pixels, and differences among the pixel and its neighbors. The training data is extracted from user input and can be subsequently refined after the user is shown the results of the classification. The output of this classifier is a probability of each pixel, of belonging to an ant. Given the resulting probability matrix (of the same dimensions as the original image, and with values between 0 and 1), the MSER algorithm is used. The results, which are called detections, are a connected sets of pixels whose probability of belonging to an ant is similar and sufficiently different from adjacent pixels not in the detection.

**Graph pruning.** Once detections are extracted from each of the frames in the video, it is necessary to determine which detections from one frame correspond to the same ant as the detections in the previous frame (stitching). As before, this is posed as a graph-theoretical problem, in which an  $f$ -partite complete graph has its edges pruned while meeting several conditions and to maximize a score. The pruning is performed for every pair of consecutive frames, in the following three steps:

1. Edges connecting detections which are too far away in space are discarded. The notion of distance, used this time, is the distance between the edges of the detections and not the centroids. I had noticed in the previous version that, when one of the detections is large, it could happen that it was not connected to a smaller one even when the smaller was almost contained inside the larger one. This happened because the centroids of the detections were far due to the large size of the first one.
2. Edges connecting detections which are too far away in space are discarded. The notion of distance, used this time, is the distance between the edges of the detections and not the centroids. I had noticed in the previous version that, when one of the detections is large, it could happen that it was not connected to a smaller one even when the smaller was almost contained

inside the larger one. This happened because the centroids of the detections were far due to the large size of the first one.

3. Edges which are outliers, in the sense that they connect detections which have very different geometries, as determined by their areas and the orientations of the axes of ellipses with the same central moments as the detections, are discarded.

Determining, for steps 2 and 3, which edges are outliers, is done using two Isolation Forest classifiers. These are trained using the pairs of edges that, after the first step leave an unambiguous identification of detections, for example if all ants are far away from each other in both frames. This approach was originally presented by the authors of idTracker to obtain reference frames [Pérez-escudero *et al.*, 2014], and overcomes one of the limitations of the previous Ferda version: that the user would spend a long time finding thresholds to define which are outliers, and which were not useful for any other video. Each of these classifiers gives a probability of an edge of being correct, in the sense of connecting two regions that belong to the same ant. The edges that are removed in steps 2 and 3 are those whose probabilities are in the lowest decile, according to the respective classifier.

After edges are pruned in the three manners described above, it is very likely that detections remain which have more than one incoming edge in the graph: that is, that there are two or more detections in the previous frame which could enclose the same object as the current detection. When this is the case, a score is computed for each edge by multiplying the probabilities which are output by the two classifiers used for steps 2 and 3 above. Afterwards, the edge with the higher score is kept as the only one incoming to the detection, provided that its score is sufficiently higher than that of the one with second highest score, otherwise, both edges are kept.

**Cardinality classification.** The next step, which makes use of user input, is to classify each of the detections into one of four classes: a) containing a single ant, b) containing no ant at all (*e.g.* reflections or detritus), c) containing more than one ant and d) containing only part of an ant. To perform this classification, regions are

represented using a seven dimensional vector that includes simple information on the geometry of the region: its area, its perimeter, its maximum and minimum intensity, the major and minor axis of the circumscribed ellipse, and its stability (according to the MSER algorithm [Matas *et al.*, 2004]. The next step is to cluster these vectors using the K Means++ algorithm [Arthur and Vassilvitskii, 2007], with K being the number of user inputs that will be requested. The best representative of each of the resulting clusters is shown to the user, who manually labels it in each of the four categories. In the current implementation, this training is done on a small subset of the frames, before segmenting the rest of the video. Afterwards, the rest of the regions are classified depending on which of the manually classified regions is closest to it (in euclidean distance), ie, using a nearest neighbor classifier. Regions that are classified as containing no ants are removed from the graph.

**Tracklet formation.** The graph is then partitioned into strongly connected paths each of whose nodes have exactly one incoming and one outgoing edge, except for the start and end nodes that have no incoming and no outgoing edges, respectively. The paths of regions that are the result of this partitioning are called tracklets.

**Identity classification.** Ferda provides the option of assigning identities to regions, to try to disambiguate the ants that are contained in each. Since this involves additional user input and is only feasible with a small amount of ants and with videos with very good image quality, it is possible to opt out of this. In this case, the tracklets are the final output of Ferda.

If the user opts for the identity classification, then, for each region, a set of identities of possible ants is predicted. That is, if it is known that the video contains N ants, each region will receive a set of identities, each ranging from 1 to N. For this, regions are represented using the same features as used in the classifier of step 2 above, plus the Hu moments [Hu, 1962] of both a binarized and a gray-scale version of the region. With this representation a random forest classifier is trained using user-provided input. The identities of a tracklet are then determined by identities which have the higher probability in its regions, provided that a set of constraints is not violated. These constraints encode the cardinality of

each tracklet (obtained in the previous step), the fact that in every frame every ant must be accounted for, and that the set of identities assigned to tracklets cannot change in time. When these constraints are not satisfiable, the user is prompted for further input, in which case they can correct identity assignment and partition tracklets.

Identity assignment, as implemented in Ferda, is the latest solution to a problem that was posed at the beginning. Previously, I had tried in collaboration with Michael Schwarzfischer and Fabian Theis, from Helmholtz Center Munich, to match tracklets (from Ctrax) based on similarity of color histograms and an algorithm for solving the stable matching problem. I brought the experience of these previous attempts into the discussions leading to the design of Ferda's identity classification module.

The videos were recorded in a computer dedicated for video acquisition (four videos were acquired at a time). Afterwards, the videos were moved to a file server which made them accessible from both the HPC clusters and my desktop computer. Using the desktop computer, arena parameters were input, and the foreground/ background pixel classifier was trained, followed by cardinality classification. A script was executed that prepared the project for running in the HPC cluster and sent it to the processing nodes, using Grid Engine (and later Slurm). In the cluster, the following steps were done concurrently for segments of 1000 frames: image segmentation, graph pruning, cardinality classification and tracklet formation. The end result of this is a set of files that contain the tracklets present in each of the 1000-frame-long segments of the video. These files are converted, also in parallel, into a format which is readable using Matlab, such that the data for each segment is stored in the same format which Ctrax stores its data in. When these parallel processes are finished, the results are downloaded back to the desktop computer where a single data structure that holds the information for the whole video is created. These data structures were used to perform the data analysis detailed in Chapter 4 for the long term colony experiment. The configuration of the HPC cluster, including the installation of the necessary libraries was done by Alois Schoegl, IT, IST Austria, who also contributed to the design of the parallelization strategy.



## 5.4 Results

The second implementation of Ferda greatly improved the user experience as well as the processing throughput. More importantly, it was able to compete in some tracking tasks with the state of the art. To compare Ferda with idTracker, ground truth is necessary. This takes the form of a series of trajectories for which identity and position are correctly known. For this, ground truth provided by the idTracker team (Zebrafish-1) was used, as well as two datasets created ex-profeso for this (Ants-1 and Ants-3). From all, the first 4500 frames were used, and tracked by hand to create the ground truth (See Table 5.3).

Dataset	Number of animals	Number of Pixels Per Object	Origin
Ants-1	6	755	Own recording
Ants-3	10	817	Own recording
Zebrafish-1	5	781	idTracker team

Table 5.3: Summary of ground truth datasets tested

The output of the two different trackers was measured with respect to ground truth (See Table 5.4). For a detection to be correctly assigned, we required that it be no more than  $\frac{1}{3}$  the average animal length from the ground truth position and that the identities match. All possible permutations of identities were tried (and kept constant throughout the video) and we report the one with the best performance.

While idTracker performed better in the case of the ant videos, it is interesting to note that Ferda performed better in the zebrafish videos for which idTracker was originally devised. Despite lower performance, Ferda remained our best option because of the amount of videos we need to process, as well as the particular case of differently-sized ants. There is one additional step in Ferda, in which the user is asked for input regarding the match. This step could increase the number of correctly classified trajectories, the results of which are shown in [Naiser, 2017].

Dataset	Assignment	Ferda	idTracker
Ants-1	correct	59.66%	71.68%
	wrong	6.74%	0.32%
	unassigned	33.60%	28.01%
Ants-3	correct	61.24%	82.38%
	wrong	25.60%	5.25%
	unassigned	13.17%	12.37%
Zebrafish-1	correct	96.92%	88.00%
	wrong	0.27%	0.63%
	unassigned	2.81%	11.36%

Table 5.4: Comparison between Ferda and IdTracker results

## 5.5 Conclusions

Creating a multi-object tracker is a challenging enterprise. In particular, making a tracking solution scale to be able to handle large amounts of data is not straight forward. Interestingly, none of the solutions freely available take this into account, even when their tracking performance was good. It is for this reason that we opted for developing and using Ferda.

We have successfully used Ferda to generate input data for an experiment described in the next section of this chapter and for an additional experiment, which I co-authored and which was recently published [Liutkevičiute *et al.*, 2018].

In essence, after running the whole Ferda processing pipeline we end up with different detections tagged with the number of ants they hold, as well as contours of the detection themselves. Using these annotations we are able to do content-based retrieval, to extract sequences of sections of video frames that, for example, showed single ants, or pairs of ants, or that showed them in a given configuration. Extracting these sequences is useful, among other things, for the machine learning applications, which I will describe below.

That being said, many problems remain only partially tackled. Image segmentation remained a challenge when dealing with extremely noisy backgrounds. To compensate for this we built a post-processing tool to remove spurious detections. We must note, however, that the constant gathering during runtime of training data for the segmentation classifier greatly improved the performance, and we are confident that further refinement of this method will lead to a robust segmentation method that is able to adapt to changing lighting conditions.

Identity assignment worked well for datasets in which the ants were few, mostly active and neatly color coded, but was not useful in the case of the Colony Experiment (Chapter 4), where ants spent long amounts of time clustered together, near the queen. There we could rely on the fact that identities were lost only when ants entered the queen cluster, or worker clusters, but we could extract average velocities and positional information of the ‘unclustered’ ants. We made use of cluster detections to extract meaningful statistics on the global level (*e.g.* distribution of individuals in space, how many cluster near a given individual, etc.).

The limitations in identity assignment in the case of long-lasting interactions are very much related to the lack of an accurate pose estimation for ants during interactions. Likewise, shape variations in ants present a problem for identity matching and pose estimation. These problems are yet to be tackled in a satisfactory manner in any of the solutions surveyed, which still is crucial for automating behaviour annotation. Nevertheless, we believe that a machine-learning oriented approach can go around the problem of describing (an estimating) pose, and we have conducted preliminary research in that direction, as described in the next section.

## 5.6 Contribution

My contributions fall under several categories:

**Conceptualization:** formulation of research goals and aims, contribution of ideas and discussion throughout.

**Software:** design, implementation of computer code and supporting algorithms and testing of existing code components. I especially contributed to the parts dealing

with compression and preprocessing, large file handling and parallelization, the design of a correction tool and, in general, of user interaction.

**Validation:** verification of the reproducibility and scalability of results.

**Investigation:** data collection and preliminary work to select our approach

## Behavioral Classification

### 5.7 Introduction

The behavior of an animal can be described as the combination of its displacement in space and of the movement of its body parts, relative to each other, to the environment, or to other individuals. Such a general definition suggests that behavior is a high-dimensional dynamical process. This is in stark contrast with the relative ease with which human observers can identify it and describe it succinctly. These short description of behaviors are only possible because, in effect, the high dimensional dynamics of an individual can be reasonably approximated by low-dimensional descriptions [Stephens *et al.*, 2010]. The viability of such low-dimensional descriptions is of course not limited to behavior, rather, it has been argued that it is a general feature of the universe, or at least of the parts of it which we can study and understand [Simon, 1996].

The automated description of behavior makes explicit use of the low-dimensionality of animal dynamics. For example, using motion tracking technologies as those described in the previous section, one can identify simple behaviors such as an ant being present in the feeding area by simple examinations of a two-dimensional time series (as done in Chapter 4). This approach can be extended by creating a manually-curated set of dynamical features (such as velocity, acceleration, or angular momentum) and using either a supervised classifier or a clustering algorithm to identify behavioral patterns. While movement of the individual in space is sufficient to identify several behaviors, ignoring the positions of the different body parts of the individual can prevent us from identifying more fine behaviors, some of which could be of special interest (*e.g.* in the case of ants, acidopore grooming, as described in Chapter 3).

The usual approach is to augment the positional time series with variables that describe the posture of the individual. Tracking of individual body parts of an animal is not feasible with current technology, but other methods have been devised to augment the two dimensional description. An elegant example is the work on worm motion, which can be described by the progression of a single phase variable, that can be thought of as travelling wave moving up or down the worms body [Stephens *et al.*, 2008]. Many of the variables used to augment a two-dimensional time series are not as easy to interpret. Moreover, one needs to identify which regions in the state space correspond to meaningful behaviours. This assumes that the sequence of behaviors has discrete and discernible states. One way forward, is defining a dynamical representation of the behavioral series. For example, finding temporal motifs or assigning time-frequency representations, which in essence, discretize the positional and/or postural series.

Once the position and posture time series have been augmented, or replaced, by a dynamical representation, behavior can be identified by using statistical classifiers (as in the case of the position-only time series, described above), or by more intricate dynamical system analyses (*e.g.* identifying attraction basins). It is in this way that representations of sequence of behaviours of an animal are constructed [Berman, 2018].

## 5.8 Approach

In the case of legged animals, it remains a challenge to describe posture by identifying the relative positions of all body parts for multiple individuals. This is particularly difficult in the case of ants, whose tendency to aggregate make their simple segmentation a difficult task. More over the many degrees of freedom of their six legs and antennae make a geometrical description impractical. Recent efforts have made it feasible to track body-part positions of freely moving animals, using a minimally supervised machine learning approach [Pereira *et al.*, 2019]. We have also approached the problem of behavioral detection using machine learning, but without pose estimation, and leveraging the vast amounts of hand-annotated behaviours we have scored (See Chapter 3).

The general approach can be defined as feeding a neural network, sections of video

frames centered around an ant (or sequences thereof), and training it to recognize the behavior being performed. Since we have as described in Chapter 3, vast amounts of manually annotated videos in which ants have been color marked, generating training data is as simple as matching the annotations with a tracked video and finding in the frame a set of pixels corresponding to the ant's mark. When this classifier is trained, it should be able to take tracked video sequences for automated annotation.

We opted for Deep Learning algorithms for image classification, since these apply very well to the constraints of our setup outlined above. Deep-learning algorithms are a form of artificial neural network, a computational model proposed in the 1940s, inspired by the physiology of natural neurons. In brief, an artificial neural network is made up of a set of simple processing units, called neurons, arranged in a succession of layers. The neurons from one layer take as input the outputs from the neurons in the previous layer, weight them and output a highly non-linear function on its sum (*e.g.* tanh), which is then taken as input by the next layer. As such, artificial neural networks can be seen as a function that takes an input (in this case an image) and produces an output (in this case, the class of behavior there represented). The exact function that is computed by the network as a whole depends on the weights of the connections between the different neurons, as well as the particular order in which these are connected. Arriving at the function that correctly classifies the images is a process known as training, and consists, roughly speaking, of iteratively comparing the output of the network with the desired output in a set of manually labeled examples, computing its error, and adjusting the weights to descend on the gradient of the error (as a function of the weights). Deciding on the order in which neurons are connected (its architecture) is done before the training starts, and is based on the experience of the practitioner and the available literature.

Until recently, machine-learning algorithms based on artificial neural networks relied on researchers to process the raw information into more meaningful form before feeding it to computational models. This process, known as feature engineering, is akin to defining the dynamical descriptions mentioned above. Today, a neural network has layers to find meaningful relationships embedded in the input (*e.g.* edges embedded in pixels, and faces embedded in edges). These additional layers, which allow the input to enter unprocessed into the network, is what give an artificial neural network the

designation of “Deep”.

Another common feature of Deep Neural Networks is having slightly more intricate architectures, some of which are specially suited to fit the domain of the problem. In the case of image recognition, Convolutional Neural Networks (CNN) have become commonplace, since their architecture keeps in mind two characteristics of images: i) that they contain features and patterns which are local in space (such as edges) and ii) that the defining characteristics of an image, for the purpose of interest, need to be always in the same relative position (*e.g.* the center) within the image. Furthermore, specialized CNN architectures have been developed for image classification tasks, and we make use of one of them in this work.

The type of deep neural network that was used in this work was based on a network of the InceptionV3 architecture, an architecture that has shown very good results in other image classification tasks. InceptionV3 is a complex architecture of convolutional neural networks consisting of two identical modules, each of which is characterized by performing convolutions with different kernel sizes on the input and then combining them together. This choice of architecture removes the need for finding the correct convolution kernel size, but greatly increases the number of connections between neurons. The authors of the original InceptionV3 architecture [Szegedy *et al.*, 2014] have come up with some interesting tricks to reduce the total number of training weights, but the task of training the network remains computationally intensive.

To counter such hunger for expensive data, a method called Transfer Learning has been devised. This method exploits the ability of neural networks to apply classification prowess acquired from one data type to another type. That is, to use a network trained on other datasets, tweak only some layers to fit the problem in hand, and learn from a smaller dataset. Using transfer learning, Deep Neural Networks do not start from scratch but start the learning process using what was learned to solve a different task, for example, the ability to recognize edges, regions, or transitions. This operates under the assumption that some “low level” features are present in both the dataset at hand, and that on which the network was originally trained. This assumption is valid for most real world images (as opposed to artificially generated ones), but still, transfer learning is not always ‘appropriate’ and experimentation is required to determine whether knowledge can be transferred from one domain to another.

The particular network that we based our classifier on was pre-trained to solve the ImageNet task, a benchmark task of classifying images into 1000 categories. These categories are, of course, not any of the categories we are interested in (which correspond to the behaviors which are of interest to us), but rather general image categories such as different animals or types of scenes. However, the first layers of the network have been adjusted so that the activation of the neurons therein occurs when certain patterns occur in the input image, with said patterns being useful for classifying the images in the benchmark dataset into any of the 1000 categories.

So far, the preliminary experiments described below take only single frames as input.

## 5.9 Method

We implemented an image classification method, which takes as input an image and from it outputs a label for five behavioral categories. This image classification was a time-ignorant CNN which was pre-trained on the ImageNet database, following the transfer learning paradigm.

The five behavioral categories, all correspond to individual ants (*i.e.* no interaction), which are stationary or in place, doing some type of self-grooming (SG), resting or doing something else. The categories are defined as follows: (1) “Resting” where there is only some very slow movement of the head and antenna, (2) “SG lateral” where the ant body bends to one side to stroke her side and mid legs with her front legs, (3) “SG antennal” where antennae are stroked with the front legs (*i.e.* passed through the strigil, a cleaner structure), (4) “SG gastertip” where the ant bends over her abdomen (gaster) to reach the acidopore, an opening of the formic and dufour glands (5) “Other”, where ants were doing something else (*e.g.* ants resting against a wall, digging). See Figure 5.1, below.

We created a toy dataset of images categorized as above. For this we used a video sequence of six ants (18 fps, ant length ~150 pixels), for which we obtained motion trajectories. We selected frames where an ant stayed in position (*i.e.* velocity under 6 pixels / frame, less than 1 body length per second) and others were not too close (*i.e.*





Figure 5.1: Examples of dataset and behavioral categories

distance threshold = 100 pixels) and cut the selected frames around the ant (150 x 150 pix). We manually scored the behaviours of 530 clips to obtain 33,000 labelled frames.

The starting network was an InceptionV3 network, from which we removed the last layer of neurons, which in the benchmark task are used to perform the final classification task into each of the 1000 categories. We replaced these layer with three more layers: one with 512 neurons with rectifying activation function, followed by a drop-out layer, and finally 5 softmax layers. Each layer was connected to the previous in a dense manner (*i.e.* each neuron of a layer was connected to all neurons in the previous one). The neurons with rectifying activation functions activate only when the input is positive, in which case the output is equal to the input, and is widely used in deep neural networks for computer vision tasks as it has shown to increase performance. The dropout neurons are neurons that, in each training iteration, discard a fraction of their input (50% in our case), in effect introducing noise to avoid overfitting. Finally, the softmax neurons are used as the standard classification layer, as their output is proportional to the largest of their input, thus serving as a means of collecting the input of the previous layers.

We used the Python library for Deep Learning, Keras, to train the network so constructed. It needed 30 minutes to re-train on the ant videos to achieve 90% accuracy. The split into training and test data was done for each movie, so that all images from a single were either in the train or in the test set. Furthermore, to take class imbalance into account, stratification was performed, meaning that the training and testing sets have the same proportions of each class as the entire dataset. Importantly, images had to be resized to fit the network's size of 299x299 pixels, and color conversion was performed in the same way as in the training of InceptionV3 to Imagenet: it was converted from RGB to BGR, and from each channel, the mean of the ImageNet datasets was

subtracted (zero centering). The training was done in two steps, first only the weights behind each of the newly added layers were adjusted, and afterward, all weights were re-adjusted, including those that came from the pre-trained inceptionV3 network.

## 5.10 Results

The results of the classification experiment are summarized in the following table:

Categories	Precision	Recall	F1-score	Support
Rest	0.95	0.97	0.96	11011
SG(antennal)	0.72	0.85	0.78	1047
SG(lateral)	0.89	0.85	0.87	2109
other	0.87	0.58	0.70	1431
SG(gaster)	0.61	1.00	0.76	344

Table 5.5: Results CNN

For a given category, precision ( $p$ ) is the number of correctly classified images, divided by the number of all images classified with this category, and recall ( $r$ ) is the number of correctly classified images divided by the number of images truly belonging to this category (*i.e.* matching the manual labels). F1-score, takes both precision and recall into account, as a their balanced harmonic mean, *i.e.*  $F1 = 2pr / (p+r)$ . Support is the number of occurrences of each category.

These results show good classification performance overall, considering that the training was done on a small dataset. Selfgrooming behaviours, for which the dataset had few examples, were well classified, in particular, lateral self-grooming.

An additional insight was obtained from visualization using partial occlusion, a standard sanity check in the learning process [Zeiler and Fergus, 2014]. With this visualization technique one sees the importance of different parts of an image on classification. An example visualization (Picasso [Henderson and Rothe, 2017]) is shown in Figure 5.2 In general, our results are encouraging since they showed that a good

separation is made between foreground and background, and that other ants present in a frame are not taken into account.

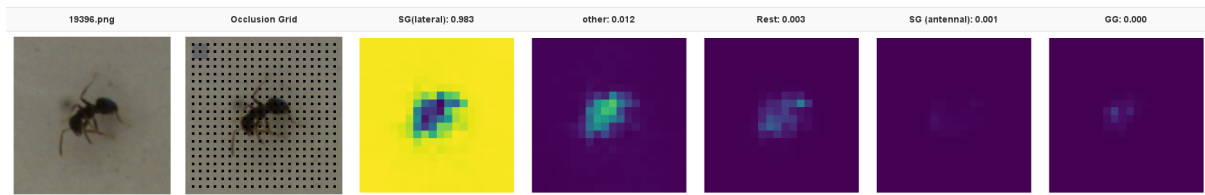


Figure 5.2: Partial occlusion visualization in Picasso visualizer. Classification is done several times on an image, blocking different parts of the image (second panel, shaded occlusion square). The image shown was classified by the model, with 98% classification probability of “SG(lateral)”. Dark blue parts of the image correspond to lower probability of the given classification, *i.e.* if those parts are occluded probability of classification decreased. For instance, if we blocked parts of the ant body or legs, the probability of “SG(lateral)” decreased, which means that without these parts it is hard for the model to recognize that the ant is in position for this selfgrooming category.

## 5.11 Conclusions

Classification using the state-of-the-art deep neural network showed mixed results, which suggest that additional experiments are needed and that more hand-labeled training data must be procured for other behaviors. While the current results are not sufficient to replace a human annotator, the experiments are too preliminary to rule out this possibility. Still, the time needed to re-train the network for this particular problem is smaller than the time needed to train a human annotator that can achieve comparable results, especially when using only still images.

The most satisfactory result is that, based on single images (not sequences), the network is capable of quite reliably detecting when ants are resting. This suggests that pose estimation was successfully achieved by the network, at least to the point of recognizing movement. Let us also recall, that the input to the classifier were images, not any sort of description, derived from human-defined criteria, of the pose of the ant. This simple classification is already enough to pre-select sequences of the video that a human annotator must observe, greatly reducing the time needed for annotation.

Several further steps can be tested to improve classification accuracy.

First, the classifier must be adapted to take sequences of images as input, to have access to information about the movement of the ant's limbs. This can be done in three different ways. The simplest is to apply the current CNN on each frame and then pass this sequence of classes to a statistical classifier, such as a Support Vector Machine. We will also try a more advanced classifier, such as a Recurrent Neural Network, which is especially suited for processing sequential data. Finally, re-purposing the current CNN to take volumes as input, which would involve much more retraining.

Second, and of utmost interest to the biological community, would be to attempt a classification of behaviors involving several individuals. The dataset that we have produced includes annotations of such behaviors, so as soon as a suitable single-individual-behavior classifier is found, it can be retrained for the multiple individuals' case.

Finally, it is possible to implement the above-mentioned hybrid system of annotation, that takes into account tracking information (even if not complete), and uses such a classifier to point a human annotator only to the important parts of the video recording.

## 5.12 Contribution

In brief, my contributions fall under two categories:

**Conceptualization:** formulation of research goals and aims and discussion.

**Investigation:** dataset creation, data curation and preliminary work (*e.g.* behaviour classification (SVG) trials with motion trajectory features) to select our approach

## Bibliography

- [Alaux *et al.*, 2012] Cédric Cedric Alaux, Nele Kemper, Andre André Kretzschmar, and Yves Le Conte, “Brain, physiological and behavioral modulation induced by immune stimulation in honeybees (*Apis mellifera*): a potential mediator of social immunity?,” *Brain Behavior and Immunity*, 26(7):1057–1060, 2012.
- [Anderson and McShea, 2001] C Anderson and D W McShea, “Individual versus social complexity, with particular reference to ant colonies,” *Biological Review*, 76(2):211–237, 2001.
- [Anderson and May, 1979] Roy M Anderson and Robert M May, “Population biology of infectious diseases: Part I,” *Nature*, 280(5721):361–367, 1979.
- [Arathi *et al.*, 2000] H S Arathi, I Burns, and M Spivak, “Ethology of hygienic behaviour in the honey bee *Apis mellifera* L-(Hymenoptera : Apidae): behavioural repertoire of hygienic bees,” *Ethology*, 106(4):365–379, 2000.
- [Aron *et al.*, 2009] Serge Aron, Nathalie Steinhauer, and Denis Fournier, “Influence of queen phenotype , investment and maternity apportionment on the outcome of fights in cooperative foundations of the ant *Lasius niger*,” *Animal Behaviour*, 77(5):1067–1074, 2009.
- [Arthur and Vassilvitskii, 2007] David Arthur and Sergei Vassilvitskii, “K-means++: the advantages of careful seeding,” In *In Proceedings of the 18th Annual ACM-SIAM Symposium on Discrete Algorithms*, 2007.
- [Aubert and Richard, 2008] A Aubert and F J Richard, “Social management of LPS-induced inflammation in *Formica polyctena* ants,” *Brain Behavior and Immunity*, 22(6):833–837, 2008.

- [Bansal *et al.*, 2010] Shweta Bansal, Jonathan Read, Babak Pourbohloul, and Lauren Ancel Meyers, “The dynamic nature of contact networks in infectious disease epidemiology,” *Journal of Biological Dynamics*, 4(5):478–489, 2010.
- [Baracchi and Cini, 2014] David Baracchi and Alessandro Cini, “A Socio-Spatial Combined Approach Confirms a Highly Compartmentalised Structure in Honeybees,” *Ethology*, 120(12):1167–1176, 2014.
- [Baracchi *et al.*, 2012] David Baracchi, Antonio Fadda, and Stefano Turillazzi, “Evidence for antiseptic behaviour towards sick adult bees in honey bee colonies,” *Journal of Insect Physiology*, 2012.
- [Baracchi *et al.*, 2010] David Baracchi, Marco Zaccaroni, Rita Cervo, and Stefano Turillazzi, “Home range analysis in the study of spatial organization on the comb in the paper wasp *Polistes dominulus*,” *Ethology*, 116(7):579–587, 2010.
- [Barthelemy *et al.*, 2005] M Barthelemy, A Barrat, R Pastor-Satorras, and A Vespignani, “Dynamical patterns of epidemic outbreaks in complex heterogeneous networks,” *Journal of Theoretical Biology*, 235(2):275–288, 2005.
- [Bates *et al.*, 2016] Douglas Bates, Martin Maechler, Ben Bolker, and Steven Walker, *lme4: Linear Mixed-Effects Models using 'Eigen' and S4*, 2016.
- [Benjamini and Hochberg, 1995] Yoav Benjamini and Yosef Hochberg, “Controlling the False Discovery Rate: A Practical and Powerful Approach to Multiple Testing,” *Journal of the Royal Statistical Society. Series B (Methodological)*, 57(1):289–300, 1995.
- [Berman, 2018] Gordon J. Berman, “Measuring behavior across scales,” *BMC Biology*, 16(1):1–11, 2018.
- [Bischoff *et al.*, 2009] Joseph F Bischoff, Stephen A Rehner, Richard A Humber, Joseph F Bischoff, Stephen A Rehner, Richard A Humber A, Joseph F Bischoff, and Richard A Humber, “A multilocus phylogeny of the *Metarhizium anisopliae* lineage A multilocus phylogeny of the *Metarhizium anisopliae* lineage,” *Mycologia*, 5514(101):512–530, 2009.

- [Bisset and Marathe, 2009] K Bisset and M Marathe, "A cyber environment to support pandemic planning and response," 2009.
- [Blonder and Dornhaus, 2011] Benjamin Blonder and Anna Dornhaus, "Time-ordered networks reveal limitations to information flow in ant colonies," *PLoS ONE*, 6(5):e20298, 2011.
- [Bolker *et al.*, 2008] Benjamin M Bolker, Mollie E Brooks, Connie J Clark, Shane W Geange, John R Poulsen, M Henry H Stevens, and Jada-simone S White, "Generalized linear mixed models : a practical guide for ecology and evolution," *Trends in Ecology and Evolution*, 24(3), 2008.
- [Boomsma and Gawne, 2018] Jacobus J. Boomsma and Richard Gawne, "Superorganismality and caste differentiation as points of no return: how the major evolutionary transitions were lost in translation," *Biological Reviews*, 93(1):28–54, 2018.
- [Bordoni, 2017] Adele Bordoni, "Long-term assessment reveals the hidden and hiding effects of experimental stress on ant colonies," *Behavioral Ecology and Sociobiology*, 71:144, 2017.
- [Bos *et al.*, 2012] N Bos, T Lefevre, A B Jensen, and P D'Ettoire, "Sick ants become unsociable," *Journal of Evolutionary Biology*, 25(2):342–351, 2012.
- [Bourke *et al.*, 1995] Andrew F G Bourke, Nigel R Franks, and Nigel R Franks, *Social evolution in ants*, Princeton University Press, 1995.
- [Branson *et al.*, 2009] Kristin Branson, Alice Robie, John Bender, Pietro Perona, and Michael Dickinson, "High-throughput Ethomics in Large Groups of *Drosophila*," *Nature Methods*, 6(6):451–457, 2009.
- [Buechel and Schmid-Hempel, 2016] Denise Buechel and Paul Schmid-Hempel, "Colony pace : a life-history trait affecting social insect epidemiology," *Proceedings of the Royal Society B-Biological Sciences*, 2016.
- [Burchill and Moreau, 2016] A. T. Burchill and C. S. Moreau, "Colony size evolution in ants: macroevolutionary trends," *Insectes Sociaux*, 63(2):291–298, 2016.

- [Buscarino *et al.*, 2010] Arturo Buscarino, Agnese Di Stefano, Luigi Fortuna, Mattia Frasca, and Vito Latora, "Effects of motion on epidemic spreading," *International Journal of Bifurcation and Chaos*, 20(3):765–773, 2010.
- [Calleri II *et al.*, 2006] D V Calleri II, R B Rosengaus, and J F A Traniello, "Disease and colony establishment in the dampwood termite *Zootermopsis angusticollis* : survival and fitness consequences of infection in primary reproductives," *Insectes Sociaux*, 53:204–211, 2006.
- [Calleri II *et al.*, 2007] D V Calleri II, R B Rosengaus, and J F A Traniello, "Immunity and reproduction during colony foundation in the dampwood termite, *Zootermopsis angusticollis*," *Physiological Entomology*, 32:136–142, 2007.
- [Charbonneau *et al.*, 2013] D Charbonneau, Benjamin Blonder, and Anna Dornhaus, "Social insects: a model system for network dynamics," In Petter Holme and Jari Saramäki, editors, *Temporal Networks, Understanding Complex Systems*, pages 217–244. Springer-Verlag, Berlin Heidelberg, 2013.
- [Chultz and Eifert, 2005] Roland S Schultz and Bernhard S Eifert, "*Lasius neglectus* ( Hymenoptera : Formicidae )— a widely distributed tramp species in Central Asia," *Myrmecological News*, 7(September):47–50, 2005.
- [Cole, 2009] Blaine J Cole, "The ecological setting of social evolution: the demography of ant populations," *New Frontiers for Behavior Ecology: From Gene to Society*, pages 74–104, 2009.
- [Cremer *et al.*, 2007] Sylvia Cremer, Sophie A.O. Armitage, and Paul Schmid-Hempel, "Social Immunity," *Current Biology*, 17(16):1–8, 2007.
- [Cremer *et al.*, 2018] Sylvia Cremer, Christopher D Pull, and Matthias A. Fürst, "Social Immunity: Emergence and Evolution of Colony-Level Disease Protections," *Annual Review of Entomology*, 63:105–123, 2018.
- [Cremer and Sixt, 2009] Sylvia Cremer and Michael Sixt, "Analogies in the evolution of individual and social immunity," *Philosophical Transactions: Biological Sciences*, 364:129–142, 2009.



- [Cremer *et al.*, 2006] Sylvia Cremer, Line V Ugelvig, Suzanne Lommen, Klaus S Petersen, and Jes S Pedersen, "Attack of the invasive garden ant : aggression behaviour of *Lasius neglectus* ( Hymenoptera : Formicidae ) against native *Lasius* species in Spain," *Myrmecological News*, 9:13–19, 2006.
- [Cronin *et al.*, 2013] Adam L. Cronin, Mathieu Molet, Claudie Doums, Thibaud Monnin, and Christian Peeters, "Recurrent Evolution of Dependent Colony Foundation Across Eusocial Insects," *Annual Review of Entomology*, 58(1):37–55, 2013.
- [Currie and Stuart, 2001] Cameron R Currie and Alison E Stuart, "Weeding and grooming of pathogens in agriculture by ants," *Proceedings of the Royal Society B: Biological Sciences*, 2001.
- [de Mendiburu, 2016] Felipe de Mendiburu, *agricolae: Statistical Procedures for Agricultural Research*, 2016.
- [de Roode and Lefèvre, 2012] Jacobus C de Roode and Thierry Lefèvre, "Behavioral Immunity in Insects," *Insects*, 3(4):789–820, 2012.
- [de Souza *et al.*, 2008] Danival José de Souza, Johan Van Vlaenderen, Yannick Moret, and Alain Lenoir, "Immune response affects ant trophallactic behaviour," *Journal of Insect Physiology*, 54(5):828–832, 2008.
- [Deacon, 2013] Jim W Deacon, *Fungal biology*, John Wiley & Sons, 2013.
- [Dell *et al.*, 2014] Anthony I. Dell, John A. Bender, Kristin Branson, Iain D. Couzin, Gonzalo G. de Polavieja, Lucas P.J.J. Noldus, Alfonso Pérez-Escudero, Pietro Perona, Andrew D. Straw, Martin Wikelski, and Ulrich Brose, "Automated image-based tracking and its application in ecology," *Trends in Ecology and Evolution*, 29(7):417–428, 2014.
- [Depickère *et al.*, 2004] S. Depickère, D. Fresneau, and J. L. Deneubourg, "Dynamics of aggregation in *Lasius niger* (Formicidae): Influence of polyethism," *Insectes Sociaux*, 51(1):81–90, 2004.
- [Dussaubat *et al.*, 2013] C Dussaubat, A Maisonnasse, D Crauser, D Beslay, G Costagliola, S Soubeyrand, A Kretzchmar, and Y Le Conte, "Flight behavior and

- pheromone changes associated to *Nosema ceranae* infection of honey bee workers (*Apis mellifera*) in field conditions,” *Journal of Invertebrate Pathology*, 113(1):42–51, 2013.
- [Dussaubat *et al.*, 2010] Claudia Dussaubat, Alban Maisonnasse, Cedric Alaux, Sylvie Tchamitchan, Jean-Luc Brunet, Erika Plettner, Luc P Belzunces, and Yves Le Conte, “*Nosema* spp. infection alters pheromone production in honey bees (*Apis mellifera*),” *Journal of Chemical Ecology*, 36(5):522–525, 2010.
- [Eisner and Happ, 1962] B Y T Eisner and G M Happ, “THE INFRABUCCAL POCKET OF A FORMICINE ANT : A SOCIAL FILTRATION DEVICE,” *Psyche (New York)*, 1962.
- [Elena B. Lopatina, 2018] Elena B. Lopatina, “Structure, diversity and adaptive traits of seasonal cycles and strategies in ants,” *Intech open*, 2:64, 2018.
- [Evans and Spivak, 2010] Jay D Evans and Marla Spivak, “Socialized medicine: individual and communal disease barriers in honey bees,” *Journal of Invertebrate Pathology*, 103:S62–S72, 2010.
- [Farish, 1972] B Y D J Farish, “THE EVOLUTIONARY IMPLICATIONS OF QUALITATIVE VARIATION IN THE GROOMING BEHAVIOUR OF THE HYMENOPTERA ( INSECTA ),” *Animal Behaviour*, pages 662–676, 1972.
- [Fefferman *et al.*, 2007] Nina H Fefferman, James F A Traniello, Rebeca B Rosengaus, and Daniel V Calleri, “Disease prevention and resistance in social insects: modeling the survival consequences of immunity, hygienic behavior, and colony organization,” *Behavioral Ecology and Sociobiology*, 61(4):565–577, 2007.
- [Feigenbaum and Naug, 2010] C Feigenbaum and D Naug, “The influence of social hunger on food distribution and its implications for disease transmission in a honey-bee colony,” *Insectes Sociaux*, 57(2):217–222, 2010.
- [Ferguson-Gow *et al.*, 2014] Henry Ferguson-Gow, Seirian Sumner, Bourke, Andrew F. G., and Kate E. Jones, “Colony size predicts division of labour in attine ants,” *Proceedings of the Royal Society of London B: Biological Sciences*, 281(1793), 2014.

- [Fernández-Marín *et al.*, 2015] Hermógenes Fernández-Marín, David R. Nash, Sarah Higginbotham, Catalina Estrada, Jelle S. Van Zweden, Patrizia D’Ettorre, William T. Wcislo, and Jacobus J. Boomsma, “Functional role of phenylacetic acid from metapleural gland secretions in controlling fungal pathogens in evolutionarily derived leaf-cutting ants,” *Proceedings of the Royal Society B: Biological Sciences*, 282(1807), 2015.
- [Fernández-Marín *et al.*, 2006] Hermógenes Fernández-Marín, Jess K. Zimmerman, Stephen A. Rehner, and William T. Wcislo, “Active use of the metapleural glands by ants in controlling fungal infection,” *Proceedings of the Royal Society B: Biological Sciences*, 273(1594):1689–1695, 2006.
- [Fowler *et al.*, 1986] H G Fowler, V Pereira-da Silva, L C Forti, and N B Saes, *Population dynamics of leaf-cutting ants: a brief review*, Westview Press, 1986.
- [Frank *et al.*, 2018] Erik T Frank, Marten Wehrhahn, K Eduard Linsenmair, Am Hubland, and Erik T Frank, “Wound treatment and selective help in a termite-hunting ant,” *Proceedings of the Royal Society B: Biological Sciences*, 2018.
- [Goblirsch *et al.*, 2013] Mike Goblirsch, Zachary Y Huang, and Marla Spivak, “Physiological and behavioral changes in honey bees (*Apis mellifera*) induced by *Nosema ceranae* infection,” *PLoS ONE*, 8(3):e58165, 2013.
- [Gordon and Mehdiabadi, 1999] Deborah M Gordon and Natasha J Mehdiabadi, “Encounter rate and task allocation in harvester ants,” *Behavioral Ecology and Sociobiology*, 45(5):370–377, 1999.
- [Graystock and Hughes, 2011] Peter Graystock and William O.H. H Hughes, “Disease resistance in a weaver ant, *Polyrhachis dives*, and the role of antibiotic-producing glands,” *Behavioral Ecology and Sociobiology*, 65(12):2319–2327, 2011.
- [Haatanen *et al.*, 2015] Marja Katariina Haatanen, Tapio van Ooik, and Jouni Sorvari, “Effects of overwintering temperature on the survival of the black garden ant (*Lasius niger*),” *Journal of Thermal Biology*, 49-50:112–118, 2015.

- [Hagenaars *et al.*, 2004] T J Hagenaars, C A Donnelly, and N M Ferguson, “Spatial heterogeneity and the persistence of infectious diseases,” *Journal of Theoretical Biology*, 229(3):349–359, 2004.
- [Hamilton *et al.*, 2011] Casey Hamilton, Brian T. Lejeune, and Rebeca B. Rosengaus, “Trophallaxis and prophylaxis: social immunity in the carpenter ant *Camponotus pennsylvanicus*,” *Biology Letters*, 7(1):89–92, 2011.
- [Hart and Ratnieks, 2001] A G Hart and F L W Ratnieks, “Task partitioning, division of labour and nest compartmentalisation collectively isolate hazardous waste in the leafcutting ant *Atta cephalotes*,” *Behavioral Ecology and Sociobiology*, 49(5):387–392, 2001.
- [Hart and Ratnieks, 2002] A G Hart and F L W Ratnieks, “Waste management in the leaf-cutting ant *Atta colombica*,” *Behavioral Ecology*, 13(2):224–231, 2002.
- [Heinze and Walter, 2010] Juergen Heinze and Bartosz Walter, “Moribund ants leave their nests to die in social isolation,” *Current Biology*, 20(3):249–252, 2010.
- [Helanterä *et al.*, 2009] Heikki Helanterä, Joan E Strassmann, Juli Carrillo, and David C Queller, “Unicolonial ants : where do they come from , what are they and where are they going ?,” *Trends in Ecology & Evolution*, pages 1–9, 2009.
- [Henderson and Rothe, 2017] Ryan Henderson and Rasmus Rothe, “Picasso: A modular framework for visualizing the learning process of neural network image classifiers,” *arXiv preprint arXiv:1705.05627*, 2017.
- [Hiruma and Kaneko, 2013] Kiyoshi Hiruma and Yu Kaneko, *Hormonal Regulation of Insect Metamorphosis with Special Reference to Juvenile Hormone Biosynthesis*, volume 103, Elsevier Inc., 1 edition, 2013.
- [Hock and Fefferman, 2012] Karlo Hock and Nina H Fefferman, “Social organization patterns can lower disease risk without associated disease avoidance or immunity,” *Ecological Complexity*, 12:34–42, 2012.
- [Hothorn *et al.*, 2016] Torsten Hothorn, Frank Bretz, and Peter Westfall, *multcomp: Simultaneous Inference in General Parametric Models*, 2016.

- [House and Keeling, 2011] Thomas House and M J Keeling, “Epidemic prediction and control in clustered populations,” *Journal of Theoretical Biology*, 272(1):1–7, 2011.
- [Howard and Tschinkel, 1975] Dennis F Howard and Walter R Tschinkel, “Aspects of necrophoric behaviour in the red imported fire ant, *Solenopsis invicta*,” *Behaviour*, 1975.
- [Hu, 1962] Ming-Kuei Hu, “Visual Pattern Recognition by Moment Invariants,” *Information Theory, IRE Transactions*, 8(2):179–187, 1962.
- [Hughes *et al.*, 2002] W O H Hughes, J Eilenberg, and J J Boomsma, “Trade-offs in group living: transmission and disease resistance in leaf-cutting ants,” *Proceedings of the Royal Society B-Biological Sciences*, 269(1502):1811–1819, 2002.
- [Jaccoud *et al.*, 1999] D B Jaccoud, W O H Hughes, and C W Jackson, “The epizootiology of a *Metarhizium* infection in mini-nests of the leaf-cutting ant *Atta sexdens rubropilosa*,” *Entomologia Experimentalis et Applicata*, pages 51–61, 1999.
- [Jander, 1976] Rudolf Jander, “Grooming and pollen manipulation in bees ( Apoidea ): the nature and evolution of movements involving the foreleg,” *Physiological Entomology*, 1:179–194, 1976.
- [Jandt and Dornhaus, 2009] Jennifer M Jandt and Anna Dornhaus, “Spatial organization and division of labour in the bumblebee *Bombus impatiens*,” *Animal Behaviour*, 77(3):641–651, 2009.
- [Janet, 1907] Charles Janet, *Anatomie du corselet et histolyse des muscles vibrateurs, après le vol nuptial: chez la reine de la fourmi (Lasius niger)*, volume 1, Impr.-librairie Ducourtieux et Gout, 1907.
- [Jeanson, 2012] Raphaël Jeanson, “Long-term dynamics in proximity networks in ants,” *Animal Behaviour*, 83(4):915–923, 2012.
- [Kabra *et al.*, 2013] Mayank Kabra, Alice A. Robie, Marta Rivera-Alba, Steven Branson, and Kristin Branson, “JAABA: Interactive machine learning for automatic annotation of animal behavior,” *Nature Methods*, 10(1):64–67, 2013.

- [Keeling, 2005] M Keeling, “The implications of network structure for epidemic dynamics,” *Theoretical Population Biology*, 67(1):1–8, 2005.
- [Keller *et al.*, 2003] Siegfried Keller, Philip Kessler, and Christian Schweizer, “Distribution of insect pathogenic soil fungi in Switzerland with special reference to *Beauveria brongniartii* and *Metharhizium anisopliae*,” *BioControl*, 48:307–319, 2003.
- [Khoury *et al.*, 2013] David S Khoury, Andrew B Barron, and Mary R Myerscough, “Modelling food and population dynamics in honey bee colonies,” *PLoS ONE*, 8(5):e59084, 2013.
- [Konrad *et al.*, 2018] Matthias Konrad, Christopher D. Pull, Sina Metzler, Katharina Seif, Elisabeth Naderlinger, Anna V. Grasse, and Sylvia Cremer, “Ants avoid superinfections by performing risk-adjusted sanitary care,” *Proceedings of the National Academy of Sciences*, page 201713501, 2018.
- [Konrad *et al.*, 2012] Matthias Konrad, Meghan L Vyleta, Fabian J Theis, Miriam Stock, Simon Tragust, Martina Klatt, Verena Drescher, Carsten Marr, Line V Ugelvig, and Sylvia Cremer, “Social transfer of pathogenic fungus promotes active immunisation in ant colonies,” *Plos Biology*, 10(4):e1001300, 2012.
- [Kramer *et al.*, 2016] Boris H. Kramer, Ralf Schaible, and Alexander Scheuerlein, “Worker lifespan is an adaptive trait during colony establishment in the long-lived ant *Lasius niger*,” *Experimental Gerontology*, 85:18–23, 2016.
- [Krause *et al.*, 2009] J Krause, D Lusseau, and R James, “Animal social networks: an introduction,” *Behavioral Ecology and Sociobiology*, 63(7):967–973, 2009.
- [Krause and Ruxton, 2002] J Krause and G. D. Ruxton, *Living in Groups*, Oxford University Press, 2002.
- [Leboeuf *et al.*, 2016] Adria C. Leboeuf, Patrice Waridel, Colin S. Brent, Andre N. Gonçalves, Laure Menin, Daniel Ortiz, Oksana Riba-Grognuz, Akiko Koto, Zamira G. Soares, Eyal Privman, Eric A. Miska, Richard Benton, and Laurent Keller, “Oral transfer of chemical cues, growth proteins and hormones in social insects,” *eLife*, 5(NOVEMBER2016), 2016.

- [Leclerc and Detrain, 2016] Jean Baptiste Leclerc and Claire Detrain, “Ants detect but do not discriminate diseased workers within their nest,” *Science of Nature*, 103(7), 2016.
- [Lentz *et al.*, 2012] Hartmut H K Lentz, Thomas Selhorst, and Igor M Sokolov, “Spread of infectious disease in directed and modular metapopulation networks,” *Physical Review E*, 85(6):66111, 2012.
- [Leoncini *et al.*, 2004] I Leoncini, Y Le Conte, G Costagliola, E Plettner, A L Toth, M W Wang, Z Huang, J M Becard, D Crauser, K N Slessor, and G E Robinson, “Regulation of behavioral maturation by a primer pheromone produced by adult worker honey bees,” *Proceedings of the National Academy of Sciences of the United States of America*, 101(50):17559–17564, 2004.
- [Lindholm and Britton, 2007] Mathias Lindholm and Tom Britton, “Endemic persistence or disease extinction: the effect of separation into sub-communities,” *Theoretical Population Biology*, 72(2):253–263, 2007.
- [Liutkevičiute *et al.*, 2018] Zita Liutkevičiute, Esther Gil-mansilla, Thomas Eder, Barbara Casillas-pérez, Giulia Di Giglio, Edin Muratspahić, Florian Grebien, Thomas Rattei, Sylvia Cremer, and Christian W Gruber, “Europe PMC Funders Group Oxytocin-like signaling in ants influences metabolic gene expression and locomotor activity,” *FASEB J.*, 32(12):6808–6821, 2018.
- [Martin and Bateson, 2007] Paul Martin and Patrick Bateson, *Measuring Behaviour: An Introductory Guide*, Cambridge University Press, third edit edition, 2007.
- [Matas *et al.*, 2004] J Matas, O Chum, M Urban, and T Pajdla, “Robust wide-baseline stereo from maximally stable extremal regions,” *Image and Vision Computing*, 22:761–767, 2004.
- [Mersch *et al.*, 2013] Danielle P Mersch, Alessandro Crespi, and Laurent Keller, “Tracking individuals shows spatial fidelity is a key regulator of ant social organization,” *Science*, 340(6136):1090–1093, 2013.
- [Miller, 2009] J Miller, “Spread of infectious disease through clustered populations,” *Journal of The Royal Society Interface*, 6(42):1121–1134, 2009.

- [Naiser, 2014] Filip Naiser, “Detection, description and tracking of ants in video sequences,” B.S. Thesis, CMP, Prague, 2014.
- [Naiser, 2017] Filip Naiser, “Tracking, Learning and Detection of Multiple Objects in Video Sequences,” Master’s thesis, CMP, Prague, 2017.
- [Naug and Camazine, 2002] D Naug and S Camazine, “The role of colony organization on pathogen transmission in social insects,” *Journal of Theoretical Biology*, 215(4):427–439, 2002.
- [Naug, 2008] Dhruba Naug, “Structure of the social network and its influence on transmission dynamics in a honeybee colony,” *Behavioral Ecology and Sociobiology*, 62(11):1719–1725, 2008.
- [Naug and Gibbs, 2009] Dhruba Naug and Ann Gibbs, “Behavioral changes mediated by hunger in honeybees infected with *Nosema ceranae*,” *Apidologie*, 40(6):595–599, 2009.
- [Naug and Smith, 2007] Dhruba Naug and Brian Smith, “Experimentally induced change in infectious period affects transmission dynamics in a social group,” *Proceedings of the Royal Society B-Biological Sciences*, 274(1606):61–65, 2007.
- [Newman, 2010] M E J Newman, “Epidemics on networks,” In M E J Newman, editor, *Networks: An Introduction*. Oxford University Press, 2010.
- [Newman and Girvan, 2004] M E J Newman and M Girvan, “Finding and evaluating community structure in networks,” *Physical Review E*, 69(2), 2004.
- [Nieuwenhuis *et al.*, 2017] Rense Nieuwenhuis, Ben Pelzer, and Manfred te Grotenhuis, *influence.ME: Tools for Detecting Influential Data in Mixed Effects Models*, 2017.
- [Nunn *et al.*, 2015] Charles L. Nunn, Ferenc Jordan, Collin M. Mc-Cabe, Jennifer L. Verdolin, and Jennifer H. Fewell, “Infectious disease and group size: More than just a numbers game,” *Philosophical Transactions of the Royal Society B: Biological Sciences*, 370(1669), 2015.



- [Okuno *et al.*, 2012] Masaki Okuno, Kazuki Tsuji, Hiroki Sato, and Kenji Fujisaki, “Plasticity of grooming behavior against entomopathogenic fungus *Metarhizium anisopliae* in the ant *Lasius japonicus*,” *Journal of Ethology*, 30(1):23–27, 2012.
- [Otterstatter and Thomson, 2007] Michael C Otterstatter and James D Thomson, “Contact networks and transmission of an intestinal pathogen in bumble bee (*Bombus impatiens*) colonies,” *Oecologia*, 154(2):411–421, 2007.
- [Pamminger *et al.*, 2016] Tobias Pamminger, Thomas Steier, and Simon Tragust, “High temperature and temperature variation undermine future disease susceptibility in a population of the invasive garden ant *Lasius neglectus*,” *Science of Nature*, 103(5):2–5, 2016.
- [Pedras *et al.*, 2002] M Soledade C Pedras, L Irina Zaharia, and Dale E Ward, “The destruxins : synthesis , biosynthesis , biotransformation , and biological activity,” *Phytochemistry*, 59:579–596, 2002.
- [Peeters and Ito, 2015] Christian Peeters and Fuminori Ito, “Wingless and dwarf workers underlie the ecological success of ants (Hymenoptera: Formicidae),” *Myrmecological News*, 21(June):117–130, 2015.
- [Pei and Makse, 2013] Sen Pei and Hernán A Makse, “Spreading dynamics in complex networks,” *Journal of Statistical Mechanics: Theory and Experiment*, 2013(12):P12002, 2013.
- [Pereira *et al.*, 2019] Talmo D Pereira, Diego E Aldarondo, Lindsay Willmore, Mikhail Kislin, Samuel S Wang, Mala Murthy, and Joshua W Shaevitz, “neural networks,” *Nature Methods*, 16(January), 2019.
- [Pérez-escudero *et al.*, 2014] Alfonso Pérez-escudero, Julián Vicente-page, Robert C Hinz, Sara Arganda, and Gonzalo G De Polavieja, “idTracker : tracking individuals in a group by automatic identification of unmarked animals,” *Nature Methods*, 11(7), 2014.
- [Pie *et al.*, 2004] M R Pie, R B Rosengaus, and J F A Traniello, “Nest architecture, activity pattern, worker density and the dynamics of disease transmission in social insects,” *Journal of Theoretical Biology*, 226(1):45–51, 2004.

- [Pinter-Wollman *et al.*, 2014] Noa Pinter-Wollman, Elizabeth A Hobson, Jennifer E Smith, Andrew J Edelman, Daizaburo Shizuka, Shermin de Silva, James S Waters, Steven D Prager, Takao Sasaki, George Wittemyer, Jennifer Fewell, and David B McDonald, “The dynamics of animal social networks: analytical, conceptual, and theoretical advances,” *Behavioral Ecology*, 25(2):242–255, 2014.
- [Pinter-Wollman *et al.*, 2011] Noa Pinter-Wollman, Roy Wollman, Adam Guetz, Susan Holmes, and Deborah M Gordon, “The effect of individual variation on the structure and function of interaction networks in harvester ants,” *Journal of the Royal Society Interface*, 8(64):1562–1573, 2011.
- [Porter and Tschinkel, 1986] Sanford D. Porter and Walter R. Tschinkel, “Adaptive Value of Nanitic Workers in Newly Founded Red Imported Fire Ant Colonies (Hymenoptera: Formicidae),” *Annals of the Entomological Society of America*, 79(3):723–726, 1986.
- [Pull *et al.*, 2013] Christopher D Pull, William O H Hughes, and Mark J F Brown, “Tolerating an infection: an indirect benefit of co-founding queen associations in the ant *Lasius niger*,” *Naturwissenschaften*, 100(12):1125–1136, 2013.
- [Pull *et al.*, 2018] Christopher D Pull, Line V Ugelvig, Florian Wiesenhofer, Anna V Grasse, Simon Tragust, Thomas Schmitt, Mark J F Brown, and Sylvia Cremer, “Destructive disinfection of infected brood prevents systemic disease spread in ant colonies,” *eLife*, pages 1–29, 2018.
- [Quevillon *et al.*, 2015] Lauren E. Quevillon, Ephraim M. Hanks, Shweta Bansal, and David P. Hughes, “Social, spatial, and temporal organization in a complex insect society,” *Scientific Reports*, 5:1–11, 2015.
- [R Core Team, 2013] R Core Team, *R: A Language and Environment for Statistical Computing*, R Foundation for Statistical Computing, Vienna, Austria, 2013.
- [Read *et al.*, 2008] Jonathan M Read, Ken T D Eames, and W John Edmunds, “Dynamic social networks and the implications for the spread of infectious disease,” *Journal of the Royal Society Interface*, 5(26):1001–1007, 2008.

- [Reber *et al.*, 2011] A Reber, J Purcell, S D Buechel, P Buri, and M Chapuisat, “The expression and impact of antifungal grooming in ants,” *Journal of Evolutionary Biology*, 24(5):954–964, 2011.
- [Renfree and Fenelon, 2017] Marilyn B. Renfree and Jane C. Fenelon, “The enigma of embryonic diapause,” *Development*, 144(18):3199–3210, 2017.
- [Richard *et al.*, 2008] F J Richard, A Aubert, and C M Grozinger, “Modulation of social interactions by immune stimulation in honey bee, *Apis mellifera*, workers,” *BMC Biology*, 6(1):50, 2008.
- [Richard *et al.*, 2012] F J Richard, Holly L Holt, and Christina M Grozinger, “Effects of immunostimulation on social behavior, chemical communication and genome-wide gene expression in honey bee workers (*Apis mellifera*),” *BMC Genomics*, 13:558, 2012.
- [Richardson *et al.*, 2015] Thomas O Richardson, Thomas E Gorochowski, and Thomas O Richardson, “Beyond contact-based transmission networks : the role of spatial coincidence,” *J R Soc Interface*, 2015.
- [Roberts and St. Leger, 2004] Donald W. Roberts and R. J. St. Leger, “*Metarhizium* spp ., Cosmopolitan Insect-Pathogenic Fungi : Mycological Aspects,” *Advances in Applied Microbiology*, 54, 2004.
- [Romero-ferrero *et al.*, 2018] Francisco Romero-ferrero, Mattia G Bergomi, Robert Hinz, and J H Francisco, “idtracker . ai : Tracking all individuals in large collectives of unmarked animals,” *arXiv*, 2018.
- [Rosengaus *et al.*, 1999] R B Rosengaus, C Jordan, M L Lefebvre, and J F A Traniello, “Pathogen alarm behavior in a termite: a new form of communication in social insects,” *Naturwissenschaften*, 86(11):544–548, 1999.
- [Rosengaus *et al.*, 1998a] R B Rosengaus, A B Maxmen, L E Coates, and J F A Traniello, “Disease resistance: a benefit of sociality in the dampwood termite *Zootermopsis angusticollis* (Isoptera : Termopsidae),” *Behavioral Ecology and Sociobiology*, 44(2):125–134, 1998.

- [Rosengaus *et al.*, 1998b] Rebeca B Rosengaus, A B Maxmen, Laran E Coates, and James F A Traniello, "Disease resistance : a benefit of sociality in the dampwood termite *Zootermopsis angusticollis* (Isoptera : Termopsidae)," *Behavioral Ecology and Sociobiology*, 44:125–134, 1998.
- [Rosengaus and Traniello, 1997] Rebeca B Rosengaus and James F A Traniello, "Pathobiology and disease transmission in dampwood termites [ *Zootermopsis angusticollis* ( Isoptera : Termopsidae )] infected with the fungus *Metarhizium anisopliae* ( Deuteromycotina : Hypomycetes," *Sociobiology*, 30(2):185–195, 1997.
- [Rueppell *et al.*, 2010] O Rueppell, M K Hayworth, and N P Ross, "Altruistic self-removal of health-compromised honey bee workers from their hive," *Journal of Evolutionary Biology*, 23(7):1538–1546, 2010.
- [Salathe and Jones, 2010] M Salathe and J H Jones, "Dynamics and control of diseases in networks with community structure," *Plos Computational Biology*, 6(4):e1000736, 2010.
- [Schmid-Hempel, 1998] P Schmid-Hempel, *Parasites in social insects*, Princeton University Press, Princeton, New Jersey, 1998.
- [Schmid-Hempel and Schmid-Hempel, 1993a] P Schmid-Hempel and R Schmid-Hempel, "Transmission of a pathogen in *Bombus terrestris*, with a note on division of labor in social insects," *Behavioral Ecology and Sociobiology*, 33(5):319–327, 1993.
- [Schmid-Hempel, 2017] Paul Schmid-Hempel, "Parasites and Their Social Hosts," *Trends in Parasitology*, 33(6):453–462, 2017.
- [Schmid-Hempel and Schmid-Hempel, 1993b] Paul Schmid-Hempel and Regula Schmid-Hempel, "Transmission of a pathogen in *Bombus terrestris*, with a note on division of labour in social insects," *Behavioral Ecology and Sociobiology*, 1993.
- [Scholl and Naug, 2011] Jacob Scholl and Dhruva Naug, "Olfactory discrimination of age-specific hydrocarbons generates behavioral segregation in a honeybee colony," *Behavioral Ecology and Sociobiology*, 65(10):1967–1973, 2011.

- [Schwenke *et al.*, 2017] Robin A Schwenke, Brian P Lazzaro, and Mariana F Wolfner, "Reproduction – Immunity Trade-Offs in Insects," *Annual Review of entomology*, pages 239–256, 2017.
- [Seeley, 1982] T D Seeley, "Adaptive significance of the age polyethism schedule in honeybee colonies," *Behavioral Ecology and Sociobiology*, 11(4):287–293, 1982.
- [Seifert, 2000] Bernhard Seifert, "Rapid range expansion in *Lasius neglectus* (Hymenoptera, Formicidae) -an Asian invader swamps Europe," 2000.
- [Sendova-Franks and Franks, 1995] A B Sendova-Franks and N R Franks, "Demonstrating new social interactions in ant colonies through randomization tests: separating seeing from believing," *Animal Behaviour*, 50:1683–1696, 1995.
- [Sendova-Franks *et al.*, 2010] A B Sendova-Franks, R K Hayward, B Wulf, T Klimek, R James, R Planque, N F Britton, and N R Franks, "Emergency networking: famine relief in ant colonies," *Animal Behaviour*, 79(2):473–485, 2010.
- [Shao and Jiang, 2012] Fei Shao and GuoPing Jiang, "Traffic driven epidemic spreading in homogeneous networks with community structure," *Journal of Networks*, 7(5):850–855, 2012.
- [Simon, 1996] Herbert A Simon, *The Sciences of the Artificial Third edition*, MIT Press, third edit edition, 1996.
- [Solé *et al.*, 1993] R V Solé, O Miramontes, and B C Goodwin, "Emergent Behavior in Insect Societies: Global Oscillations, Chaos and Computation," In Hermann Haken and A Mikhailov, editors, *Interdisciplinary Approaches to Nonlinear Complex Systems*, pages 77–88, Berlin, Heidelberg, 1993. Springer Berlin Heidelberg.
- [Sommer *et al.*, 1995] K Sommer, B Hölldobler, Theodor-boveri Institut, Zoologie li, Am Hubland, and D Würzburg, "Colony founding by queen association and determinants of reduction in queen number in the ant *Lasius niger*," *Animal Behaviour*, pages 287–294, 1995.
- [Starks *et al.*, 2000] Philip T Starks, Caroline A Blackie, and Thomas D Seeley, "Fever in honeybee colonies," *The Science of Nature*, 87(December):10–13, 2000.

- [Stephens *et al.*, 2008] Greg J. Stephens, Bethany Johnson-Kerner, William Bialek, and William S. Ryu, “Dimensionality and dynamics in the behavior of *C. elegans*,” *PLoS Computational Biology*, 4(4), 2008.
- [Stephens *et al.*, 2010] Greg J. Stephens, Leslie C. Osborne, and William Bialek, “Searching for simplicity: Approaches to the analysis of neurons and behavior,” *Proceedings of the National Academy of Sciences*, 108:15565–15571, 2010.
- [Stroeymeyt *et al.*, 2014] Nathalie Stroeymeyt, Barbara Casillas-Pérez, and Sylvia Cremer, “Organisational immunity in social insects,” *Current Opinion in Insect Science*, 5:1–15, 2014.
- [Stroeymeyt *et al.*, 2018] Nathalie Stroeymeyt, Anna V. Grasse, Alessandro Crespi, Danielle P. Mersch, Sylvia Cremer, and Laurent Keller, “Social network plasticity decreases disease transmission in a eusocial insect,” *Science*, 362(6417):941–945, 2018.
- [Sumpter, 2006] D J T Sumpter, “The principles of collective animal behaviour,” *Philosophical Transactions of the Royal Society B: Biological Sciences*, 361(November 2005):5–22, 2006.
- [Sun and Zhou, 2013] Qian Sun and Xuguo Zhou, “Corpse management in social insects,” *International Journal of Biological Sciences*, 9(3):313–321, 2013.
- [Szegedy *et al.*, 2014] Christian Szegedy, Vincent Vanhoucke, and Jon Shlens, “Rethinking the Inception Architecture for Computer Vision,” *Conference on Computer Vision and Pattern Recognition*, 2014.
- [Theis *et al.*, 2015] Fabian J Theis, Line V Ugelvig, Carsten Marr, Sylvia Cremer, and Sylvia Cremer, “Opposing effects of allogrooming on disease transmission in ant societies,” *Philosophical Transactions: Biological Sciences*, 2015.
- [Tragust *et al.*, 2013] Simon Tragust, Barbara Mitteregger, Vanessa Barone, Matthias Konrad, Line V Ugelvig, and Sylvia Cremer, “Ants Disinfect Fungus-Exposed Brood by Oral Uptake and Spread of Their Poison,” *Current Biology*, 23(1):76–82, 2013.
- [Traniello *et al.*, 2002] J F A Traniello, R B Rosengaus, and K Savoie, “The development of immunity in a social insect: evidence for the group facilitation of disease

- resistance,” *Proceedings of the National Academy of Sciences of the United States of America*, 99(10):6838–6842, 2002.
- [Trible and Kronauer, 2017] Waring Trible and Daniel J. C. Kronauer, “Caste development and evolution in ants: it’s all about size,” *The Journal of Experimental Biology*, 220(1):53–62, 2017.
- [Tschinkel, 1998] W. Tschinkel, “Sociometry and sociogenesis of the harvested ant *Pogonomyrmex badius*,” *Insectes Sociaux*, 45:385–410, 1998.
- [Tschinkel, 2010] Walter R. Tschinkel, “Back to basics: Sociometry and sociogenesis of ant societies (Hymenoptera: Formicidae),” *Myrmecological News*, 14(January):49–54, 2010.
- [Ugelvig and Cremer, 2007] Line V Ugelvig and Sylvia Cremer, “Report Social Prophylaxis : Group Interaction Promotes Collective Immunity in Ant Colonies,” *Current Biology*, 17:1967–1971, 2007.
- [Ugelvig *et al.*, 2008] Line V Ugelvig, Falko P Drijfhout, Daniel J C Kronauer, Jacobus J Boomsma, Jes S Pedersen, and Sylvia Cremer, “The introduction history of invasive garden ants in Europe : Integrating genetic , chemical and behavioural approaches,” *BMC Biology*, 14:1–14, 2008.
- [Ugelvig *et al.*, 2010] Line V Ugelvig, Daniel J C Kronauer, Alexandra Schrempf, and Sylvia Cremer, “Rapid anti-pathogen response in ant societies relies on high genetic diversity,” *Proceedings of the Royal Society B-Biological Sciences*, 277(May):2821–2828, 2010.
- [van Zweden and D’Ettorre, 2010] Jelle S van Zweden and Patrizia D’Ettorre, “Nest-mate recognition in social insects and the role of hydrocarbons,” In Anne-Geneviève Bagnères and Gary J Blomquist, editors, *Insect Hydrocarbons: Biology, Biochemistry, and Chemical Ecology*, pages 222–243. Cambridge University Press, Cambridge, 2010.
- [Venables and Ripley, 2002] W N Venables and B D Ripley, *Modern Applied Statistics with S*, Springer, New York, fourth edition, 2002.

- [Walker and Hughes, 2009] Tom N. Walker and William O.H. Hughes, “Adaptive social immunity in leaf-cutting ants,” *Biology Letters*, 5(4):446–448, 2009.
- [Wang and Moeller, 1970] D I Wang and F E Moeller, “Division of labor and queen attendance behavior of Nosema-infected worker honey bees (Hymenoptera, Apidae),” *Journal of Economic Entomology*, 63(5):1539–1541, 1970.
- [Ward, 2014] Philip S Ward, “The Phylogeny and Evolution of Ants,” *Annual Review of Ecology, Evolution, and Systematics*, 2014.
- [Wheeler, 1911] William Morton Wheeler, “The ant-colony as an organism,” *J Morphol*, 22:307–325, 1911.
- [Wickham *et al.*, 2018] Hadley Wickham, Winston Chang, Lionel Henry, Thomas Lin Pedersen, Kohske Takahashi, Claus Wilke, and Kara Woo, *ggplot2: Create Elegant Data Visualisations Using the Grammar of Graphics*, 2018.
- [Wickham *et al.*, 2017] Hadley Wickham, Romain Francois, Lionel Henry, and Kirill Müller, *dplyr: A Grammar of Data Manipulation*, 2017.
- [Wills *et al.*, 2018] Bill D. Wills, Scott Powell, Michael D. Rivera, and Andrew V. Suarez, “Correlates and Consequences of Worker Polymorphism in Ants,” *Annual Review of Entomology*, 63(1):575–598, 2018.
- [Wilson-Rich *et al.*, 2009] Noah Wilson-Rich, Marla Spivak, Nina H Fefferman, and Philip T Starks, “Genetic, Individual, and Group Facilitation of Disease Resistance in Insect Societies,” *Annual Review of Entomology*, 54(1):405–423, 2009.
- [Woyciechowski and Moron, 2009] M Woyciechowski and D Moron, “Life expectancy and onset of foraging in the honeybee (*Apis mellifera*),” *Insectes Sociaux*, 56(2):193–201, 2009.
- [W.R. Tschinkel, 1993] W.R. Tschinkel, “Sociometry and sociogenesis of colonies of the fire ant *Solenopsis invicta* during one annual cycle,” *Ecological Monographs*, 63(4):452–457, 1993.
- [Wyrebek *et al.*, 2011] Michael Wyrebek, Cristina Huber, Ramanpreet Kaur Sasan, and Michael J Bidochka, “Three sympatrically occurring species of *Metarhizium* show plant rhizosphere specificity,” *Microbiology*, 157:2904–2911, 2011.



- [Yanagawa *et al.*, 2011] Aya Yanagawa, Nao Fujiwara-Tsujii, Toshiharu Akino, Tsuyoshi Yoshimura, Takashi Yanagawa, and Susumu Shimizu, "Behavioral changes in the termite, *Coptotermes formosanus* (Isoptera), inoculated with six fungal isolates," *Journal of Invertebrate Pathology*, 107(2):100–106, 2011.
- [Yanagawa *et al.*, 2009] Aya Yanagawa, Fumio Yokohari, and Susumu Shimizu, "The role of antennae in removing entomopathogenic fungi from cuticle of the termite, *Coptotermes formosanus*," *Journal of Insect Science*, 9(6), 2009.
- [Yang, 2007] Andrew S. Yang, "Thinking outside the Embryo: The Superorganism as a Model for EvoDevo Studies," *Biological Theory*, 2(4):398–408, 2007.
- [Yek *et al.*, 2013] Sze H. Yek, Jacobus J. Boomsma, and Morten Schiøtt, "Differential gene expression in *Acromyrmex* leaf-cutting ants after challenges with two fungal pathogens," *Molecular Ecology*, 22(8):2173–2187, 2013.
- [Zeiler and Fergus, 2014] Matthew D Zeiler and Rob Fergus, "Visualizing and Understanding Convolutional Networks," *European Conference on Computer Vision*, 2014.